DAMPING INTERAREA OSCILLATIONS IN POWER SYSTEMS WITH DFIG

A Thesis
Submitted to The Graduate Faculty
of the
North Dakota State University
of Agriculture and Applied Science

By

Ravi Chandra Thapa

In Partial Fulfillment of the Requirements
for the Degree of
MASTER OF SCIENCE

Major Department:
Electrical and Computer Engineering

April 2011

Fargo, North Dakota

North Dakota State University
Graduate School

Title

DAMPING INTERAREA OSCILLATIONS IN POWER SYSTEMS WITH DFIG

By

RAVI CHANDRA THAPA

The Supervisory Committee certifies that this ***disquisition*** complies with North Dakota State University's regulations and meets the accepted standards for the degree of

MASTER OF SCIENCE

ABSTRACT

Thapa, Ravi Chandra, M.S., Department of Electrical and Computer Engineering, College of Engineering and Architecture, North Dakota State University, April 2011. Damping Interarea Oscillations in Power Systems with DFIG. Major Professor: Dr. Rajesh Kavasseri.

With rapid depletion of fossil fuels and increasing environmental concerns, the trend to capture renewable energy, especially through wind energy resources, is increasing. The doubly fed induction generator (DFIG) is the most widely used generator for wind energy conversion because of its various advantages over other types of generators. In a DFIG, the rotor is fed through back to back converters via slip rings. The converters enable the generation control. This control property can be used to support reliable operation of a grid network system.

Interarea oscillation has been a major factor in limiting power transfers in interconnected power systems. Poorly damped modes can trigger oscillatory instability, potentially leading to cascading blackouts in such systems. We consider a two-area system where DFIG based wind generation is integrated with conventional synchronous generators. A simple controller is proposed for the DFIG to improve damping of interarea oscillations. To support the proposition, case studies are conducted in Matlab/Simulink. The effectiveness of the proposed controller is then analyzed by eigenvalue analysis and verified with time domain simulation results. The results show that a properly tuned controller can increase the damping of dominant oscillatory mode by nearly 5% while improving the area transfer by about 200 MW of wind power. The results further show that with the proposed control strategy, damping of dominant oscillatory mode increased by more than 10%.

ACKNOWLEDGEMENTS

I owe my deepest gratitude to my advisor, Dr. Rajesh Kavasseri, for providing me the opportunity to work on this project. His invaluable guidance and encouragement has been of great help to me throughout the course of my M.S. studies.

I am grateful to Dr. Subbaraya Yuvarajan, Dr. Lingling Fan, Dr. Bei Gou and Dr. Sumathy Krishnan as instructors and also as members of my graduate committee for their advice and guidance that enabled me to develop and understand the subject.

I would like to thank the NDSU graduate school and the ECE Department for providing me with financial support. I am thankful to Priscilla Schlenker and Laura Dallmann for their effort in helping me with administrative matters.

I am indebted to my friends Rasool Aghaterani, Munir Kaderbhai and all others for their unconditional support and encouragement.

Finally my deepest gratitude to my parents and relatives for their entire support; without them, I would not have reached this point in my life.

TABLE OF CONTENTS

LIST OF TABLES

LIST OF FIGURES

LIST OF APPENDIX FIGURES

CHAPTER 1. INTRODUCTION

1.1. Overview

This chapter presents a brief introduction on renewable energy resources and harvesting of wind energy. Stability problems related to power systems are presented. Stability problems that might arise due to introduction of large scale power generation units in the system are discussed. The objective is to provide an overview on wind power, stability problems and develop general idea on problem statement of the thesis.

1.2. Renewable Energy Resources

Depletion of fossil fuel resources and increase in environmental concerns have led to ever rising usage of renewable energy resources such as wind, sunlight, hydro power and geothermal heat. Abundant and pollution free nature of these resources have led to further interest in their usage for bulk power production. Power supplied from renewable energy sources have seen an upsurge in the total energy supplied recently in most countries and the trend is likely to continue forever. Renewable energy sources contribute about nineteen percent of the total global energy consumed today [1]. With higher targets set to obtain more energy from renewable energy sources and the increasing investments made in this sector, it is certain bulk power from renewable energy harvesting technologies will be added to the power grid system.

Wind energy being economically competent to other energy resources nowadays, it is becoming a significant source of renewable energy. Wind energy is abundant, requires no fuel cost, pollution free and wind power generation units require small area for construction. Growth in wind farms connection to grid system recently and prospective grid connection of wind generation units show the popularity of wind energy generation.

1.3. Wind Energy Harvesting

Wind power has been in use since a long time back. The earliest known use of wind power is the sail boats [2]. The first windmills were developed to automate the tasks of grain-grinding and water-pumping and the earliest known design is the vertical axis system developed in Persia about 500-900 A.D. Wind energy harvesting technologies have transformed a lot since then.

Wind power installations have been increasing at a fast pace and at the highest rate among renewable energy harvesting technologies used recently. More wind power capacity was added during 2009 than any other renewable energy harvesting technologies. New technologies and larger sized wind turbines to harvest wind energy have been of great importance these days. Development of large size wind turbines and large wind farms have led to bulk power grid integration of wind power. Strict grid integration requirements [3-4] of electrical power from wind requires further improvement in technologies to control wind power generation. Intermittent nature of the wind resource and remote location of generation units from consumers is hindering development of large sized wind farms and grid integration.

Electricity was generated successfully in the late 19^{th} century using multi-blade windmill design. Charles F. Brush generated electricity from a large wind mill for the first time in Cleveland, Ohio in 1888. However, bulk power production at utility scale from wind did not flourished till it was first undertaken in Russia in 1931 with 100KW Balaclava wind generator. Subsequent experimental wind plants were established in the United States, Denmark, France, Germany, and Great Britain during the period 1935-1970. Since then wind energy installation has seen various developments and large wind farms

have been installed and proposed to be built in the near future. Some of the large scale wind farms built or planned in the USA are Buffalo Gap Wind farm (524 MW, Texas), Capricorn Ridge Wind farm (662.5 MW, Texas), Fowler Ridge Wind farm (600 MW, Indiana), Lone Star Wind farm (400 MW, Texas), Panther Creek Wind farm (458 MW, Texas), Horse Hollow Wind farm (735.5 MW, Texas), Roscoe Wind farm (781.5 MW, Texas), Pampa Wind Project (4000 MW, Texas), Shepherds Flat Wind Farm (845 MW, Oregon).

A wind generation unit has a wind turbine coupled to a generator. The turbine captures kinetic energy from wind. The captured energy is then transformed to electric energy via a generator. The generating unit is equipped with a synchronous or an asynchronous (induction) generator. Recent wind turbines are mostly equipped with variable speed generators as doubly fed induction generator. Variable speed wind generation captures more energy compared to fixed speed wind generation. In addition doubly fed induction generator can support grid network with reactive power and have other control advantages too. A doubly fed induction generator is an induction generator that consists of accessible rotor via slip rings. The stator of the doubly fed induction generator is connected to the grid network and the rotor is fed via back to back converters that enable generator control.

1.4. Power System Stability Problems

Successful operation of power systems network depends on reliable and uninterrupted power supply to consumers. For this to happen, synchronous generators in grid network should run in parallel and interconnecting transmission lines should operate in sound conditions to maintain power flow without any interruption. Operating states

continuously change with varying operating conditions of a system. A successfully operating network system should be able to regain equilibrium states after a disturbance. This property of power systems network is defined as power system stability. Disturbances or changes in practical power systems network are unavoidable. Disturbances lead to oscillatory phenomenon that is reflected as fluctuations in rotor angle, power flow etc. Excessive fluctuations with poor damping lead to oscillatory instability inducing protection devices to trip power system components. Power system stability is generally categorized as small signal stability and transient stability. Small signal stability problems involve small disturbances whereas transient stability is the ability of power systems network to regain equilibrium state after severe disturbances.

1.5. Wind Energy and Power System Stability

With increasing large scale grid integration of wind generators, stability problems have attained a lot of interest recently. A lot of work is ongoing with voltage stability. However, rotor angle stability problem hasn't been properly investigated with small scale grid integration of wind generators in power systems network. With the rise in large scale grid integration of wind power, rotor angle stability problem recently has attained some interest. Large scale wind generation supports more power and as well introduces many challenges against secured power system operation. Large scale grid integrated wind generators are considered new machines in power systems network. Wind generating units are undergoing various improvements to support power systems network. Their operation should be well studied and understood for successful operation of power systems network. Wind generating units as induction generators connected to the grid directly or via wind generators provide low or no and slower inertial response compared to conventional

synchronous generators. This may hamper the stability of the system. Further, intermittent power production introduces power fluctuations and remote location of wind generating units requires long transmission lines that are prone to stability problems.

1.6. Objective of the Thesis

The objective of the thesis is to study the impact of grid connection of large scale wind farms equipped with doubly fed induction generator on interarea oscillation. Inter area oscillation is a serious problem related to small signal stability of interconnected systems. Failing to damp interarea oscillation leads to cascading blackouts. A control strategy to improve interarea damping is to be proposed and investigated for its effectiveness.

1.7. Contributions of the Thesis

The major contribution of this thesis is the study of impact of grid integrated doubly fed induction generator on interarea oscillation and its damping by addition of a simple controller. In doing so, the idea behind doubly fed induction generator modeling and controller design in Matlab/Simulink is discussed in details. The effect of various control procedures on oscillations is shown. Additional control is proposed to modulate wind power generation with an attempt to damp interarea oscillations. The effectiveness of the proposed control action is analyzed with eigenvalue study and verified with time domain simulation results.

1.8. Outline of Thesis

Chapter -2 presents the literature review for the thesis. It has sections relating to wind energy systems and related previous work.

Chapter -3 presents system modeling. It contains sections with the theoretical background for development of wind generator model and control concept.

Chapter -4 describes small signal stability study and the method utilized. It paves the way for analysis.

Chapter-5 depicts the results and discusses them to support the proposal on damping interarea oscillation.

Chapter-6 presents conclusion of the research and suggestions for future work is recommended.

1.9. Summary

This chapter presents an overview of the thesis and gives us a general idea on what the work is about. Interarea oscillation is a small signal stability problem that leads to cascading blackouts. Damping of interarea oscillation is important for successful operation of power systems network. Before integration of large scale wind farms equipped with DFIG, their impact on power systems network should be studied in details. Poor damping of interarea modes results instability. Large scale grid connected generation units should be capable of damping these oscillatory modes properly. Further, the chapter presents an outline of the thesis and gives us a basic idea about the latter sections.

CHAPTER 2. LITERATURE REVIEW

2.1. Overview

This chapter presents wind energy conversion and various wind turbine generators. The chapter explains doubly fed induction generator as a widely used variable speed wind generator. Low frequency oscillation is reviewed to state the problem to be studied. Impact of wind power connection and corrective measures taken by others to damp interarea oscillation are reviewed.

2.2. Wind Energy Integration

Energy consumption has been increasing day by day. With cost competitive generation technology wind energy harvesting has attained a lot of interest recently. Many researches are being conducted to solve relative issues for this promising energy resource.

The various issues currently related to wind power studies are location of wind power resources, fluctuating nature of wind power, generator technologies used and their control. Study of these issues helps us to have knowledge about impact of wind power on power systems network, its' stability and required reinforcement for safe and normal operation of the system. As grid integration of wind power increases, wind generation no longer remains as simple generation units that can be shut off and connected occasionally during and after faults. Impact of wind generation is more important with the installation of larger wind farms.

Interaction between wind power and power systems network should be well understood for reliable operation of power grid. Increased penetration of wind power with newer technology introduces challenges as well as place for improvements in stability of power systems network. New grid codes for grid connection of wind power require strong

performance against variations in voltage and frequency, capability of voltage control, fault ride through capability etc. Preservation of grid reliability remains the most important aspect in terms of connection of any power source. Large wind power resources grid integration gaining momentum recently may introduces new problems to the stability of power grid. Research on control of wind generation for network support has gained a lot of attention recently [5-10]. Voltage dip, effects of severe transient faults and small disturbances resulting oscillatory phenomenon as interarea oscillation are major threats to the security of interconnected power systems network [11]. These threats lead to cascading outages with sudden loss of generation units [12]. Potential contribution of wind farms to support power systems network against these threats is of great importance for secured and reliable supply of power to consumers.

2.3. Mechanics of Wind Power Conversion

A wind turbine generation system basically consists of tower, blades and nacelle. The tower supports the blades that rotate to capture kinetic energy of wind. The nacelle houses gearbox, generator and control equipments. It functions to convert linear kinetic energy of wind to electrical energy as illustrated in Figure 2-1. The captured energy is transferred to the generator via the shaft and gear box. Mechanical energy captured by the rotor is transformed to electrical energy by the generator. The control equipments work to facilitate grid integration by producing right frequency and voltage [13].

For a wind turbine, power available is a function of kinetic energy of the air flow through the rotor per unit time [14].

Kinetic energy = 0.5*air mass*V^2 (2.1)

then, if P = available power in wind (watts)

V = wind velocity (m/s)

ρ = air density (Kg/m^3)

A = area swept by the rotor blades (m^2)

Air mass flow rate = $\rho*A*V$

And, $P = 0.5* \rho*A*V^3$ (2.2)

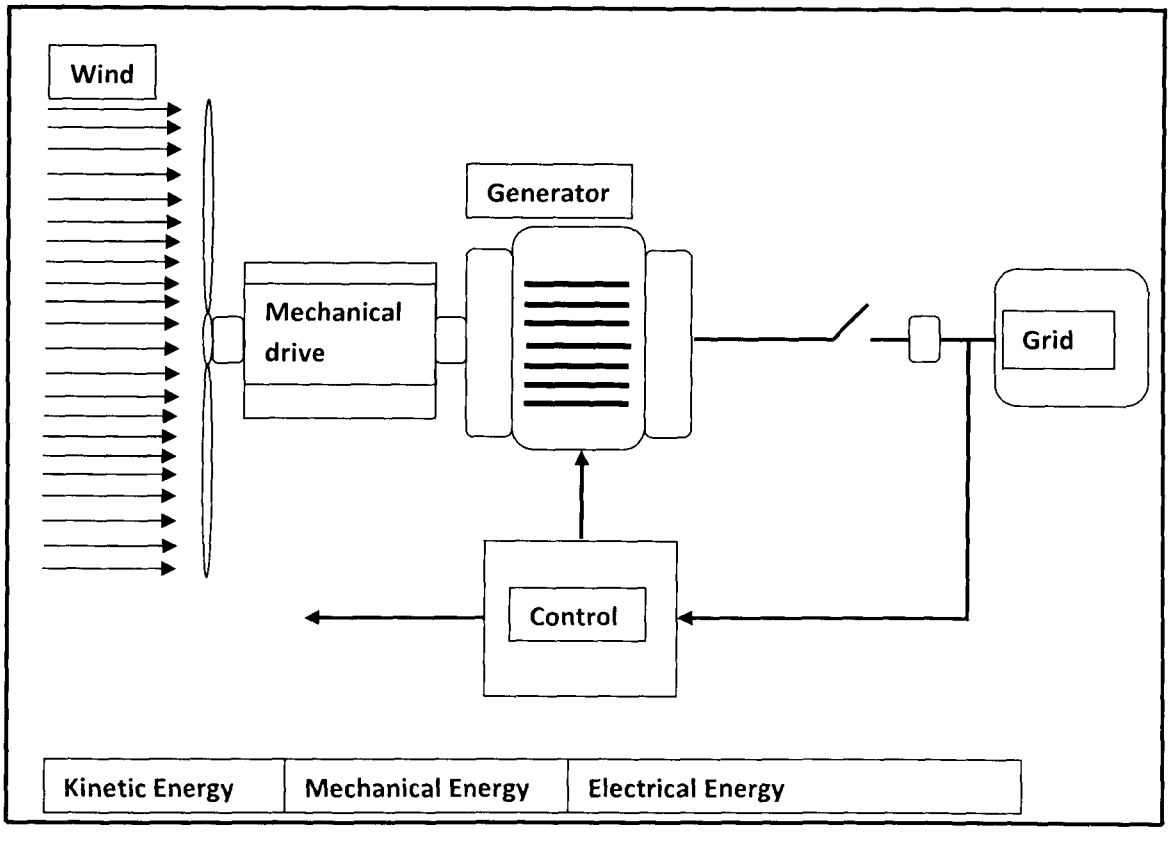

Figure 2-1: Functional Structures and Power Transfer in a Wind Energy Conversion Unit

However, only a part of the available energy can be captured by wind turbine and transformed to electrical energy. In practice a maximum of about 45% of the available wind energy is captured by the best modern horizontal axis wind turbines [14]. The deliverable power is a function of aerodynamic efficiency or power coefficient (C_p) of the wind turbine.

i.e. P_{actual} (deliverable power) = P* C_p

or, $P_{actual} = 0.5 * C_p * \rho * A * V^3$ (2.3)

Further, electrical power output of the machine considering individual efficiency is given by the following equation:

P_e(electrical power output) = $\eta_g * \eta_m * P_{actual}$ (2.4)

where η_g = efficiency of generator

η_m = efficiency of gear system

Coefficient of performance or power coefficient is the function of tip speed ratio (TSR). TSR is the ratio of linear blade speed to incoming wind speed.

i.e. TSR (λ) = blade tip speed/ wind speed

$= \omega * R/V$ (2.5)

where, ω is the rotor angular velocity, R the radius of the turbine and V is the wind speed. Variation of C_p with TSR for various types of wind turbines is discussed in [15]. A C_p vs. TSR characteristic typical to horizontal axis wind turbine is shown in Figure 2-2. The maximum theoretical value of C_p defined as Betz limit is $16/27 \approx 0.593$ for an ideal aeroturbine. However, practically wind turbines tend to have an aerodynamic efficiency less than this maximum value. Modern wind turbines achieve a C_p value of around 0.4 [16]. From Figure 2-2 we can observe that a particular value of TSR will yield the maximum value of C_p and hence the maximum output power. So it is important to control the system such that the TSR is constant throughout the operating range of wind speeds, corresponding to the maximum C_p value, thereby harnessing the maximum possible energy from wind. By operating the machine constantly at or near the optimum tip speed ratio; the turbine depending on turbine aerodynamics and wind on average can collect up to 10% more

annual energy [17]. This means a huge uplift in the collection of revenue over a period of 20-30 years of its operation.

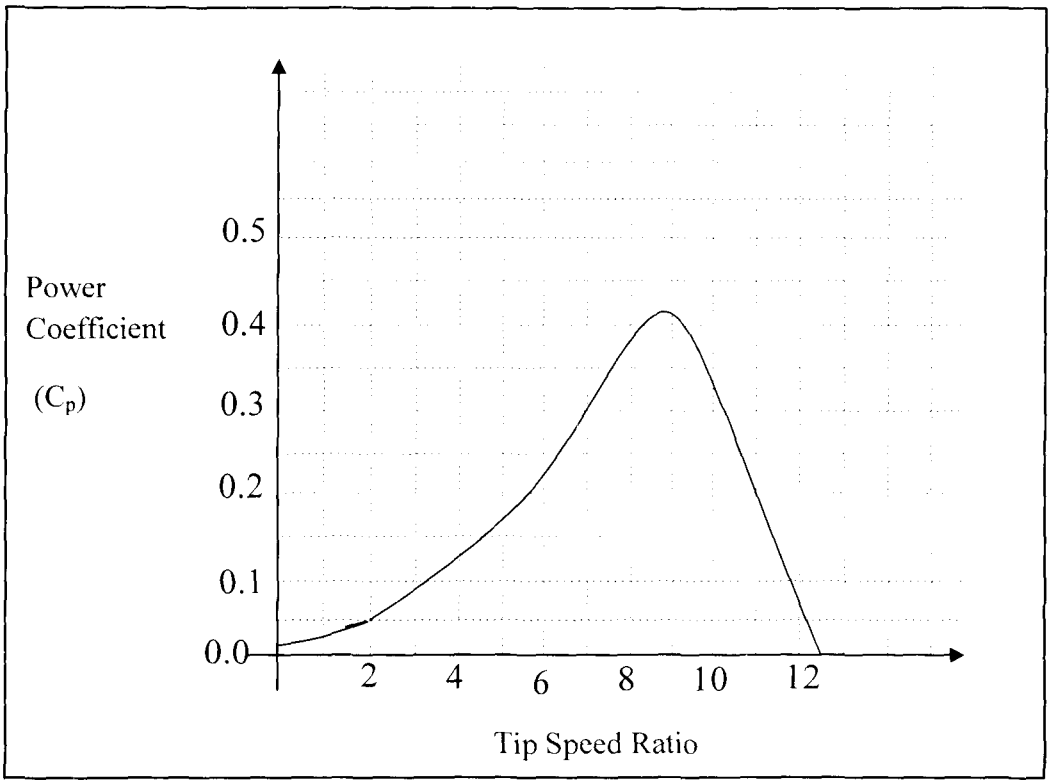

Figure 2-2: C_p vs. TSR Characteristic Typical to Horizontal Axis Wind Turbines

2.4. Wind Turbine Technology

Different types of wind turbines are used for various applications as pumping water at remote locations to bulk electric power production in modern facilities. The schemes for harvesting wind energy in terms of the speed of rotation of the wind turbine can be basically classified as follows:-

Fixed Speed Wind Turbine

Variable Speed Wind Turbine

2.4.1. Fixed Speed Wind Turbine

A fixed speed wind turbine is directly connected to the grid. The rotor and generator must turn at a certain speed to produce power at a constant frequency. Thus, the frequency of the grid system determines the rotational speed of the generator. Due to simple and inexpensive construction, induction generator is mainly used for this system. However, due to constant speed characteristics of the system; it requires a stiff grid for stable operation and expensive mechanical construction to absorb high mechanical stress caused by wind gust that produces fluctuations in the output power. Further they require reactive power compensators for reactive power demand of the generator [18].

2.4.2. Variable Speed Wind Turbine

Many variable speed architectures have been used to capture wind energy [17]. Variable speed wind turbine is connected to the grid through power electronic devices. Synchronous generators as well as asynchronous generators (induction generator) both are used for this type of system. A full converter connected generator has power converter connected to stator via the grid. A converter for a variable speed full converter connected generator has rating similar to the generator rating. The rating of the converter should be such to convey the full power generated by the wind turbine generator system. An induction generator can be connected to grid via a back to back partially rated converter at the rotor. With such connections the rotor is allowed to rotate freely with wind. The converter converts variable frequency at generator output to the grid frequency.

Induction machines are either cage rotor types or wound rotor types. Cage rotor type induction machines have conducting bars in the rotor of the machine. These conducting bars are shorted at each end of the rotor with short rings. Wound rotor on the

other hand has three phase windings in the rotor with the leads of the windings brought out to slip rings mounted on the armature. This makes the rotor of wound rotor induction machine accessible.

Forcing torque at the rotor of an induction machine produces electric energy at the stator opposite to the behavior of motor. Characteristics of an induction machine can be discussed presenting it as a motor. Implementation of stator voltage to an induction machine results flow of current in the stator windings. This current propagates a magnetic field which rotates within the stator winding. The speed of rotation of magnetic field known as synchronous speed and is dictated by the input frequency at the stator. It is given by the following equation:-

$$\eta_{sync} = \frac{120f}{P} \tag{2.6}$$

where, η_{sync}, is the synchronous speed in rpm, 'f' is the input frequency in hertz and P is the number of poles.

When the rotating magnetic field rotates across the rotor windings a current is induced on the rotor as per Faraday's law of induction. With current flowing in the windings, a force is induced on the rotor winding according to Lorentz law. On the opposite rotating mechanical energy can be transformed to electrical energy based on electromagnetic induction. A typical torque speed characteristics of an induction machine is shown in Figure 2-3.

From Figure 2-3 the machine produces no torque at synchronous speed and acts as a generator at speed greater to synchronous speed. Difference in speed of the stator magnetic field and rotor field is defined as slip.

$$s = \frac{Nsync - Nmech}{Nsync} * 100\% \quad (2.7)$$

then, the rotor frequency $f_r = s * f_s$ (2.8)

where 's' is the slip, 'Nsync' is the synchronous speed, 'Nmech' the mechanical speed, 'f_r' rotor frequency and 'f_s' the synchronous frequency.

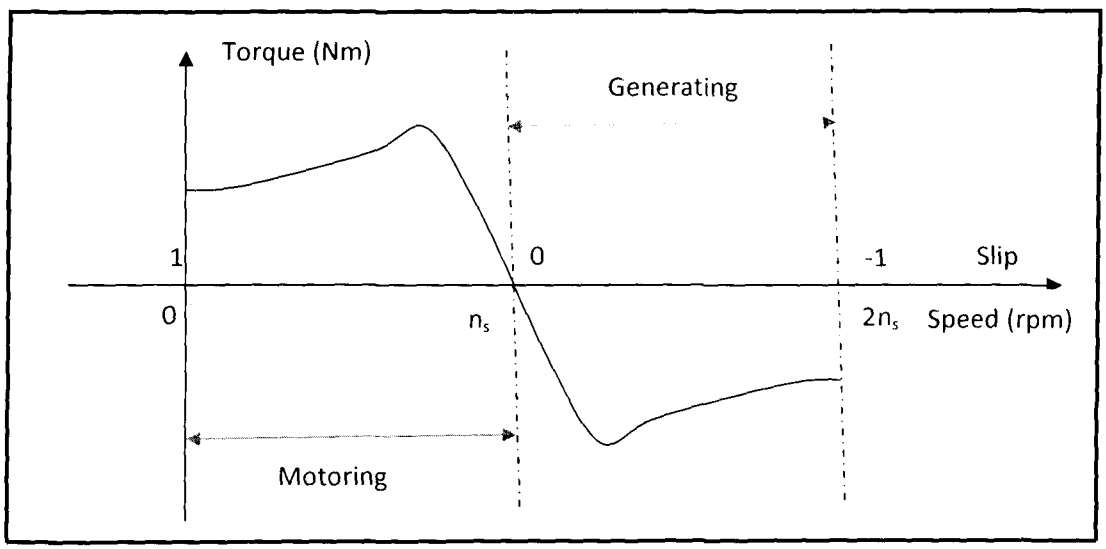

Figure 2-3: Torque Speed Characteristics of an Induction Generator

Thus, from this we know the rotor frequency can be externally changed to vary the slip and the machine may be forced to operate in generating mode as shown in Figure 2-3.

2.5. Doubly Fed Induction Generator (DFIG)

Doubly Fed Induction Generator [19] is rugged, captures more wind energy, costs less and has flexible control capability compared to various types of generators used to harvest wind power. Because of these advantages it is widely used in large scale wind energy system these days [17]. DFIG is a wound rotor induction machine controlled by AC/DC/AC; a back to back converter connected to the rotor of induction generator as shown in Figure 2-4. As name suggests a doubly fed machine is fed from the stator as well as the rotor. The converters are named as rotor and grid side converter according to their

location shown in Figure 2-4. The converter used here is rated at about 25-30% of the generator rating. The rating of the converter used is significantly less compared to full converter connected variable speed generators. Smaller the rating of converter results lower cost. DFIG serves variable speed operation with significant increase in the capacity factor compared to fixed speed wind turbine generators and less cost compared to the full converter connected generators. Further, decreased power loss at the converter has also made it more popular among the wind energy conversion systems, despite its control complexities.

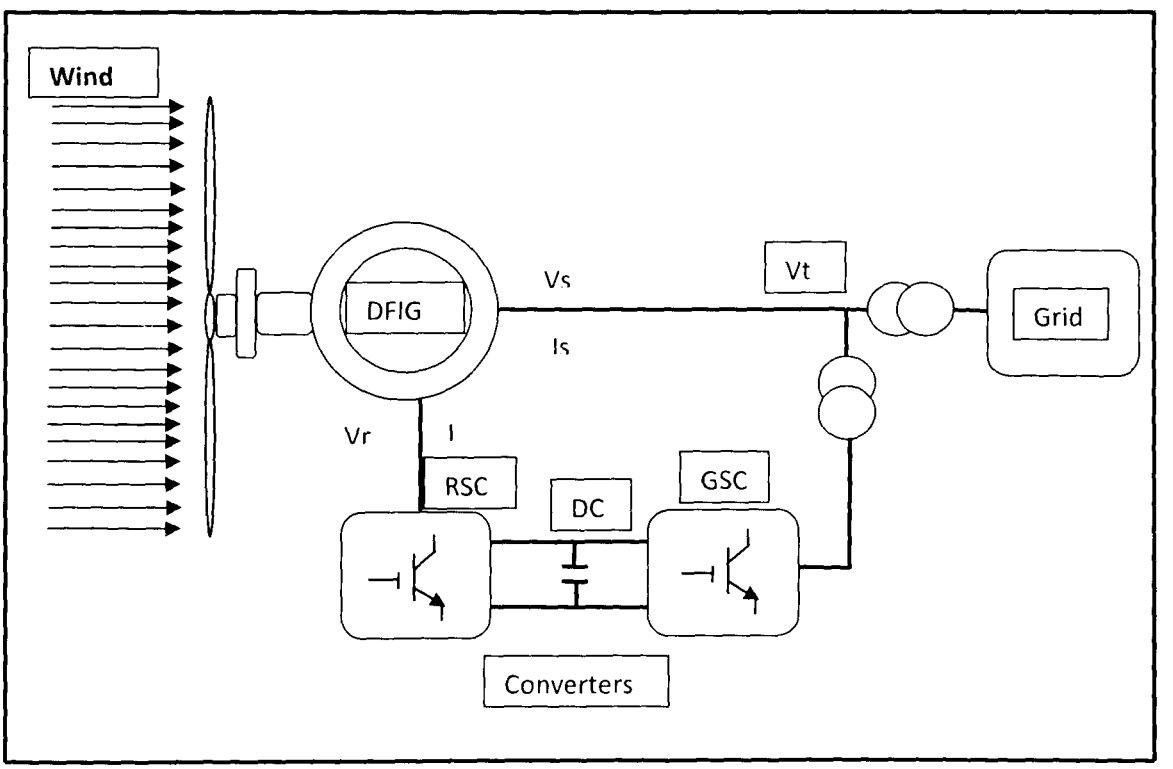

Fig 2-4: Doubly Fed Induction Generator (DFIG)

Variable frequency input through the rotor is fed to manipulate the frequency of rotor voltage. The speed of the wind varies from time to time. This results in variable angular speed of the wind turbine 'ω_t' and corresponding generator speed 'ω_g'. With the

rotor input frequency being 'ω_r', stator angular speed for operation is given by the equation; $\omega_s = \omega_g + \omega_r$ or $f_s = f_g + f_r$ [20]. The converter compensates the difference between the mechanical and electrical frequency by injecting a current with variable frequency [21]. In case of subsynchronous mode of operation of the machine, generated electrical power is fed to the grid through the stator whereas some portion of the electrical power is made available as slip power at the rotor through the power converters via slip rings. During super-synchronous operating mode total electrical power supplied to the grid is supplied through the stator as well through the rotor via the power converters.

At a wind farm individual wind turbines capture wind energy and transform it to electrical energy at low or medium voltage which is stepped up to a higher voltage and transmitted to consumers locations through power grid. Then the high voltage power is stepped down to low voltage and distributed to the end users. Bulk wind generation should act as conventional power plants despite their unique operational behavior. Thus, newer connections of wind energy grid integration require wind generation units to participate in reactive power control [22]. DFIG is operated to maximize energy capture from varying wind speeds; at rated wind speed or above it the generated output is as nameplate ratings whereas below the rated wind speed maximum possible energy is captured at various wind speeds. A DFIG rotor current is controlled by a four quadrant power converter. Real and reactive power can flow in either direction of the converter [19]. Vector control approach is generally applied these days to control the rotor current. It acts to adjust electromagnetic torque in excitation which would control active and reactive power at the stator and rotor side [23]. An active power set point can be achieved using the rotor speed which in turn adjusts the current in stator flux oriented reference frame to obtain the desired active

power. Similarly reactive power set point for the control system can be achieved for a prefixed power factor or required reactive power for a desired voltage level at the output terminal [24- 25].

Grid studies conducted on large scale wind power integration have shown that impact of wind power on damping of power system oscillations depend on the type of wind turbine (constant or variable speed) and on wind power penetration [26]. Studies related to DFIG have shown an inter mix of increment and decrease in damping whereas fixed speed wind turbines is shown to damp inter area mode oscillations [27], [28], [29].

2.6. Low Frequency Oscillations

Low frequency Oscillations are generator rotor angle oscillation having frequency ranging between 0.1-2.0 Hz [30]. They are defined as local modes and interarea oscillation as their location in power systems network. The local modes normally have a frequency in the range of 0.7-2.0 Hz. Interarea modes which are of special interest here are the oscillation associated with group of generators in different areas connected with a tie line. Interarea modes have frequencies in the range of 0.1-0.8 Hz. Presence of low frequency oscillations in power grid network limits the amount of power transfer between interconnected areas. They can be harmful as their introduction may result in outages leading to cascading blackouts, so should be dealt properly.

Figure 2-5 shows a simple two area system consisting generators in area one connected to area two via a weak transmission line. Generators in area one oscillates with generators in area two i.e. interarea oscillations.

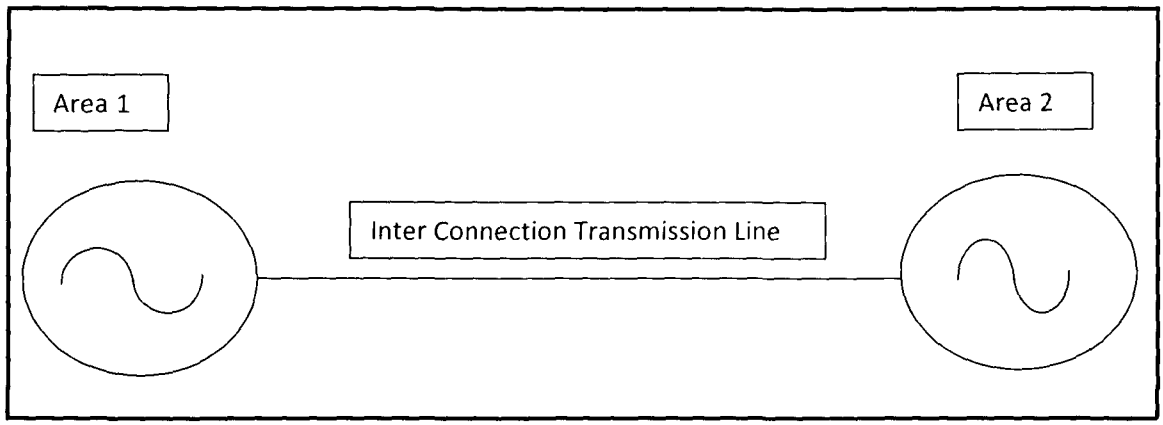

Figure 2-5: Electrical Two Area System

The two area electrical system can be perfectly described with a mechanical analog as shown in Figure 2-6 [31]. Two engines as shown in Figure 2-6, show the mechanical equivalent of the power generation in the two areas.

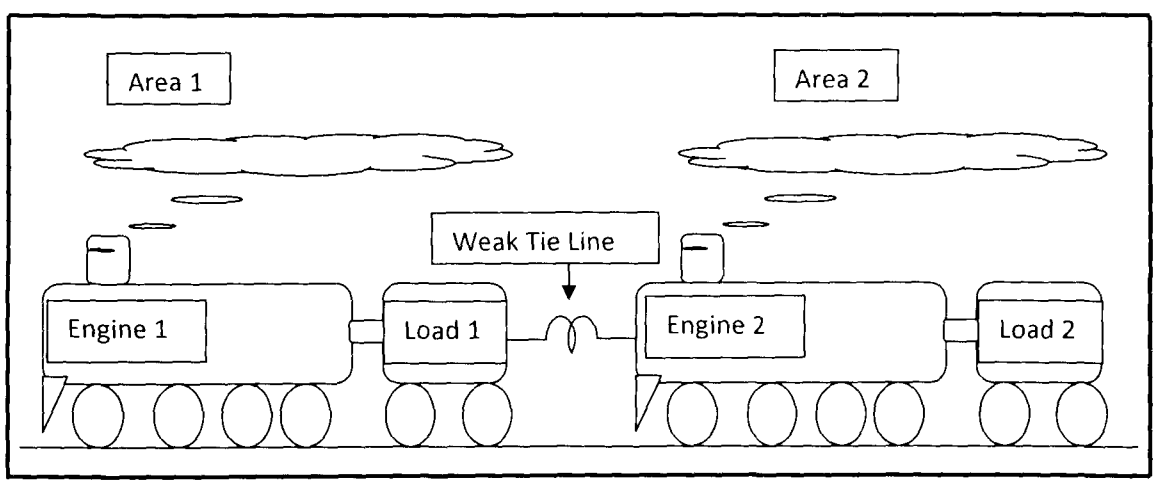

Figure 2-6: Mechanical Analog of Two Area System {Figure Modified from [31]}

The engines are assumed to be moving at steady state, a change in load introduces change in the velocity of the engines. At the same time power at tie spring representing the weak tie line varies and hence oscillation in the spring is initiated. Similarly a change in one of

the generators or load introduces electromechanical oscillation in the tie line for our electrical system.

2.7. Previous Work

Power systems oscillations and damping associated with conventional generating units are well studied [30]. Insignificant amount of wind energy integrated to power grid so far had limited studies related to bulk power transmission abnormalities as power systems oscillation. However, with the trend of establishing large wind farms and immense growth in wind energy grid integration studies related to bulk wind power integration has attained some interest recently. Research work is going on to study the behavior of new generating units and power systems to operate it reliably. With bulk wind power generation and integration at remote locations from consumers and a possibility of replacement of conventional generators by newer technologies in the future, problems as power systems oscillations and its damping has to be studied properly.

J. G. Slootweg and W. L. Kling treated the impact of variable speed wind turbines on power system oscillations with a constant power model in [26]. The effect of increasing wind power on oscillations was investigated by gradually replacing power generated by synchronous generator with wind power. Both constant and variable speed generators were considered for the study. It was observed that the effect of wind power on power systems oscillation was dependent on the type of wind turbine used. Constant speed wind turbine was found to damp power systems oscillation more than variable speed wind turbines.

Lasantha et al in [28] studied the impact of wind technology mix on interarea oscillations. The study was carried out with intermix of fixed speed induction generator and doubly fed induction generator and only doubly fed induction generator. The damping ratio

for increased wind power penetration with doubly fed induction generator was observed to be reduced. The observation was drawn showing output power oscillating noticeably during tie-line disturbances in network systems consisting wind farm equipped with doubly fed induction generator.

L. Fan et al in [29] have shown that increasing the penetration of wind power improves damping significantly. Increasing the voltage control loop gain as well improved damping where as other control loops such as pitch control and phase locked loops, have negligible impacts on interarea oscillation.

Espen et al in [32] studied large scale wind power integration in Norway and impact on damping in the Nordic Grid. A temporary three phase fault was applied to study the oscillations and prony's method [33] which yields eigenvalues for the oscillating signal obtained was used for analysis. Simulation was carried for different cases with and without wind power integrated in the system. From the study it was concluded that squirrel cage induction machine improves damping where as direct drive synchronous generator and doubly fed induction generator deteriorate damping of interarea modes.

G. Tsourakis et al in [34] investigated the effect of increasing doubly fed induction generator penetration on interarea oscillation. The investigation was conducted employing different loading patterns and doubly fed control scheme. In the paper, a positive impact on damping of interarea oscillations with the increase in doubly fed induction generator penetration with a possible exception for some cases of voltage control mode of the reactive power controller was shown.

G. Tsourakis et al investigated the impact of wind parks with doubly fed induction generator on electromechanical oscillations in an interconnected power systems network in

[35]. They used doubly fed induction generator model with detailed control loop. It was shown that interarea mode is less damped and can even be destabilized for doubly fed induction generator with voltage control modes of operation. An improved controller tuning to avoid instability was proposed for the system.

F. M. Hughes et al in [36] proposed a power system stabilizer for a wind turbine employing a doubly fed induction generator. The contribution a power system stabilizer can make on the doubly fed induction generator based wind turbine on network damping was shown. The performance of such a system was shown superior to those provided by synchronous generator with automatic voltage regulator and power system stabilizer.

In [37] P. Ledesma et al proposed a control system intended to damp interarea power systems network oscillations. A signal proportional to the deviation of frequency was added to the active power reference with various gains to modulate active power generation.

R. D. Fernandez et al in [25] presented improvements in power systems stability that can be achieved from wind farms when adequately controlled. The oscillation is damped out in this work with the addition of corrective measure that relies in a kind of resistive characteristic in order to counter oscillations.

L. Fan et al in [38] and [39] proposed a control scheme to damp interarea oscillation. In these papers an auxiliary control loop was added to adjust the active power to damp oscillations and time domain simulations were provided to demonstrate the effectiveness of the control.

2.8. Summary

Doubly fed induction generator is widely used variable speed wind generator that has the capabilities to emulate synchronous generator behavior. Low frequency oscillation as interarea oscillation is inherent to interconnected power systems network and is a serious threat to secured power systems network operation. Doubly fed induction generator requires corrective measures to damp interarea oscillations to ensure reliable power supply to consumers. Many techniques have been employed to improve damping in systems with doubly fed induction generator. In all the cases, the corrective measures taken modulate generator output power to maintain a balance between the generated power and demand.

CHAPTER 3. SYSTEM MODELING

3.1. Overview

Theoretical background required for modeling of the power systems network will be discussed in this chapter. Simple but complete models are required for accurate stability studies. Matlab/Simulink is a powerful and widely used tool for analysis and time domain simulations studies. This chapter provides the basic theory required to develop simulink models. Simulink models and codes developed for the study are presented in the appendix at the end of the thesis.

3.2. Wind Model

Various wind models are found in many literatures. TurbSim a precise wind model simulator developed at National Renewable Energy Laboratory provides stochastic, full field, turbulent wind simulation incorporating many fluid dynamic features that adversely affect turbine aero elastic response and loading [40]. In [41] the wind model combines the deterministic and the stochastic effects. The deterministic part contains the mean wind speed and tower shadow variations where as the stochastic part of the wind model includes the coherence between the wind turbines and the rotational turbulence. Simple wind models expressed by instantaneous wind velocity as follows has been used in [42].

$$V = \overline{V} + v \text{ (m/s)} \tag{3.1}$$

where V = Instantaneous wind velocity

$\overline{V}$ = Mean wind speed

v = Turbulent component of wind

In this research work, the wind speed is assumed constant i.e. a constant mechanical torque. The assumption is reasonable for small time period (5-30 seconds) and hence the simulation is restricted to ten-thirty seconds [29, 39].

3.3. Wind Turbine Modeling

Various models of wind turbines have been developed and are in use for different purposes as in [43-45]. The design differs in terms of the different features they emphasize relevant to the study. We use a simple model of controllable horizontal wind turbine for the research as described in [46-47].

The aerodynamic power captured by the turbine is given by the nonlinear expression discussed in chapter two i.e. as follows:

$$P_a = 0.5 * \rho * A * C_p(\lambda, \beta) * V^3 \quad (3.2)$$

Operation of a variable speed wind turbine based on wind speed and the power generated can be divided into three regions as shown in Figure 3-1.

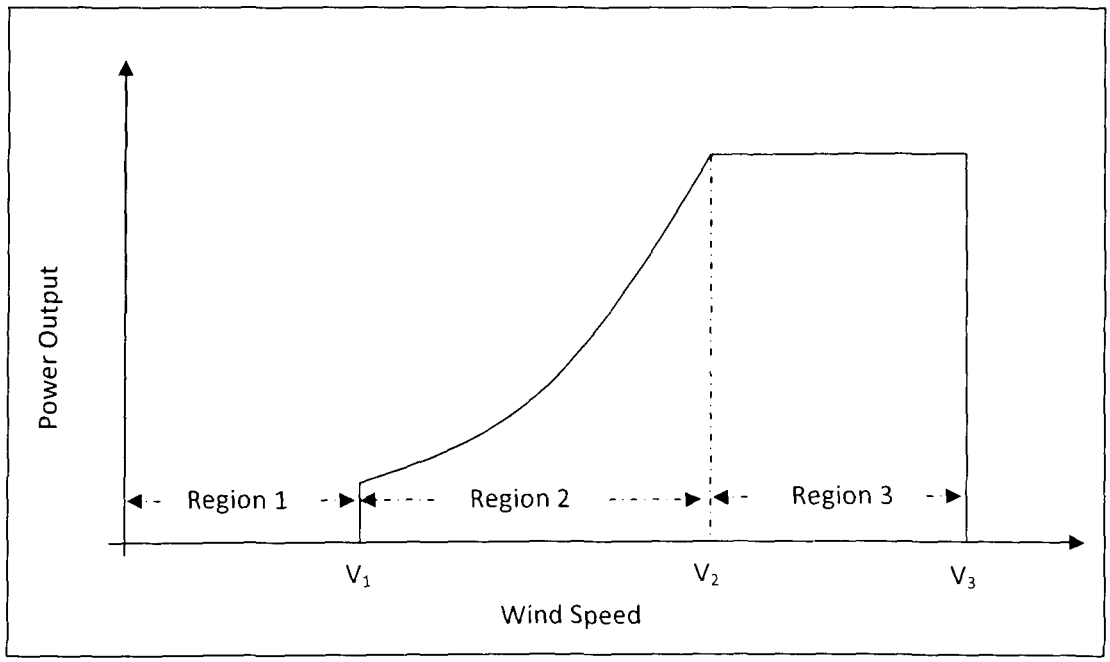

Figure 3-1: Aerodynamic Output Power of a Wind Turbine

Considering the wind speed for a certain time period at the wind turbine location to be 'V', 'V_1' is the cut in wind speed at which the wind turbine starts delivering power, 'V_2' is the rated wind speed at which maximum permissible power is generated and 'V_3' the cut out wind speed is the maximum wind speed till which the wind turbine can remain in operation for capturing wind power.

Region 1:- $V < V_1$

Region 2:- $V_1 < V < V_2$

Region 3:- $V_2 < V_3$

In region 1 and beyond region 3 no power is produced by the wind turbine. Power output of a wind turbine beyond the rated wind speed is constant. Power smoothing in this region is controlled generally by a pitch regulation or stall regulation mechanism. In region 2 variable speed operation of a wind turbine actually comes into existence. Here the coefficient of power C_p is adjusted to capture maximum possible power from wind at various speeds while the pitch is held at the optimum.

As we know that power coefficient C_p is dependent on the tip speed ratio 'λ' and blade pitch angle 'β'.

Where $\lambda = \frac{\omega * R}{V}$ (3.3)

From [42, 46] power coefficient C_p is approximated by the following expression:-

$$C_p = (0.44 - 0.0167*\beta) * \sin\left[\frac{\pi(\lambda-3)}{(15-0.3*\beta)}\right] - 0.00184 *(\lambda-3)*\beta \quad (3.4)$$

Further the aerodynamic torque is related to the power by the following relationship:

$$P_a = \omega_r * T_a \quad (3.5)$$

Then, the mechanical output torque for the wind turbine is given by the following equation:-

$$T_a = \frac{0.5 * \rho * A * R * C_p(\lambda, \beta) * V^2}{\lambda} \quad (3.6)$$

where, 'R', is the wind turbine rotor radius, 'V', is the wind velocity, 'ρ', is the air density 'ω_r', is the rotor angular velocity, 'A', is the area swept by the blades and 'T_a', is output mechanical torque.

3.4. Doubly Fed Induction Generator Modeling

The machine is modeled in Simulink/Matlab. In order to build a dynamic model of a machine we need to define electrical and mechanical characteristics of that machine first. Schematic of a three phase induction machine is shown in Figure 3-2.

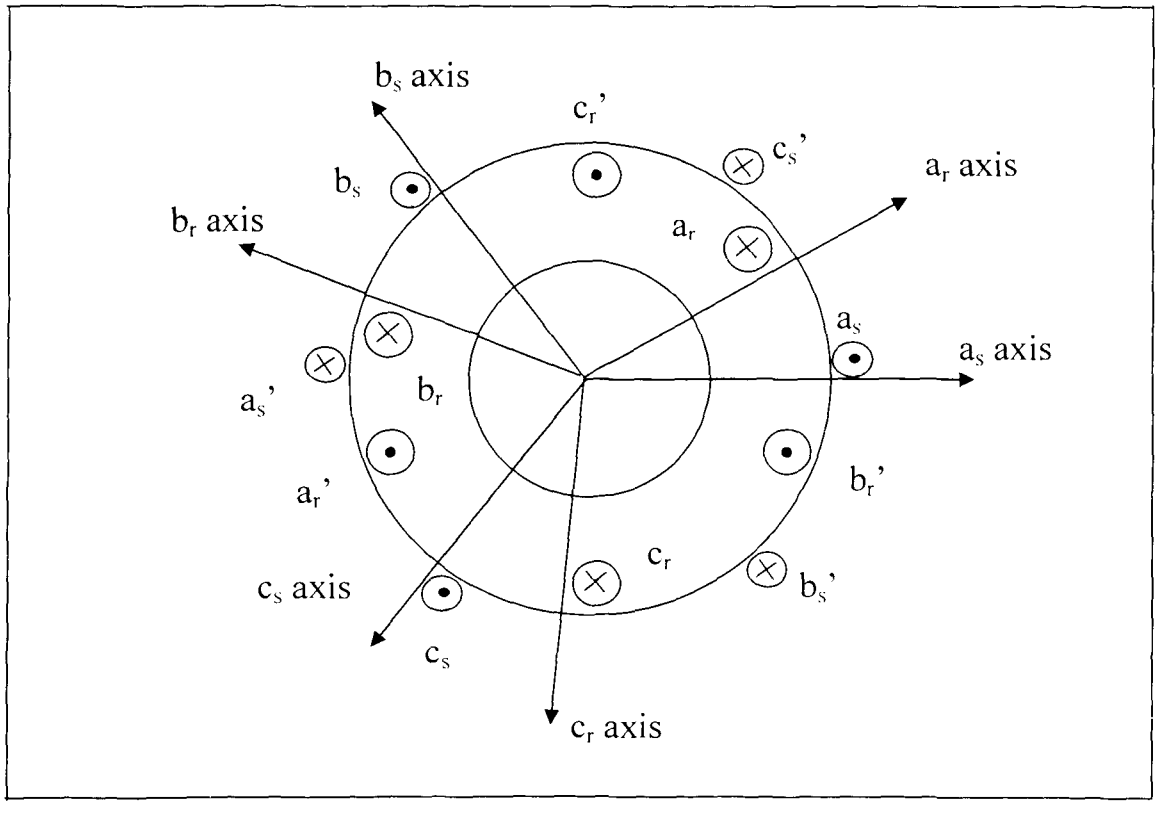

Figure 3-2: Schematics of an Induction Machine

In this thesis, the simulink model of doubly fed induction generator developed in [38] and [48] will be used for the purpose. The electrical and mechanical dynamics for the machine will be discussed initially here briefly [5, 49].

For an induction machine the stator and rotor voltages can be written as the sum of copper losses and the rate of change of flux linkages according to Kirchhoff's and Faraday's laws [5].

$$\begin{bmatrix} V_{as} \\ V_{bs} \\ V_{cs} \end{bmatrix} = R_s * \begin{bmatrix} i_{as} \\ i_{bs} \\ i_{cs} \end{bmatrix} + p \begin{bmatrix} \psi_{as} \\ \psi_{bs} \\ \psi_{cs} \end{bmatrix} \tag{3.7}$$

Similarly rotor voltages are as follows:-

$$\begin{bmatrix} V_{ar} \\ V_{br} \\ V_{cr} \end{bmatrix} = R_r * \begin{bmatrix} i_{ar} \\ i_{br} \\ i_{cr} \end{bmatrix} + p \begin{bmatrix} \psi_{ar} \\ \psi_{br} \\ \psi_{cr} \end{bmatrix} \tag{3.8}$$

where, 'V', 'R', 'i', 'p' and 'ψ' represents voltage, resistance, current, partial differentiation operator $\frac{d}{dt}$ and flux linking the windings. The subscripts 'a', 'b' and 'c' denotes the three phases. The subscripts's' and 'r' denotes the stator and rotor windings. Current flowing into the winding is considered positive for the system.

Further flux linkage can be expressed as the product of current 'i' and inductance 'L' as follows:-

$$\begin{bmatrix} \psi_{as} \\ \psi_{bs} \\ \psi_{cs} \end{bmatrix} = L_s * \begin{bmatrix} i_{as} \\ i_{bs} \\ i_{cs} \end{bmatrix} + L_m * \begin{bmatrix} i_{ar} \\ i_{br} \\ i_{cr} \end{bmatrix} \tag{3.9}$$

$$\begin{bmatrix} \psi_{ar} \\ \psi_{br} \\ \psi_{cr} \end{bmatrix} = L_m{}^T * \begin{bmatrix} i_{as} \\ i_{bs} \\ i_{cs} \end{bmatrix} + L_r * \begin{bmatrix} i_{ar} \\ i_{br} \\ i_{cr} \end{bmatrix} \tag{3.10}$$

$$\text{where, } L_s = \begin{bmatrix} L_{ls}+L_{ms} & -\frac{1}{2} L_{ms} & -\frac{1}{2} L_{ms} \\ -\frac{1}{2} L_{ms} & L_{ls}+L_{ms} & -\frac{1}{2} L_{ms} \\ -\frac{1}{2} L_{ms} & -\frac{1}{2} L_{ms} & L_{ls}+L_{ms} \end{bmatrix} \tag{3.11}$$

$$L_r = \begin{bmatrix} L_{lr}+L_{mr} & -\frac{1}{2}L_{mr} & -\frac{1}{2}L_{mr} \\ -\frac{1}{2}L_{mr} & L_{lr}+L_{mr} & -\frac{1}{2}L_{mr} \\ -\frac{1}{2}L_{mr} & -\frac{1}{2}L_{mr} & L_{lr}+L_{mr} \end{bmatrix} \quad (3.12)$$

$$L_m = L_m \begin{bmatrix} \cos\theta_r & \cos(\theta_r + \frac{2\pi}{3}) & \cos(\theta_r - \frac{2\pi}{3}) \\ \cos(\theta_r - \frac{2\pi}{3}) & \cos\theta_r & \cos(\theta_r + \frac{2\pi}{3}) \\ \cos(\theta_r + \frac{2\pi}{3}) & \cos(\theta_r + \frac{2\pi}{3}) & \cos\theta_r \end{bmatrix} \quad (3.13)$$

where, L_{ls} and L_{ms} are the leakage and magnetizing inductances of stator windings; L_{lr} and L_{mr} are the leakage and magnetizing inductances of rotor windings and L_m is the amplitude of mutual inductance between stator and rotor winding. The angular displacement of the rotor from the stator is

$$\theta_r = \int_0^t \omega_r \, dt + \theta_r(0) \quad (3.14)$$

where, ω_r is the electrical rotor speed provided by the product of no. of pole pairs and the mechanical speed of the rotor 'ω_m'. Here θ_r the angular difference between the stator and rotor quantities varies with time. This gives us varying inductance introducing complexities. It can be transformed to constant quantity using suitable arbitrary reference frame to reduce the complexities. ABC to DQ0 transformation is a procedure that transforms the three phase variables to arbitrary reference frame. For the transformation a reference frame that rotates at a speed 'ω' is considered. The 'q' axis is assumed to be 90° ahead of 'd' axis in the direction of rotation. Stator and rotor circuit frames and the reference frame are shown in Figure 3-3.

In the Figure 3-3 β_s is the angle between the stator circuit frame and the reference frame.

$$\beta_s = \int_0^t \omega \, dt + \beta_s(0) \quad (3.15)$$

β_r is the angle between the rotor circuit frame and reference frame.

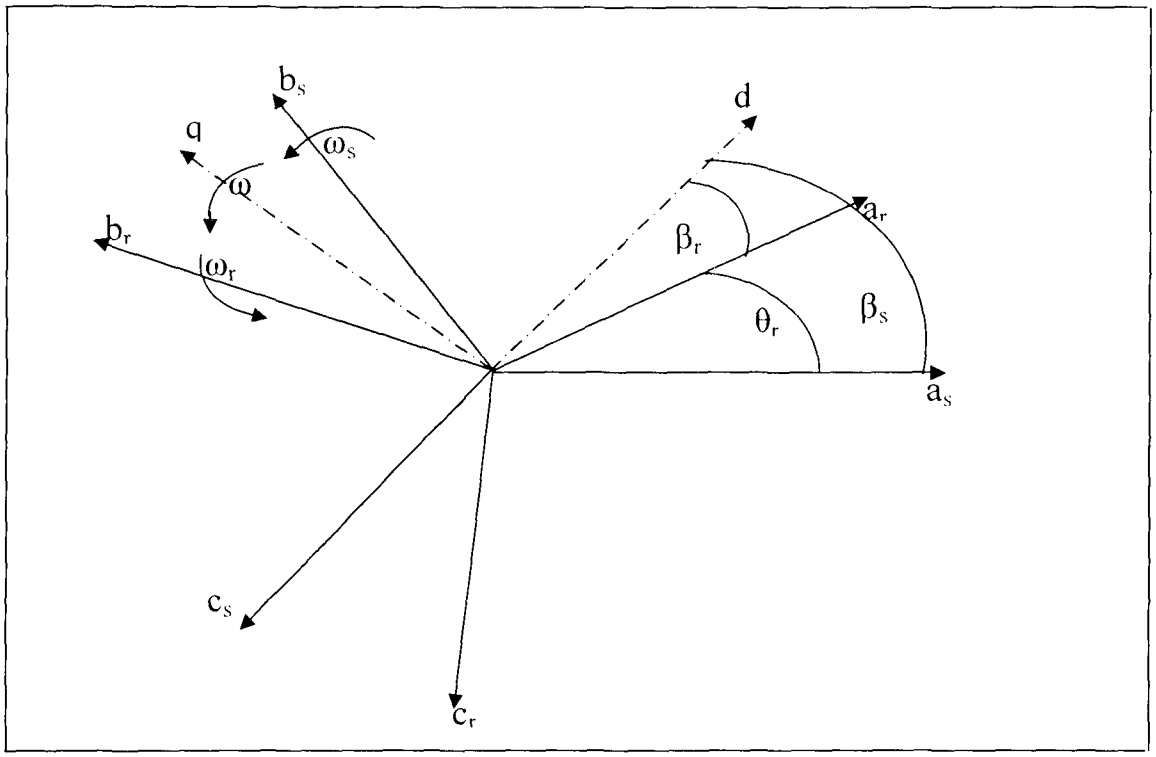

Figure 3-3: Stator and Rotor Circuit Frames and Reference Frame

where, $\beta_r = \int_0^t (\omega - \omega_r)dt + \beta_r(0)$ (3.16)

From Parks' transformation [5] the transformation of three phase variables of a circuit to arbitrary reference frame is given by

$$f_{qd0} = K_r f_{abc} \tag{3.17}$$

where, $K_r = \frac{2}{3}\begin{bmatrix} \cos\beta & \cos(\beta - \frac{2\pi}{3}) & \cos(\beta + \frac{2\pi}{3}) \\ \sin\beta & \sin(\beta - \frac{2\pi}{3}) & \sin(\beta + \frac{2\pi}{3}) \\ \frac{1}{2} & \frac{1}{2} & \frac{1}{2} \end{bmatrix}$ (3.18)

where, β is the angle between the reference frame and the frame of the circuit whose variables are to be transformed.

$$\text{Also,}\quad (K_r)^{-1} = \begin{bmatrix} \cos\beta & \sin\beta & 1 \\ \cos(\beta - \frac{2\pi}{3}) & \sin(\beta - \frac{2\pi}{3}) & 1 \\ \cos(\beta + \frac{2\pi}{3}) & \sin(\beta + \frac{2\pi}{3}) & 1 \end{bmatrix} \tag{3.19}$$

Now applying the transformation to the voltage equations (3.7) and (3.8) we get,

$$\begin{bmatrix} V_{qs} \\ V_{ds} \\ V_{0s} \end{bmatrix} = R_s * \begin{bmatrix} i_{qs} \\ i_{ds} \\ i_{0s} \end{bmatrix} + K_r(\beta_s) \frac{d}{dt}\left(K_r^{-1}(\beta_s) \begin{bmatrix} \psi_{qs} \\ \psi_{ds} \\ \psi_{0s} \end{bmatrix}\right) \tag{3.20}$$

$$\text{And} \begin{bmatrix} V_{qr} \\ V_{dr} \\ V_{0r} \end{bmatrix} = R_r * \begin{bmatrix} i_{qr} \\ i_{dr} \\ i_{0r} \end{bmatrix} + K_r(\beta_r) \frac{d}{dt}\left(K_r^{-1}(\beta_r) \begin{bmatrix} \psi_{qr} \\ \psi_{dr} \\ \psi_{0r} \end{bmatrix}\right) \tag{3.21}$$

$$\text{Also,} \begin{bmatrix} \psi_{qs} \\ \psi_{ds} \\ \psi_{0s} \end{bmatrix} = K_r(\beta_s) L_s K_r^{-1}(\beta_s) \begin{bmatrix} i_{qs} \\ i_{ds} \\ i_{0s} \end{bmatrix} + K_r(\beta_s) L_m K_r^{-1}(\beta_r) \begin{bmatrix} i_{qr} \\ i_{dr} \\ i_{0r} \end{bmatrix} \tag{3.22}$$

$$\begin{bmatrix} \psi_{qr} \\ \psi_{dr} \\ \psi_{0r} \end{bmatrix} = K_r(\beta_r) L_r K_r^{-1}(\beta_r) \begin{bmatrix} i_{qr} \\ i_{dr} \\ i_{0r} \end{bmatrix} + K_r(\beta_r) L_m^{T} K_r^{-1}(\beta_s) \begin{bmatrix} i_{qs} \\ i_{ds} \\ i_{0s} \end{bmatrix} \tag{3.23}$$

$$K_r(\beta)\frac{d}{dt}\left(K_r^{-1}(\beta) \begin{bmatrix} f_q \\ f_d \\ f_0 \end{bmatrix}\right) = K_r(\beta)\frac{d}{dt}(K_r^{-1}(\beta)) \begin{bmatrix} f_q \\ f_d \\ f_0 \end{bmatrix} + K_r(\beta)(K_r^{-1}(\beta)) \frac{d}{dt}\left(\begin{bmatrix} f_q \\ f_d \\ f_0 \end{bmatrix}\right) \tag{3.24}$$

$$= \frac{d\beta}{dt} \begin{bmatrix} 1 & 0 & 0 \\ 0 & -1 & 0 \\ 0 & 0 & 0 \end{bmatrix} + \frac{d}{dt}\left(\begin{bmatrix} f_q \\ f_d \\ f_0 \end{bmatrix}\right) \tag{3.25}$$

Then, the voltage equations can be expanded in the following form:

$$V_{qs} = r_s i_{qs} + \omega \psi_{ds} + p\psi_{qs} \tag{3.26}$$

$$V_{ds} = r_s i_{ds} - \omega \psi_{qs} + p\psi_{ds} \tag{3.27}$$

$$V_{0s} = r_s i_{0s} + p\psi_{0s} \tag{3.28}$$

$$V_{qr} = r_r i_{qr} + (\omega - \omega_r) \psi_{dr} + p\psi_{qr} \tag{3.29}$$

$$V_{dr} = r_r i_{dr} - (\omega - \omega_r) \psi_{qr} + p\psi_{dr} \tag{3.30}$$

$$V_{0r} = r_r i_{0r} + p\psi_{0r} \tag{3.31}$$

In equations (3.29)-(3.31), the rotor quantities are assumed transferred to the stator side.

Expressing all the quantities in per unit system and the flux linkage equations in terms of reactance we get,

$$V_{qs} = r_s\, i_{qs} + \frac{\omega}{\omega_b}\psi_{ds} + \frac{p}{\omega_b}\psi_{qs} \tag{3.32}$$

$$V_{ds} = r_s\, i_{ds} - \frac{\omega}{\omega_b}\psi_{qs} + \frac{p}{\omega_b}\psi_{ds} \tag{3.33}$$

$$V_{0s} = r_s\, i_{0s} + \frac{p}{\omega_b}\psi_{0s} \tag{3.34}$$

$$V_{qr} = r_r\, i_{qr} + \frac{\omega-\omega_r}{\omega_b}\psi_{dr} + \frac{p}{\omega_b}\psi_{qr} \tag{3.35}$$

$$V_{dr} = r_r\, i_{dr} - \frac{\omega-\omega_r}{\omega_b}\psi_{qr} + \frac{p}{\omega_b}\psi_{dr} \tag{3.36}$$

$$V_{0r} = r_r\, i_{0r} + \frac{p}{\omega_b}\psi_{0r} \tag{3.37}$$

Here, ω_b is the base electrical angular velocity.

Now, the flux linkage per second with the units of volts, when the inductive reactance is obtained as the product of reactance and base electrical angular velocity is as follows:

$$\psi_{qs} = X_{ls}\, i_{qs} + X_M\,(i_{qs} + i_{qr}) \tag{3.38}$$

$$\psi_{ds} = X_{ls}\, i_{ds} + X_M\,(i_{ds} + i_{dr}) \tag{3.39}$$

$$\psi_{0s} = X_{ls}\, i_{0s} \tag{3.40}$$

$$\psi_{qr} = X_{lr}\, i_{qr} + X_M\,(i_{qs} + i_{qr}) \tag{3.41}$$

$$\psi_{dr} = X_{lr}\, i_{dr} + X_M\,(i_{ds} + i_{dr}) \tag{3.42}$$

$$\psi_{0r} = X_{lr}\, i_{0r} \tag{3.43}$$

if, $X_{ss} = X_{ls} + X_M$ and $X_{rr} = X_{lr} + X_M$

$$\begin{bmatrix}\psi_{qs}\\ \psi_{ds}\\ \psi_{0s}\\ \psi_{qr}\\ \psi_{dr}\\ \psi_{0r}\end{bmatrix} = \begin{bmatrix} X_{ss} & 0 & 0 & X_M & 0 & 0\\ 0 & X_{ss} & 0 & 0 & X_M & 0\\ 0 & 0 & X_{ls} & 0 & 0 & 0\\ X_M & 0 & 0 & X_{ss} & 0 & 0\\ 0 & X_M & 0 & 0 & X_{ss} & 0\\ 0 & 0 & 0 & 0 & 0 & X_{ss}\end{bmatrix} \begin{bmatrix} i_{qs}\\ i_{ds}\\ i_{0s}\\ i_{qr}\\ i_{dr}\\ i_{or}\end{bmatrix} \tag{3.44}$$

Equation (3.44) can be rewritten to observe magnetically decoupled variables which will be used in the latter section for doubly fed induction machine control. From the obtained equation (3.38)-(3.43), a symmetrical three phase induction machine can be represented by an equivalent circuit as in Figure 3-4

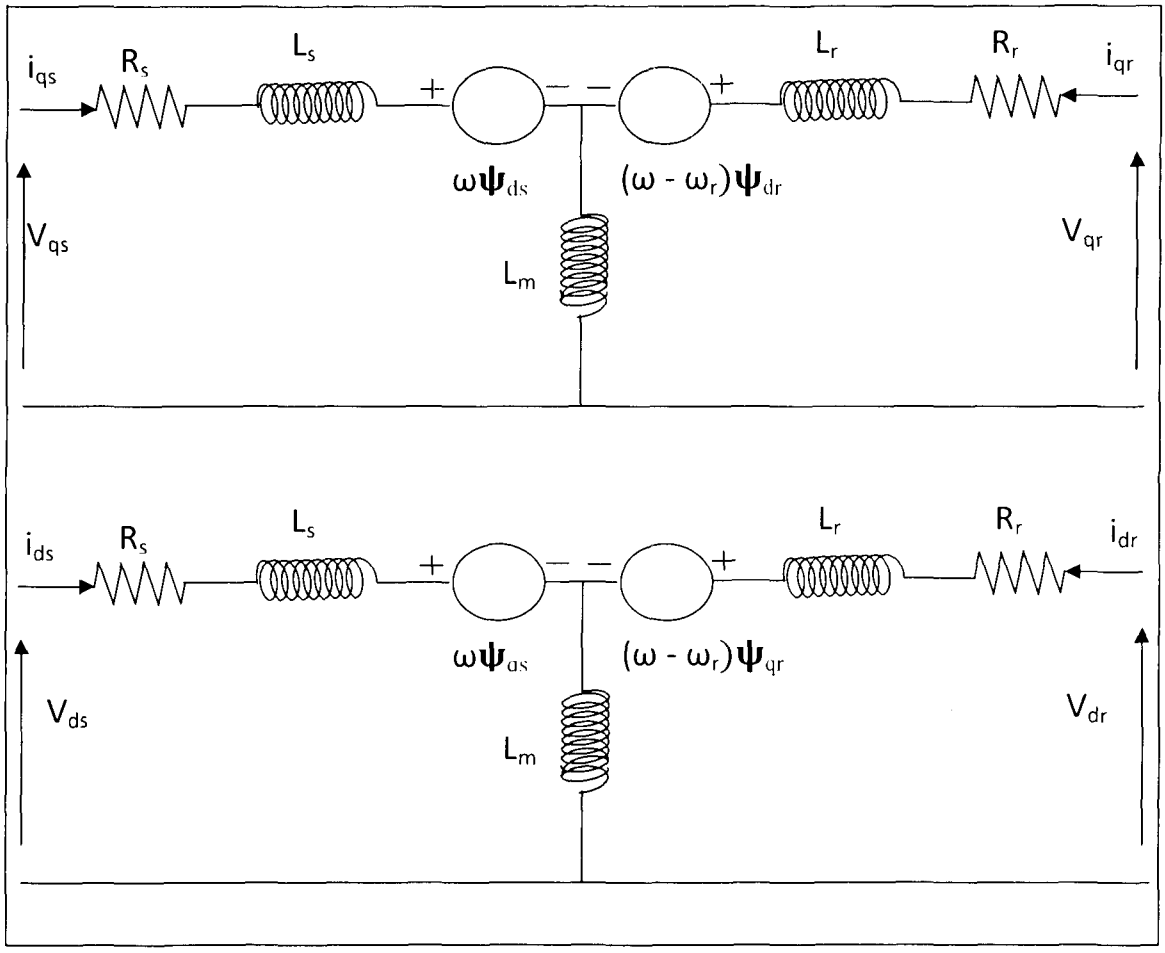

Figure 3-4: Equivalent Circuit of 3 Phase Symmetrical Induction Machine

The 0-axis has not been shown here as we are considering a symmetrical machine for which we have to deal with d and q axis components only.

Then form equations (3.32)-(3.44),

$$\begin{bmatrix} V_{qs} \\ V_{ds} \\ V_{0s} \\ V_{qr} \\ V_{dr} \\ V_{0r} \end{bmatrix} = \begin{bmatrix} r_s + \frac{p}{\omega_b} X_{ss} & \frac{\omega}{\omega_b} X_{ss} & 0 & \frac{p}{\omega_b} X_M & \frac{\omega}{\omega_b} X_M & 0 \\ -\frac{\omega}{\omega_b} X_{ss} & r_s + \frac{p}{\omega_b} X_{ss} & 0 & -\frac{\omega}{\omega_b} X_M & \frac{p}{\omega_b} X_M & 0 \\ 0 & 0 & r_s + \frac{p}{\omega_b} X_{ls} & 0 & 0 & 0 \\ \frac{p}{\omega_b} X_M & \frac{\omega-\omega_r}{\omega_b} X_M & 0 & r_r + \frac{p}{\omega_b} X_{rr} & \frac{\omega-\omega_r}{\omega_b} X_{rr} & 0 \\ -\frac{\omega-\omega_r}{\omega_b} X_M & \frac{p}{\omega_b} X_M & 0 & -\frac{\omega-\omega_r}{\omega_b} X_{rr} & r_r + \frac{p}{\omega_b} X_{rr} & 0 \\ 0 & 0 & 0 & 0 & 0 & r_s + \frac{p}{\omega_b} X_{lr} \end{bmatrix} \begin{bmatrix} i_{qs} \\ i_{ds} \\ i_{0s} \\ i_{qr} \\ i_{dr} \\ i_{0r} \end{bmatrix} \tag{3.45}$$

Assuming the angular speed of the reference frame $\omega = \omega_s$ i.e. the synchronously rotating reference frame; which is a good choice for induction machine [50]. Equation (3.37) can be written further in the state space form.

$$\dot{X} = AX + BU$$

where,

$$X = [i_{qs}\ i_{ds}\ i_{0s}\ i_{qr}\ i_{dr}\ i_{0r}]^T \tag{3.46}$$

$$B = \begin{bmatrix} \frac{X_{ss}}{\omega_b} & 0 & 0 & \frac{X_M}{\omega_b} & 0 & 0 \\ 0 & \frac{X_{ss}}{\omega_b} & 0 & 0 & \frac{X_M}{\omega_b} & 0 \\ 0 & 0 & \frac{X_{ls}}{\omega_b} & 0 & 0 & 0 \\ \frac{X_M}{\omega_b} & 0 & 0 & \frac{X_{rr}}{\omega_b} & 0 & 0 \\ 0 & \frac{X_M}{\omega_b} & 0 & 0 & \frac{X_{rr}}{\omega_b} & 0 \\ 0 & 0 & 0 & 0 & 0 & \frac{X_{lr}}{\omega_b} \end{bmatrix}^{-1} \tag{3.47}$$

$$A = B \begin{bmatrix} r_s & \frac{\omega}{\omega_b} X_{ss} & 0 & 0 & \frac{\omega}{\omega_b} X_M & 0 \\ \frac{\omega}{\omega_b} X_{ss} & r_s & 0 & \frac{\omega}{\omega_b} X_M & 0 & 0 \\ 0 & 0 & r_s & 0 & 0 & 0 \\ 0 & \frac{\omega-\omega_r}{\omega_b} X_M & 0 & r_r & \frac{\omega-\omega_r}{\omega_b} X_{rr} & 0 \\ \frac{\omega-\omega_r}{\omega_b} X_M & 0 & 0 & \frac{\omega-\omega_r}{\omega_b} X_{rr} & r_r & 0 \\ 0 & 0 & 0 & 0 & 0 & r_s \end{bmatrix} \tag{3.48}$$

Mechanical dynamics of the induction generator is defined by the swing equation:-

$$T_e - T_m = 2H \frac{d\omega_r}{dt} \tag{3.49}$$

T_e is the electromagnetic torque; T_m is the mechanical torque and H the inertia.

The instantaneous power input to the stator is

$$P_s = v_a i_a + v_b i_b + v_c i_c \tag{3.50}$$

Transformation of the variables to dq0 axes we get

$$P_s = \frac{3}{2}(V_{qs}\, i_{qs} + V_{ds}\, i_{ds}) \tag{3.51}$$

$$\text{And } Q_s = \frac{3}{2}(V_{qs}\, i_{ds} - V_{ds}\, i_{qs}) \tag{3.52}$$

$$\text{Similarly} \qquad P_r = \frac{3}{2}(V_{qr}\, i_{qr} + V_{dr}\, i_{dr}) \tag{3.53}$$

Electromagnetic torque for a machine is the division of power associated with the speed voltages by the shaft speed in mechanical radians per second [50]. The speed voltage terms associated with V_{qs} and V_{ds} are $\psi_{qs}\,\omega_s$ and $-\psi_{ds}\omega_s$. The shaft speed for this case is $-\omega_s$. Thus, the electromagnetic torque is

$$T_e = \frac{3}{2}(\psi_{qs}\, i_{ds} - \psi_{ds}\, i_{qs}) \tag{3.54}$$

Equations (3.38)-(3.43) and equation (3.46) describes a full order model of an induction machine with five states. Reduced order models as third order model that ignores the stator dynamics and first order that ignores the stator and rotor dynamics both are also found in some literature too. However, a full order model includes high bandwidth dynamics and we can use it to design current controllers as well analyze its impact on inertial response [51]. Thus full order model for the induction machine is implemented in this research.

3.5. Control of Doubly Fed Induction Generator

The control structure of a doubly fed induction generator is aimed to reliably transfer power and support the power systems network. The control system may operate to control aerodynamic power, speed, active and reactive power. Control of power plays an important role in damping oscillations; hence, only output power control of doubly fed induction generator has been discussed here.

Vector control concept using PI controllers is widely used to control a doubly fed machine. It enables us to achieve independent control of active and reactive power [52 - 55]. To facilitate the procedure the d-q axes reference frame synchronized with the stator voltage frame is chosen. Then the q axis is oriented along the stator voltage. Considering the voltage drop across the stator resistance to be negligible compared to the drop across the mutual and leakage inductance; from equation (3.7) we get,

$$V_{abcs} \approx \frac{d\psi_{abcs}}{dt} \approx j\,\omega_s\,\psi_{abcs} \tag{3.55}$$

i.e. the stator flux always lags the voltage by 90°. From equation (3.47) we also can say that the reference frame orientation to stator voltage implies orientation to stator flux as well.

Thus, when $V_{qs} = |V|$ then $V_{ds} = 0$ and $\psi_{qs} = 0$ $\psi_{ds} = \psi$ (3.56)

Then putting equation (3.48) in equation (3.43), (3.44) and (3.36) we get

$$P_s = \frac{3}{2} V_{qs}\, i_{qs} \tag{3.57}$$

$$Q_s = \frac{3}{2} V_{qs}\, i_{ds} \tag{3.58}$$

$$0 = X_{ss}\, i_{qs} + X_M\, i_{qr} \tag{3.59}$$

$$\psi = X_{ss}\, i_{ds} + X_M\, i_{dr} \tag{3.60}$$

Or, $i_{qs} = - — i_{qr}$ and $i_{ds} = — (\quad - X_M i_{dr})$ (3.61)

Then, $P_s = - - * |V| * — i_{qr}$ (3.62)

And $Q_s = - — \quad - - * |V| * — i_{dr}$ (3.63)

Hence, Active power at the stator of a doubly fed induction generator is determined by the rotor q-axis current where as the reactive power is controlled by rotor d-axis current. Thus controlling the rotor current we can control the active and reactive power of a doubly fed induction generator independently. Further, the rotor currents are controlled by rotor voltages.

Two cascaded PI controllers regulate the stator side active and reactive power for a simple control of doubly fed induction generator, as shown in Figure 3-5.

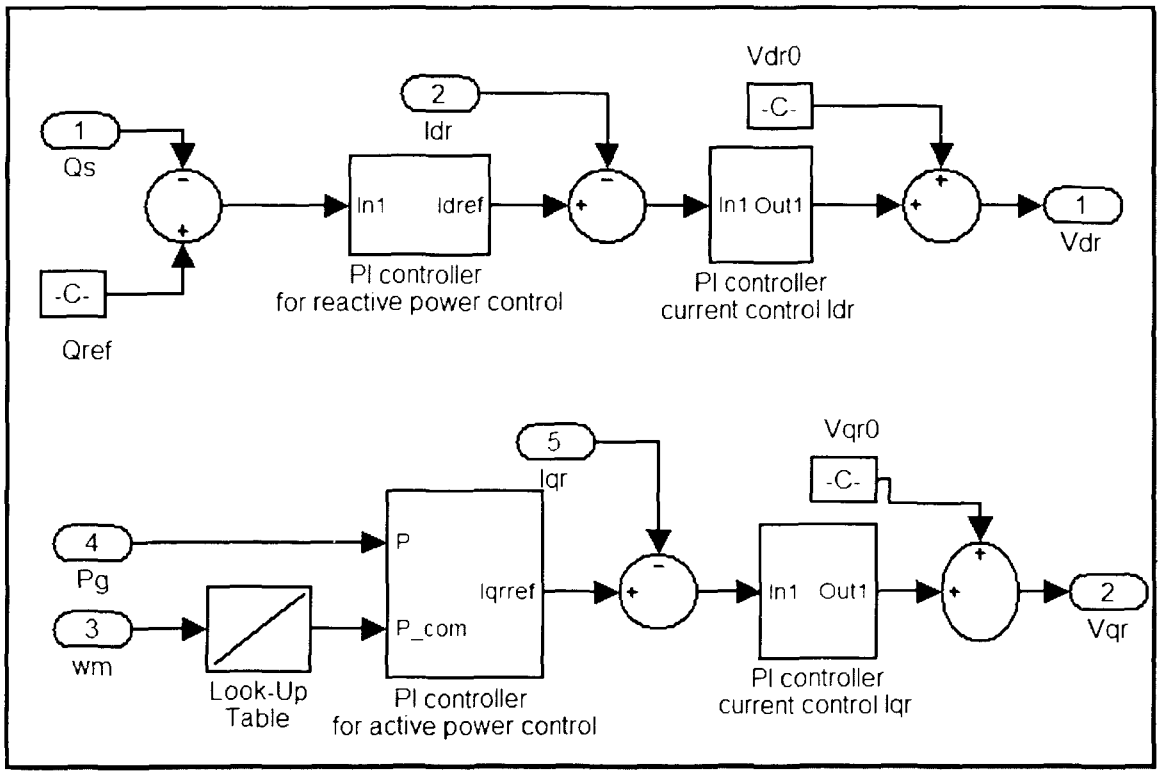

Figure 3-5: Simple Control Block Diagram for Active and Reactive Power Control

Cascaded PI controller scheme requires speed of response to increase as we move inwards. Thus, the inner control loop controlling the current is fast compared to the outer control loop controlling active and reactive power. Tuning of the controllers can be done using root locus method described in the latter parts.

The importance of consideration of detailed reactive power control loop in stability studies is stated in [35]. A detailed control loop designed to control active and reactive power described in [48] is implemented. The control design concept utilizes coordinate control method as shown in Figure 3-6 and Figure 3-7.

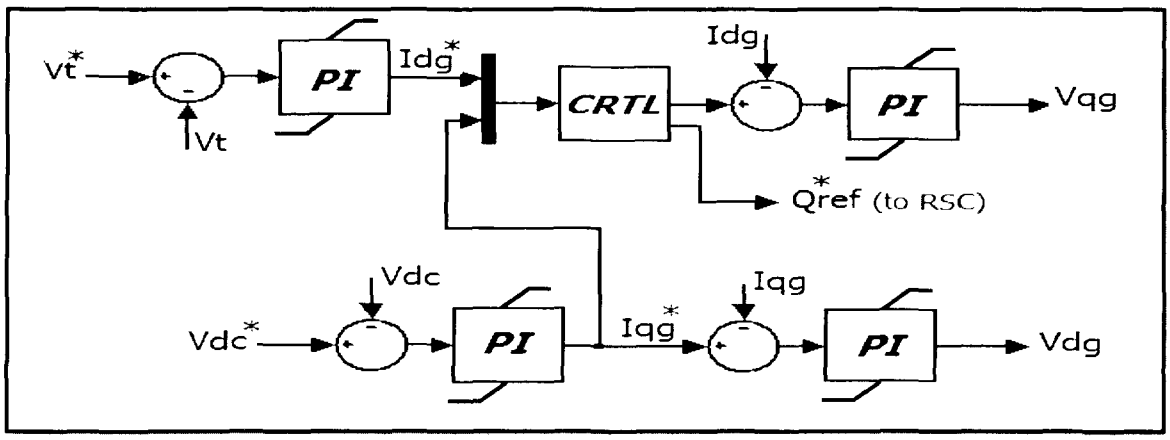

Figure 3-6: GSC Controller Block Diagram [48]

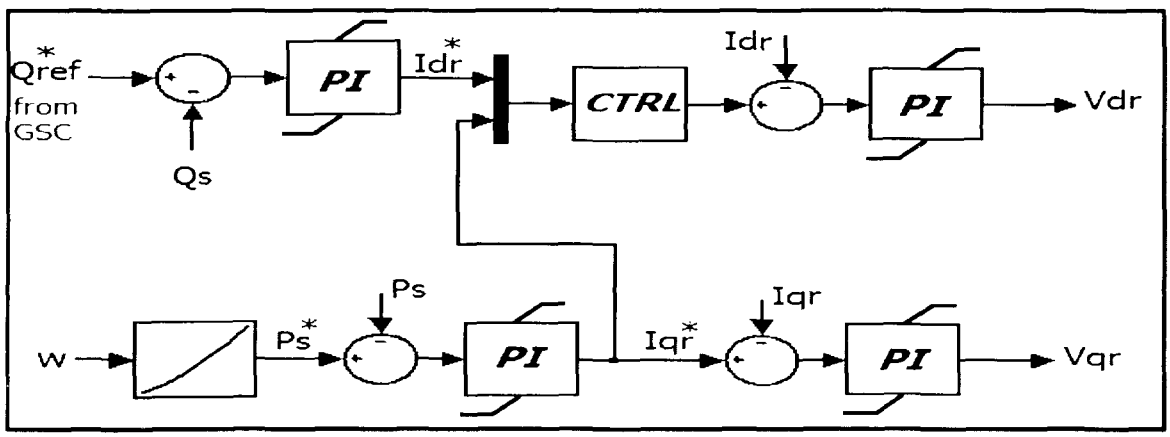

Figure 3-7: RSC Controller Block Diagram [48]

Now to damp oscillations we utilize a damping control strategy. The rotor angle difference provides a good observability of interarea oscillation mode between two areas [56]. A control signal proportional to the rotor angle deviations is added to the power references to track the deviation and make them vanish from the system [31]. Control block diagrams considered are shown in Figure 3-8, Figure 3-9 and Figure 3-10.

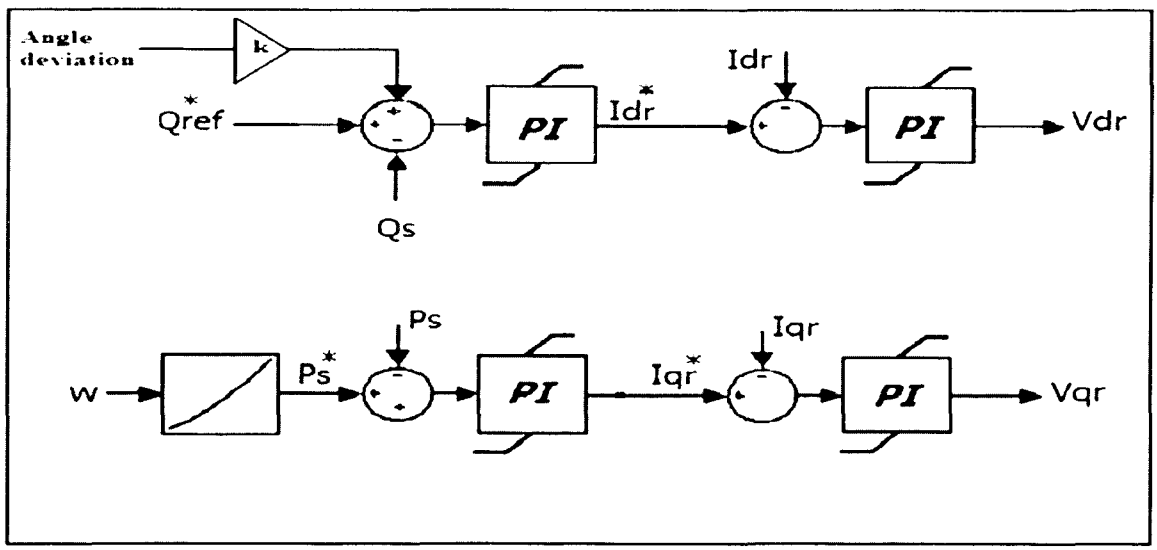

Figure 3-8: Control Block Diagram with Reactive Power Modulation

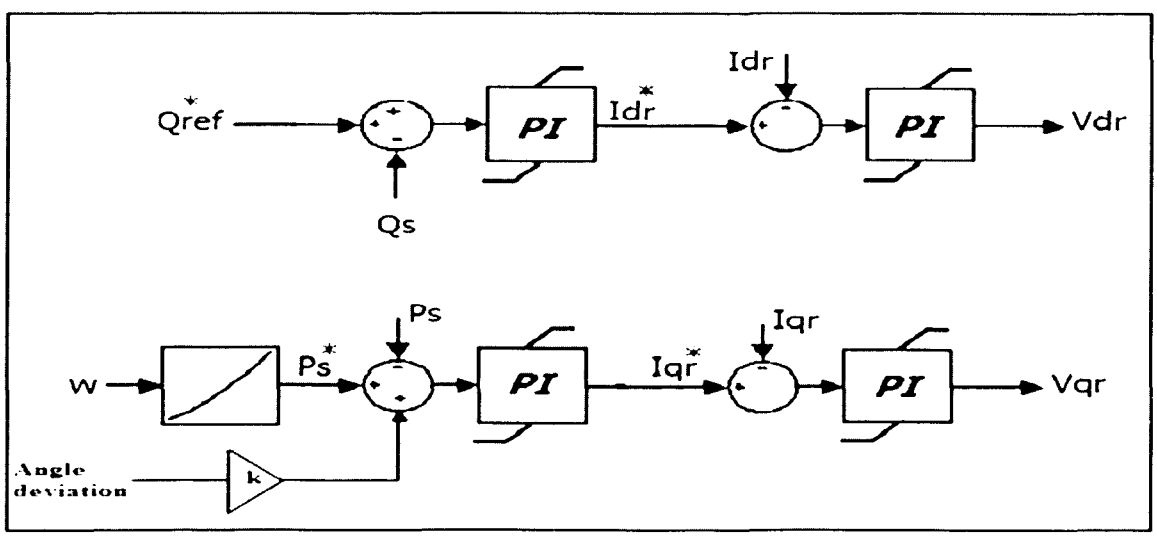

Figure 3-9: Control Block Diagram with Active Power Modulation

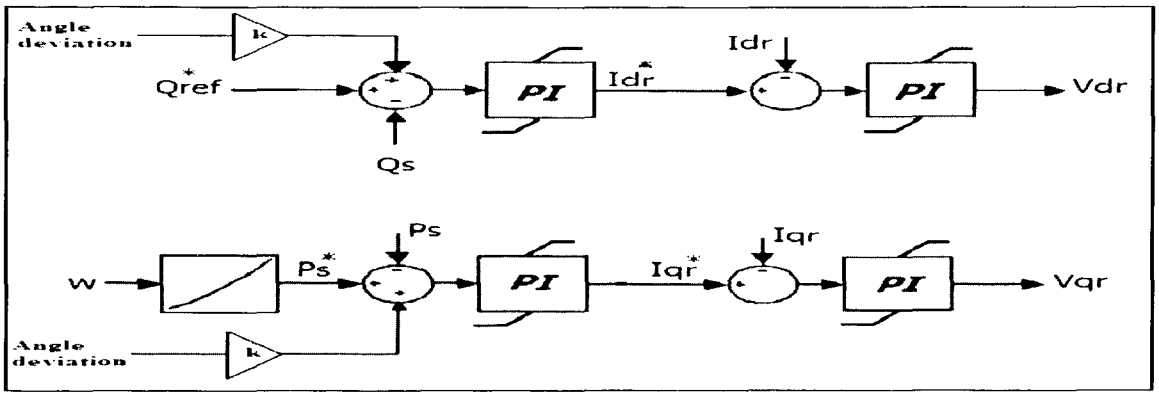

Figure 3-10: Control Block Diagram with Reactive and Active Power Modulation

Adjustments of gains can be done using the root locus plots. Root locus is used basically in control system design. It can be used to determine the value of a closed loop gain, to limit the system in stable region of operation. From the root locus plot we can know the response of the system to deviations from a set point. A very high gain generally results in an unstable system and the instability can be observed using root locus plots. For an unstable system the dominant branches of root locus plot are on the right hand side of the plane. To make the system stable the dominant branches of the root locus plot should be moved to the left side. It can be done by adjustments of the gain or by addition of an additional controller to the open loop transfer function to reshape the root loci. Further practical limits impose the gain to be less such the system to result proper output signals.

3.6. Synchronous Generator Modeling

The study of the impact of a wind farm connected to a network system requires synchronous generator models too. For the study a full order model described in [5, 42] is used which is not discussed in detail here because of its wide availability in various literature. The synchronous generator is simulated using matrix/vector control concept as

the doubly fed induction generator as described in the doubly fed induction generator modeling section.

The synchronous generator model used consists of the following electrical and mechanical equations:-

$$V_{qs}^{r} = -r_s i_{qs}^{r} + \frac{\omega_r}{\omega_b}\psi_{ds}^{r} + \frac{p}{\omega_b}\psi_{qs}^{r} \quad (3.64)$$

$$V_{ds}^{r} = -r_s i_{ds}^{r} - \frac{\omega_r}{\omega_b}\psi_{qs}^{r} + \frac{p}{\omega_b}\psi_{ds}^{r} \quad (3.65)$$

$$V_{fd}^{r'} = r_{fd}' i_{fd}^{r'} + \frac{p}{\omega_b}\psi_{fd}^{r'} \quad (3.66)$$

$$V_{kd}^{r'} = r_{kd}' i_{kd}^{r'} + \frac{p}{\omega_b}\psi_{kd}^{r'} \quad (3.67)$$

$$V_{kq1}^{r'} = r_{kq1}' i_{kq1}^{r'} + \frac{p}{\omega_b}\psi_{kq1}^{r'} \quad (3.68)$$

$$V_{kq2}^{r'} = r_{kq2}' i_{kq2}^{r'} + \frac{p}{\omega_b}\psi_{kq2}^{r'} \quad (3.69)$$

And $\frac{p}{\omega_b}\omega_r = -\frac{1}{2H}(T_e - T_m)$ and $p\theta_r = \omega_r$ (3.70)

In the equations: - d, q, r, s, f, k and ψ refer to d axis, q axis, rotor, stator, field damper winding and flux linkage quantities respectively.

3.7. Power System Network Modeling

A network is modeled treating it as admittance "Y" matrix and relating it to voltage and current [57]. The current in the network is obtained as the product of admittance matrix and voltage.

i.e. $I = Y*V$ (3.71)

Then, the voltage can be obtained using the following equation treating generators as current sources. Further all components should be represented on the same reference frame.

$V = Y^{-1}* I$ (3.72)

Figure 3-11 shows the two areas five machine one line diagram of the power systems network derived from the two areas four machine system used to study interarea oscillation modes in [30].

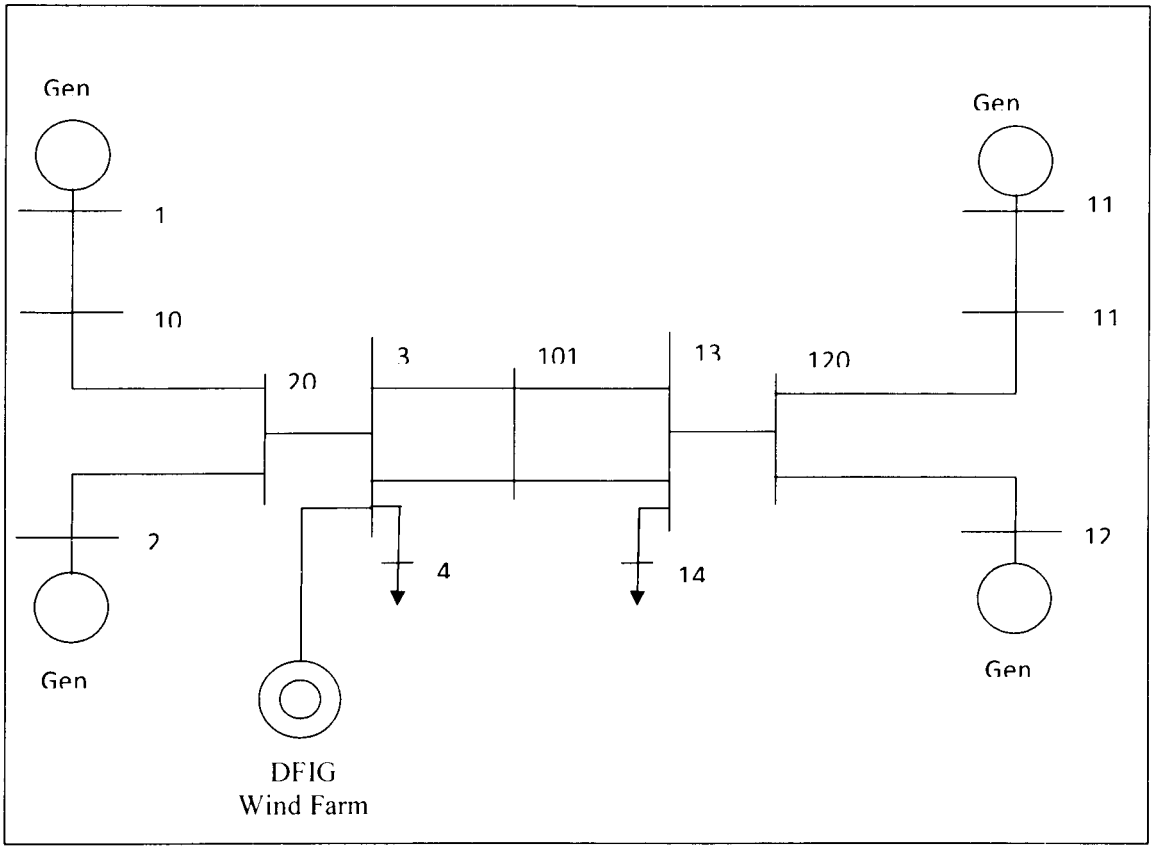

Figure 3-11: Two Area Five Machine Test System

The model is modified by addition of variable speed wind turbines equipped with doubly fed induction generator connected to bus three. Here generators 1, 2, 3 and 4 are synchronous generators without stabilizers.

3.8. Network Structure for Simulation

The network includes full order models of synchronous generators, doubly fed induction generator and network connections. A complete model is developed in Simulink

using graphically assembled blocks and sub systems defined by codes in Matlab. A basic block diagram for the power systems network in Simulink is demonstrated in Figure 3-12.

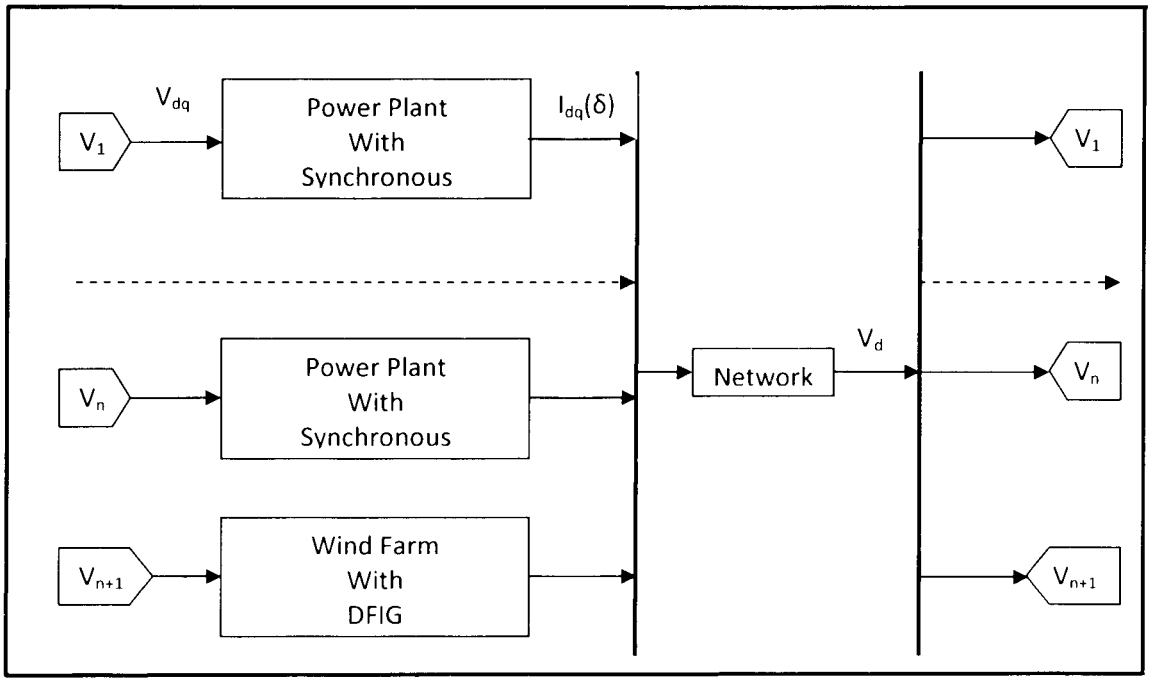

Figure 3-12: Basic Block Diagram of the Power System Network for Simulation

The block diagram shows the basic blocks of the power system network to be modeled in Simulink. It shows an input of voltage in d-q axis obtained from the transformation of measured a-b-c voltages to the generating units. The generation units are modeled as current sources to the interconnecting network system. Among the generation units the last machine is the wind farm equipped with doubly fed induction generator. Voltage from the network is fed back to the generation units to complete the modeling of the total system.

3.9. Summary

A complete model for the stability study is discussed in this chapter. Full order models of machine and model of interconnecting grid can be developed following the theoretical modeling concept discussed in this chapter. Mechanical and electrical equations

representing the dynamics of the machines in the power systems network are utilized for their modeling. Constant wind speed for a small study time period is reasonably used for the study. State space representation of the dynamic and mechanical equations simplifies modeling technique. Independent control of active and reactive power at the output of doubly fed induction generator is achieved. Further detail control loops are designed for wind generation control. Rotor angle deviation is then fed to modulate power generation, interfaced with properly tuned gain blocks to damp interarea oscillation. Simulink models so developed are included in the appendix at the end of the thesis.

CHAPTER 4. SMALL SIGNAL STABILITY STUDIES

4.1. Overview

Stability and low frequency oscillation behavior of power system has been already discussed in previous chapters. This chapter presents an overview on the procedure for small signal stability studies. Linearization, modes, root locus and impact of gain constant introduced in the damping control action is discussed. It gives the basis and method for analysis.

4.2. Small Signal Stability Analysis

Small signal stability of a system is evaluated by computing eigenvalues of the dynamic equations around steady state operating point. For eigenvalue analysis first the differential equations of the dynamic system are written. Then non linear differential equations are linearized at an equilibrium point. Further the state space matrix is generated to obtain the eigenvalues. Eigenvalues provide us the time domain response of the system to small perturbations. Time domain response of a system provides us valuable information to study stability of a system.

4.3. Linearization

Small signal stability assessment is based on linearized analysis of multi machine power system [50]. Linearization of non linear power system is carried out by approximation of differential algebraic equations by the first term of Taylor series expansion of the system at an equilibrium point. Thus, for power systems network which is not explicit of time function can be represented by differential algebraic equations as follows:-

$\dot{x}_i = f_i (x_1, x_2, \text{---------- } x_n; u_1, u_2, \text{---------- } u_m)$; i=1, 2, 3----------n; where '$\dot{x}$' is the derivative of the state variables with respect to time, 'n' is the order of the system and 'm' the no of inputs.

Or, $\dot{x} = f(x, u)$ (4.1)

where state vector $x = \begin{bmatrix} x1 \\ \vdots \\ xn \end{bmatrix}$, input vector $u = \begin{bmatrix} u1 \\ \vdots \\ un \end{bmatrix}$, and $f = \begin{bmatrix} f1 \\ \vdots \\ fn \end{bmatrix}$

Now the output can be written as $y = g(x, u)$ (4.2)

(Say 'r' is the no of outputs)

Equation (4.1) and (4.2) is then represented in generalized form as

$\dot{x} = Ax + Bu$ and $y = Cx + Du$ (4.3)

where, 'A' is nxn state matrix, 'B' is nxm input matrix and 'C' is rxn output matrix and 'D' rxm feed forward matrix.

Linearization of the system around an operating point (x_0, u_0) gives us the linearized statespace system.

$\Delta\dot{x} = A\Delta x + B\Delta u$ and $\Delta y = C\Delta x + D\Delta u$ (4.4)

where, 'Δx'; is the n state vector increment

'Δy'; is the r output vector increment

'Δu'; is the m input vector increment

The state matrix 'A' provides eigenvalues which are used to analyze stability of the network system. As the framework for all the system development has been implemented in Matlab/Simulink, a linearized model of the network system in Matlab is obtained using the 'linmod' command at a steady state point.

4.4. Eigenvalue and Stability Analysis

Eigenvalues of matrix 'A' are the non-trivial solutions of the equation $A*\Phi = \lambda* \Phi$, ('λ' are the eigenvalues and 'Φ' nx1 matrix). Eigenvalues here is calculated using the 'eig' function in Matlab. The stability of the network system is analyzed using the eigenvalues. A system is stable if all the eigenvalues lie on the left hand side of the imaginary axis of a complex plane else is unstable. Real eigenvalue corresponds to non oscillatory mode. A positive real eigenvalue means the mode increases with time whereas a negative eigenvalue implies decreasing mode over time. Complex conjugate pair as ($\sigma \pm j\omega$) of eigenvalues corresponds to oscillatory mode. Positive 'σ' means an unstable oscillatory mode. Negative 'σ' corresponds to a stable oscillatory mode that decreases over time. Further, the oscillation frequency (Hz) and damping ratio for the corresponding eigenvalue is calculated as.

Frequency (f) = $\omega/2\pi$ and Damping ratio (ζ) = $(-\sigma)/\sqrt{(\sigma^2+\omega^2)}$ (4.5)

From a single input single output system for modulation of power root locus plots can be obtained to study stability of the system. 'Rlocus' another function in matlab plots the root locus for the open loop transfer function of the linearized model. The operating point in the locus plot can be located to observe the stability of the system at this particular operation point. Root locus plot for an open loop system with gain 'k', applied is shown in Figure 4-1. The plot shows the operating points lying on the left hand side of the imaginary axis. This means that the system remains stable even after the application of damping control loop. Thus, the system is in a stable condition before and after the application of damping control. Gains 'k' for the control action should be defined or be available such that its application on the system should not force it to the unstable region.

Figure of open loop system

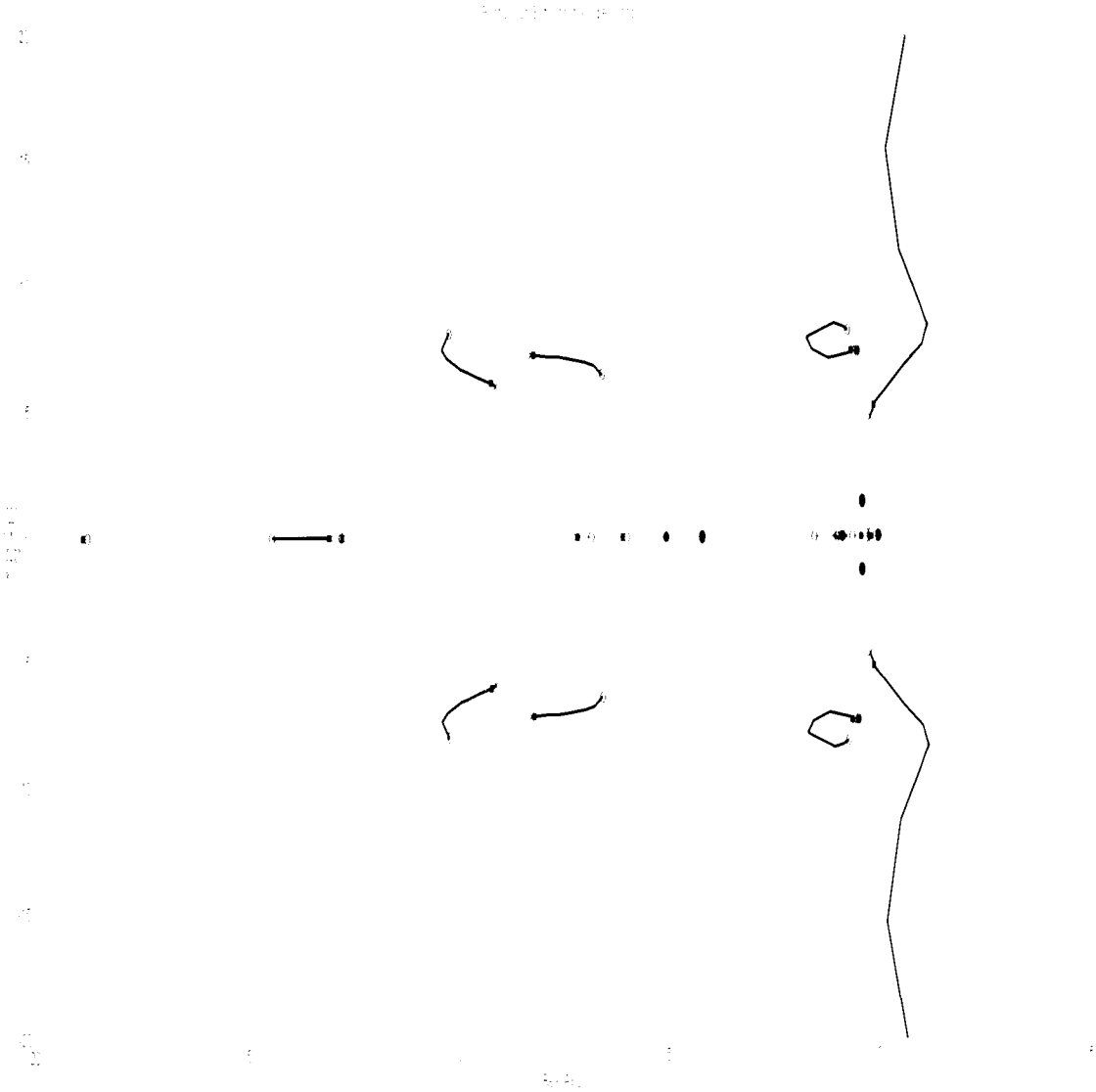

Figure 4-1: Root Locus Plot with Gain 'k' Applied to the Open Loop System

4.4. Summary

In this chapter small signal stability and eigenvalue analysis was presented. 'Linmod' and 'eig' functions in Matlab provide us the state matrix and eigenvalues. Complex eigenvalues present for the system shows oscillatory modes for the power

systems network. Positive real value in the complex eigenvalue indicates the oscillation increases over time whereas negative real value indicates the oscillation is suppressed over time, and hence, it represents a stable system.

CHAPTER 5. RESULTS AND DISCUSSION

5.1. Overview

In this chapter tabulation of eigenvalues, frequency and damping ratio for interarea mode with various case studies is presented. Case studies include test bench case with various power transfers in the tie line with synchronous generators only. Then, DFIG was added in the system to observe its impact on interarea oscillation. Further improved system was analyzed to observe the effectiveness of the proposed damping control loop.

5.2. Analysis of Base Case

Power transfer with only synchronous generators in the system: - Here, the study case system consists of four synchronous generators only to support the power flow. The results are summarized in Table 5-1.

Table 5-1: Modal Analysis of the System with Only Synchronous Generators in the Network

Power Transfer (MW)	Eigenvalue	Frequency (Hz)	Damping ratio
400	-0.0830±j4.6187	0.7351	0.018
450	-0.0678±j4.5469	0.7237	0.015
500	-0.0534±j4.4538	0.7088	0.012
550	-0.0411±j4.3252	0.6884	0.009
600	-0.0331±j4.1252	0.6565	0.008

5.3. Analysis with Simple DFIG

Power transfer with wind generator equipped with DFIG in area one picking increased load on area two is the next case considered. Simultaneously generation of synchronous generator two is reduced to match the addition by wind generation. 400MW transfer flow in the tie line is without any wind generation and is considered as the base

case. Further the load is increased in steps of 50MW and is supplied by the DFIG unit. The results for this case are summarized in Table 5-2.

Table 5-2: Modal Analysis of the System with Simple DFIG Added to the Network

Power Transfer (MW)	Eigenvalue	Frequency (Hz)	Damping ratio
400	-0.0830±j4.6187	0.7351	0.0180
450	-0.1957±j4.680	0.7450	0.0418
500	-0.2006±j4.628	0.7366	0.0433
550	-0.2088±j4.5688	0.7272	0.0456
600	-0.2204±j4.4962	0.7156	0.0490

The worst case with respect to damping is with the least wind power connected to the network i.e. 450MW of transfer of power in tie line. DFIG with var control is added to the system in the next case. Results for the case study are summarized in Table 5-3.

Table 5-3: Modal Analysis of the System with Coordinate Controlled DFIG Added to the Network

Power Transfer (MW)	Eigenvalue	Frequency (Hz)	Damping ratio
450	-0.1957±j4.6809	0.7450	0.0418

With similar GSC scheme except that the simple DFIG was entirely operated at unity power factor whereas the var controlled DFIG supplies reactive power support during voltage sag at the terminal. Both the structure provide similar damping ratio during steady state case.

5.4. Analysis with Damping Control

To improve damping now the reactive power is modulated such that the reactive power at the stator of DFIG is controlled in such a way to resist power oscillation in the tie line after fault clearance. For that the deviation of the rotor angle is fed to increase or decrease the reference of reactive power. Results are summarized in Table 5-4.

Table 5-4: Modal Analysis of the System with Reactive Power Modulated DFIG Added to the Network

Power Transfer (MW)	Eigenvalue	Frequency (Hz)	Damping ratio
450	-0.4444±j5.2606	0.837	0.0842

Next, to improve damping active power is modulated such that the active power at the stator of DFIG is controlled in such a way to resist the power oscillation at the tie line after fault clearance. For that the deviation of the rotor angle is fed to increase or decrease the reference of active power at DFIG control. Results are summarized in Table 5-5.

Table 5-5: Modal Analysis of the System with Active Power Modulated DFIG Added to the Network

Power Transfer (MW)	Eigenvalue	Frequency (Hz)	Damping ratio
450	-0.3512±j4.1423	0.6593	0.0845

Further, to improve damping combined active and reactive power is modulated such that active and reactive power at the stator of DFIG is controlled in such a way to resist the power oscillation in the tie line after fault clearance. For that the deviation of the rotor angle is fed to increase or decrease the reference of active and reactive power at DFIG control. Results are summarized in Table 5-6.

Table 5-6: Modal Analysis of the System with Active and Reactive Power Modulated DFIG Added to the Network

Power Transfer (MW)	Eigenvalue	Frequency (Hz)	Damping ratio
450	-0.5556±j4.7128	0.7501	0.1171

From the eigenvalue study we can conclude that replacement of synchronous generation by wind generation is beneficial to interarea oscillation damping. Active,

reactive and combined active and reactive power modulation techniques are effective methods to increase damping in the network system. Combined active and reactive power modulation technique is much more effective compared to individual cases of active and reactive power modulation.

5.5. Time Domain Simulation Results

Here we discuss the time domain simulation results to support the proposed technique on damping interarea oscillations in doubly fed induction generator connected power system network.

The system is operated under steady state for a certain time period and then a three phase fault occurs at 0.1 second and is cleared at 0.2 seconds. The fault initiates oscillations in the system. The worst case in terms of damping for the system with DFIG in the network is with minimum wind generation. Thus the simulation is carried out with 50MW of wind power or 450MW of transfer in the tie line as suggested by the eigenvalue study. Time domain simulations for system without DFIG, with no var controlled DFIG, with var controlled DFIG, and with damping controlled DFIG as active, reactive and combined active and reactive power modulated system in the network are plotted in latter section. The plots are shown in Figure 5-1 to Figure 5-44. The plots depict oscillation in rotor angle, tie line power, synchronous generator speed and voltage profile at the faulty bus. With application of damping control, the plots clearly depict the implication of the control design. The oscillations are suppressed faster with applying the damping control compared to the case study without any damping control. Figure 5-45 compares the damping control design for the worst case i.e. maximum power transfer with minimum wind power grid integration, without and with damping control applied.

Here the simulation is conducted without any wind power connected to the system i.e. the study case involves four synchronous generators without power system stabilizers in the power system. The power transfer between the two areas in the system considered is 450MW. The simulations show initiation of oscillations with a fault at a bus at 0.1 second which is cleared at 0.2 second. The oscillation is observed in the rotor angle deviation of the machines at two areas, power transfer in tie line and speed of synchronous generators. The oscillation gradually decreases after the fault was cleared. Without any control to damp the oscillation it takes longer time to die out, which might as well increase in negative damping cases. Further, oscillation was observed in the faulty bus voltage profile too.

5.5.2. Simulation Results with DFIG without VAR Control in the Network

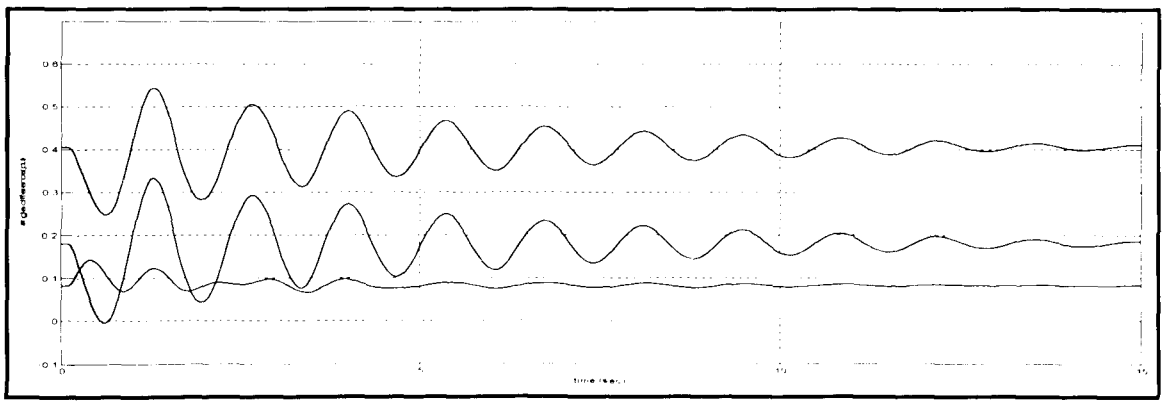

Figure 5-5: Rotor Angle Difference δ_{21}, δ_{31}, δ_{41}

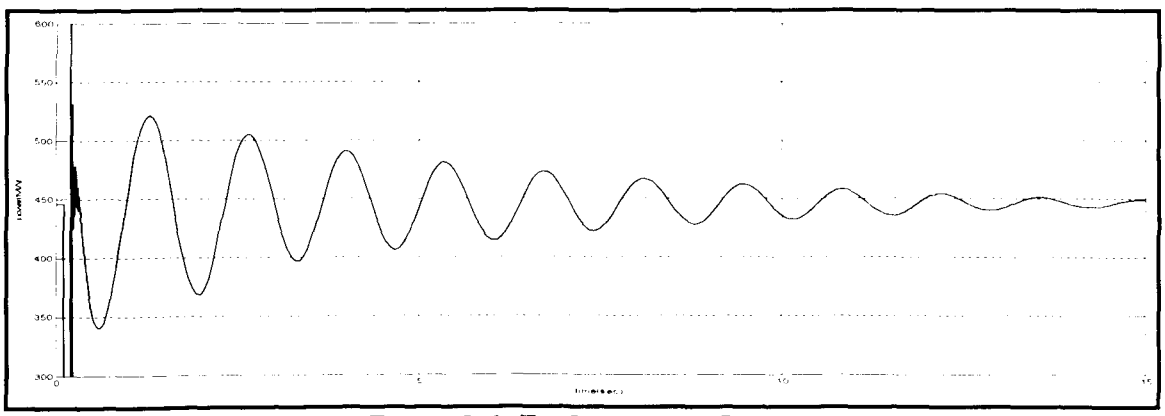

Figure 5-6: Tie Line Active Power

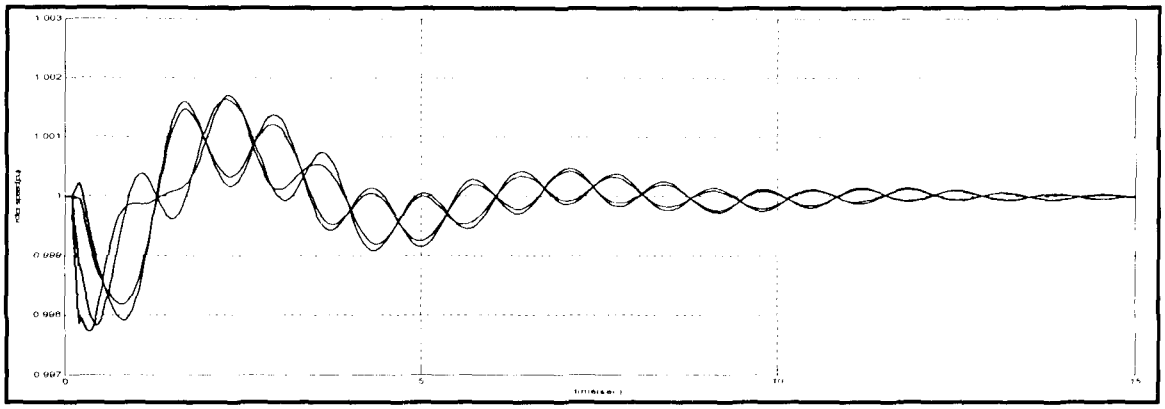

Figure 5-7: Rotor Speed of Synchronous Generators

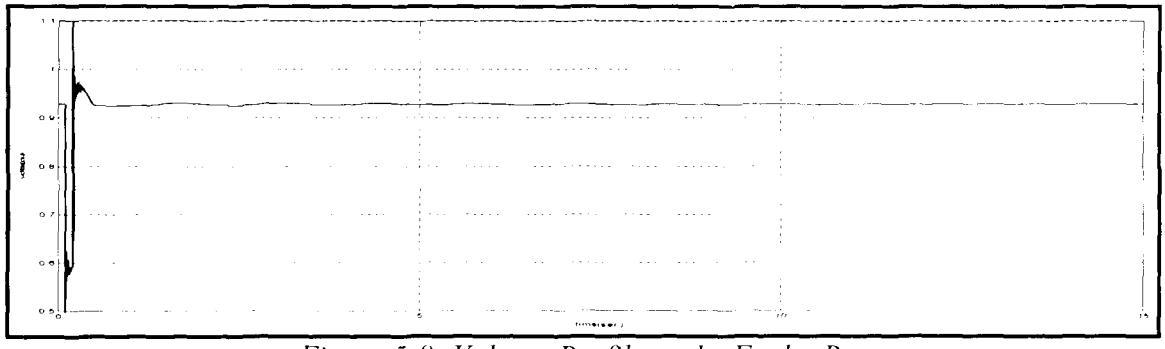

Figure 5-8: Voltage Profile at the Faulty Bus

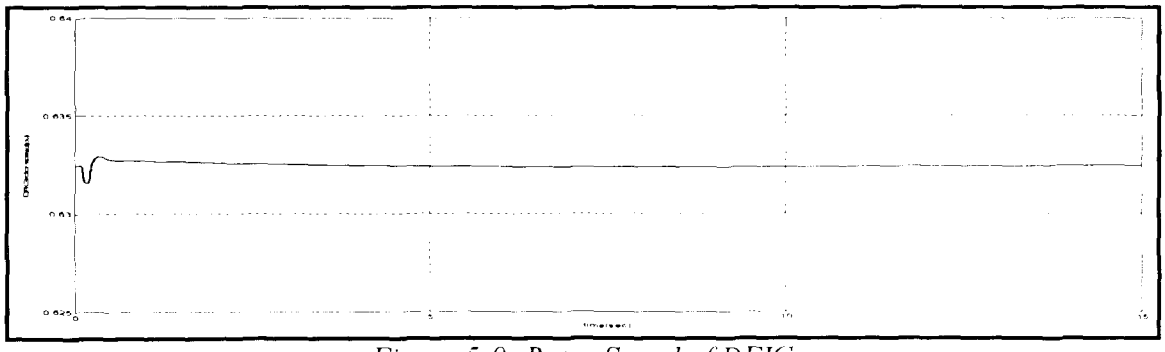

Figure 5-9: Rotor Speed of DFIG

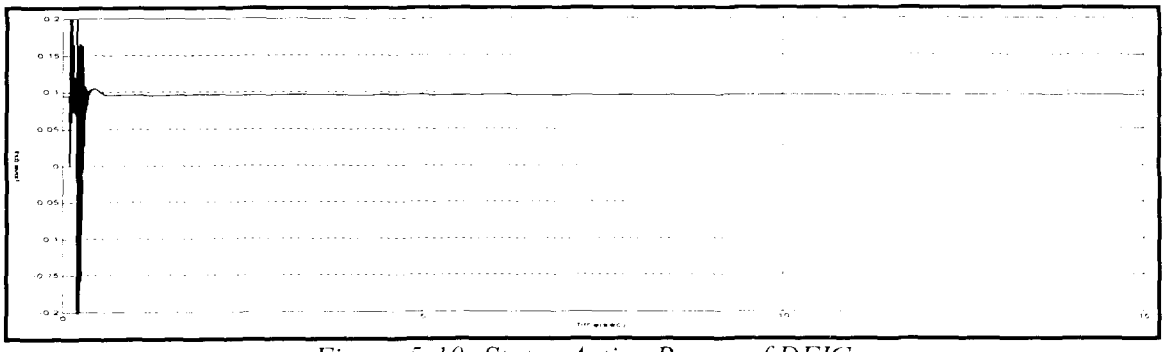

Figure 5-10: Stator Active Power of DFIG

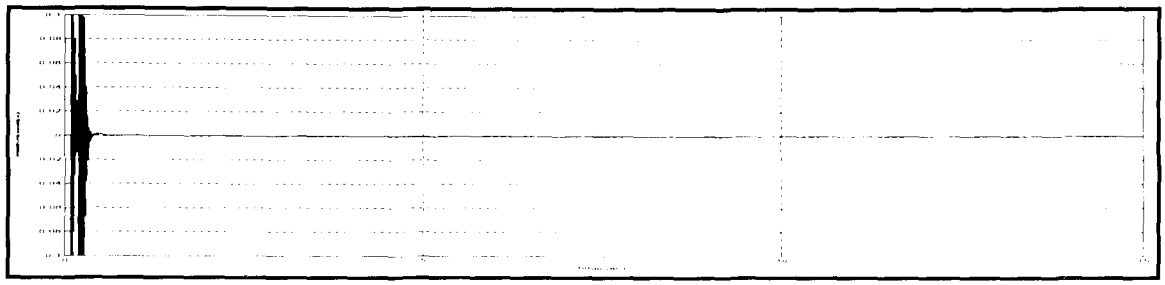

Figure 5-11: Stator Reactive Power of DFIG

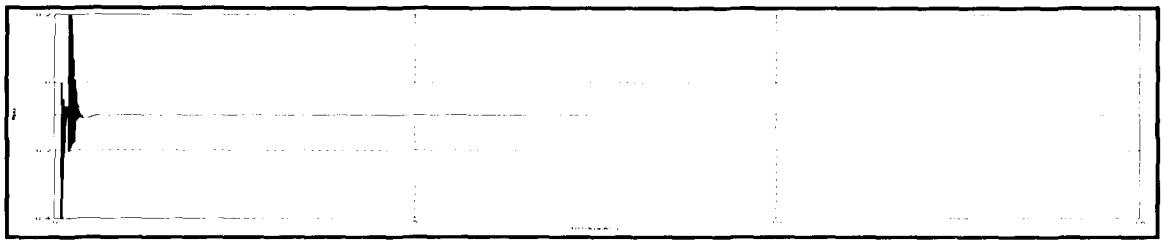

Figure 5-12: Electromagnetic Torque (Te) of DFIG

The simulations were conducted with the addition of wind power generation to the base system with four synchronous generators. 50MW of wind generation equipped with DFIG is added to pick up the load where as the power rating at synchronous generator two in area one is decreased by the same amount. DFIG considered for this case bears active power control, whereas the reactive power generation is considered zero for our case. During this operation simulation results show an increment in damping compared to the earlier case. Observation show decrease in oscillation in the rotor angle deviation, tie line transfer power and rotor speed of synchronous generators.

5.5.3. Simulation Results with DFIG with VAR Control in the Network

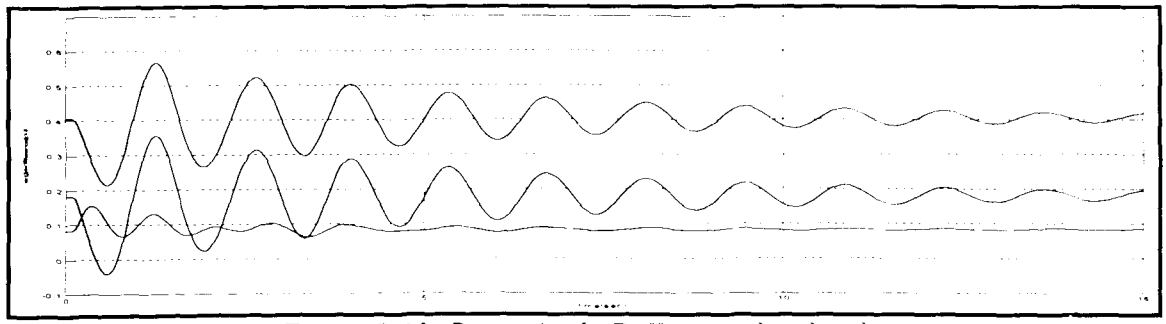

Figure 5-13: Rotor Angle Difference δ_{21}, δ_{31}, δ_{41}

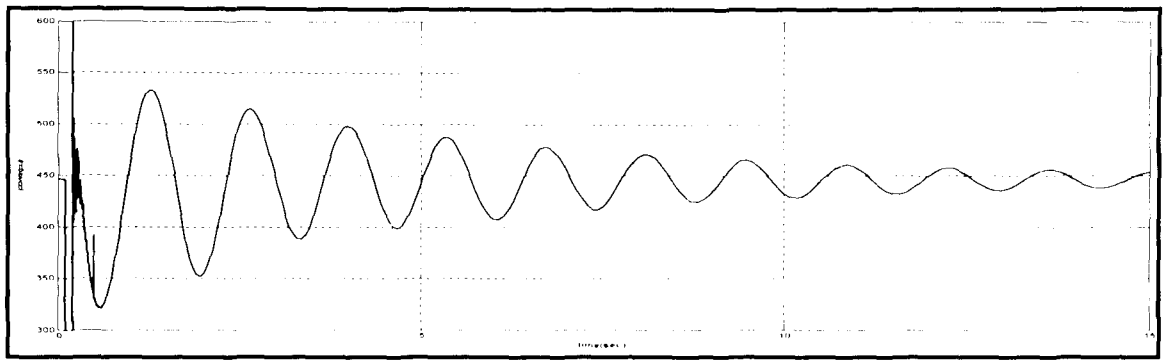

Figure 5-14: Tie Line Active Power

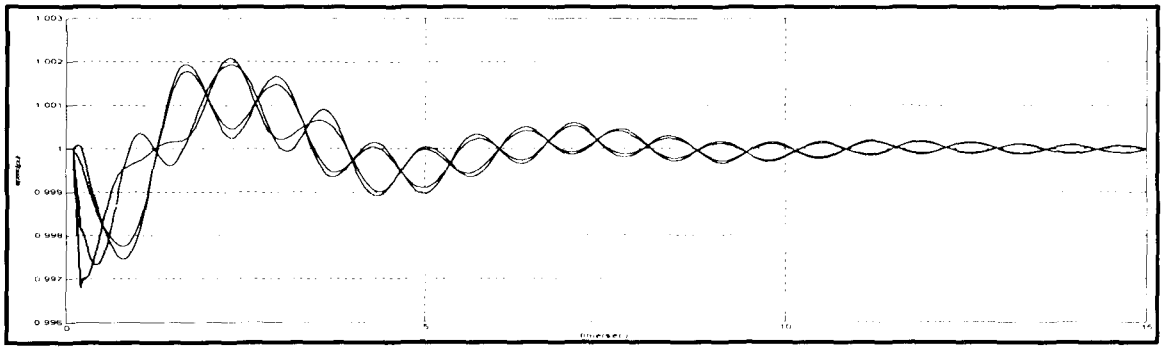

Figure 5-15: Rotor Speed of Synchronous Generators

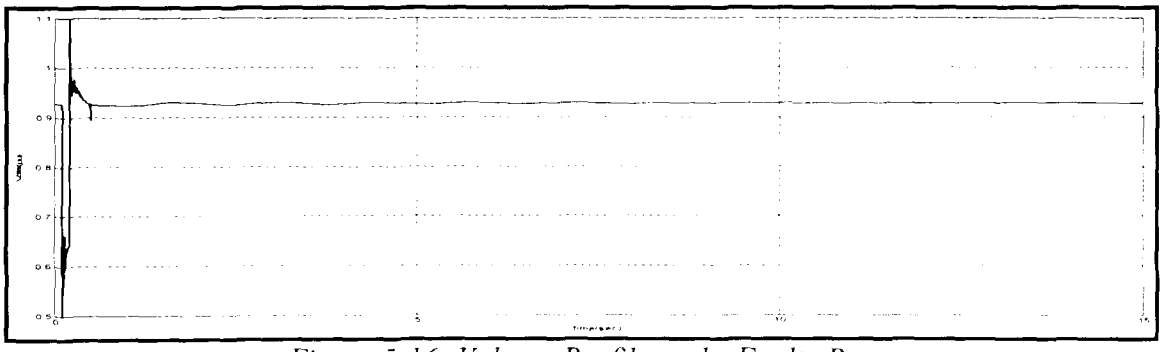

Figure 5-16: Voltage Profile at the Faulty Bus

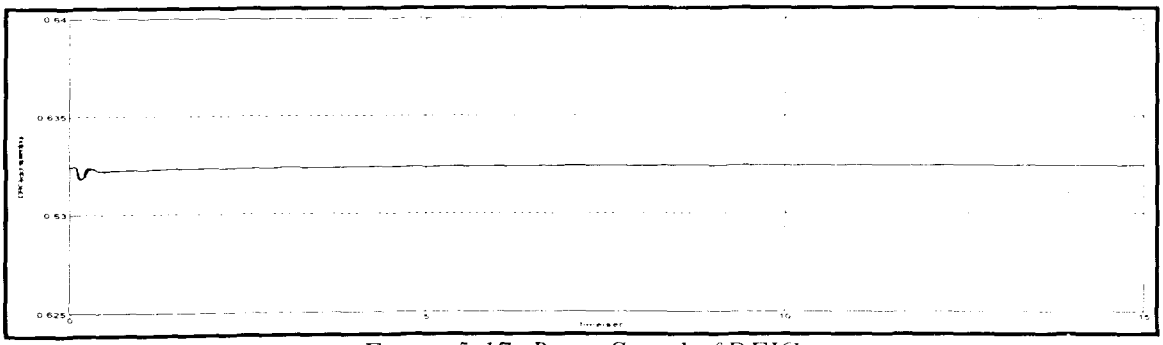

Figure 5-17: Rotor Speed of DFIG

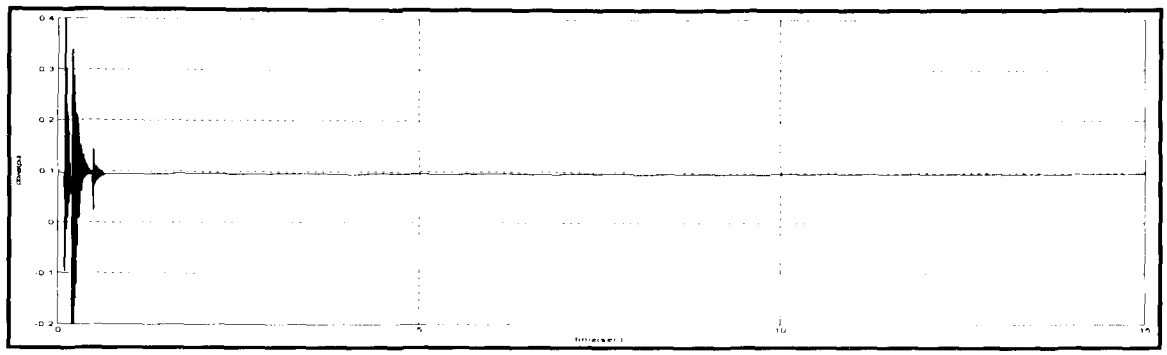

Figure 5-18: Stator Active Power of DFIG

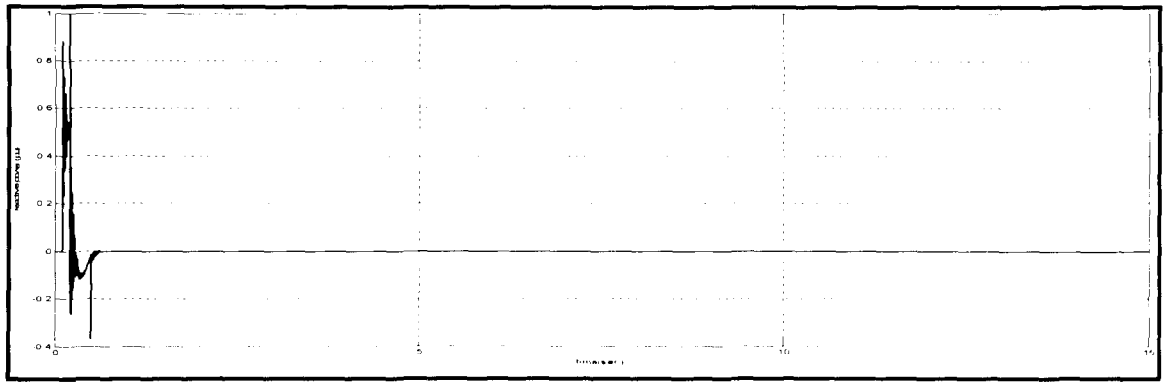

Figure 5-19: Stator Reactive Power of DFIG

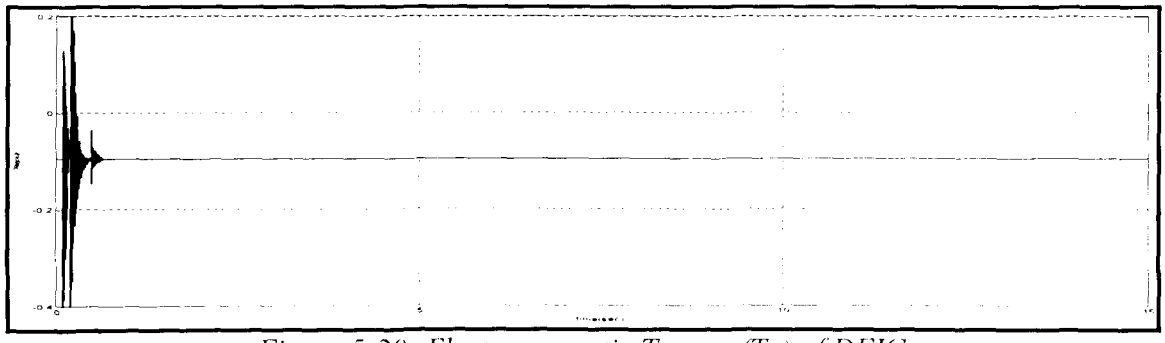

Figure 5-20: Electromagnetic Torque (Te) of DFIG

Coordinate control system was applied to control reactive power support by the doubly fed induction generator during voltage sag at the terminal of the generator. The reactive power capability of the generator is assumed to be limited. The oscillations in the rotor angle deviation, tie line power and rotor speed of synchronous generator increase. Doubly fed induction generator with var control capability tends to decrease the small

signal stability of the system. However, with reactive power support, improvements in the voltage profile were observed.

5.5.4. Simulation Results with DFIG with Reactive Power Modulation

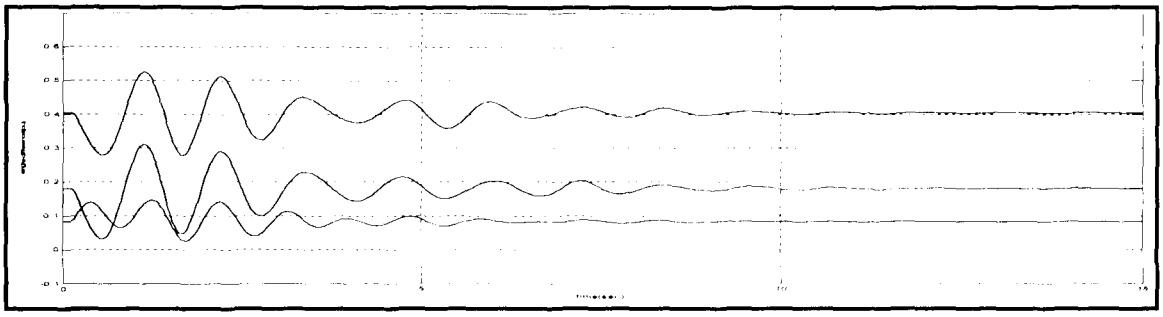

Figure 5-21: Rotor Angle Difference δ_{21}, δ_{31}, δ_{41}

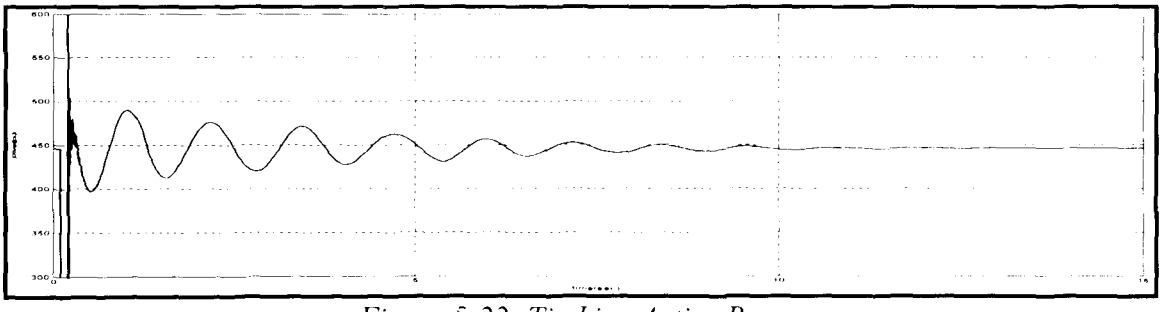

Figure 5-22: Tie Line Active Power

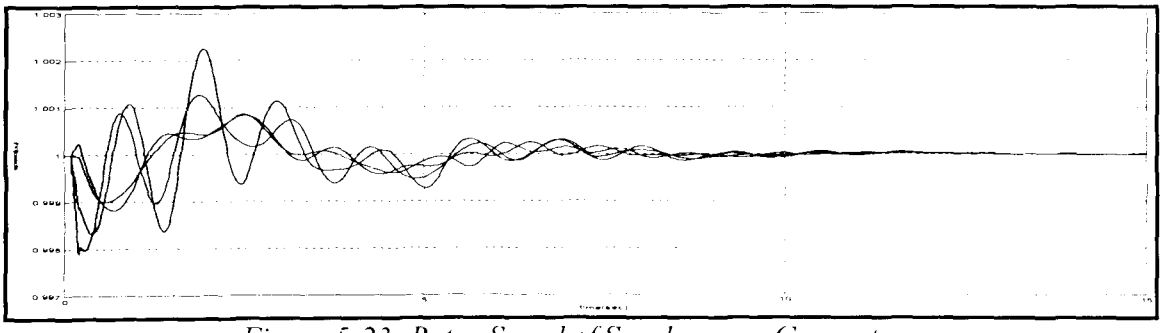

Figure 5-23: Rotor Speed of Synchronous Generators

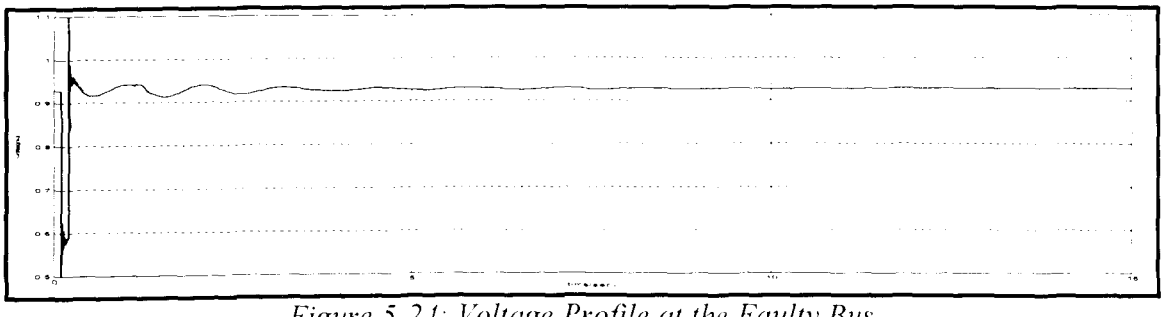

Figure 5-24: Voltage Profile at the Faulty Bus

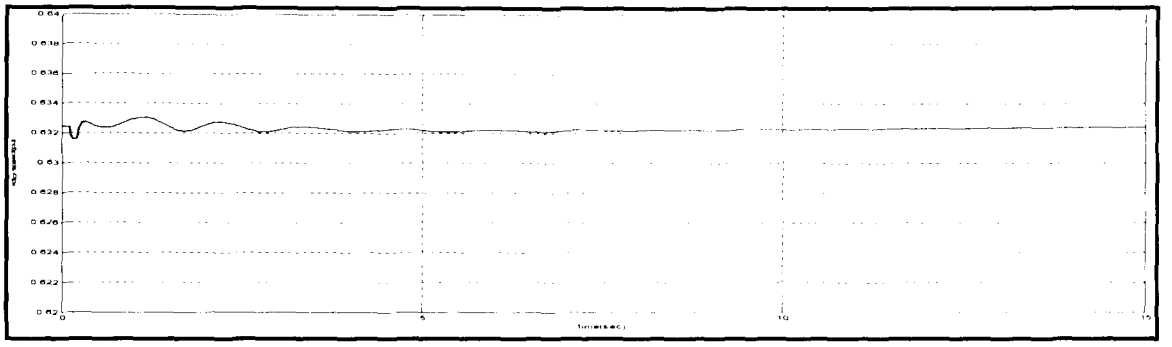

Figure 5-25: Rotor Speed of DFIG

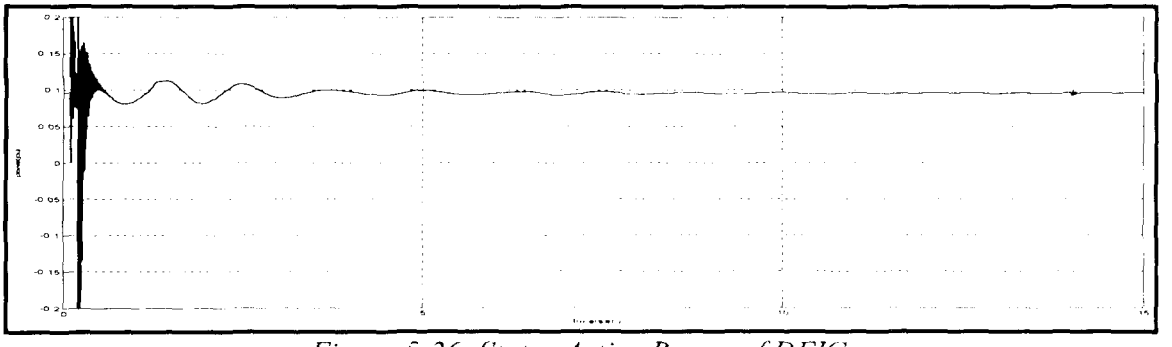

Figure 5-26: Stator Active Power of DFIG

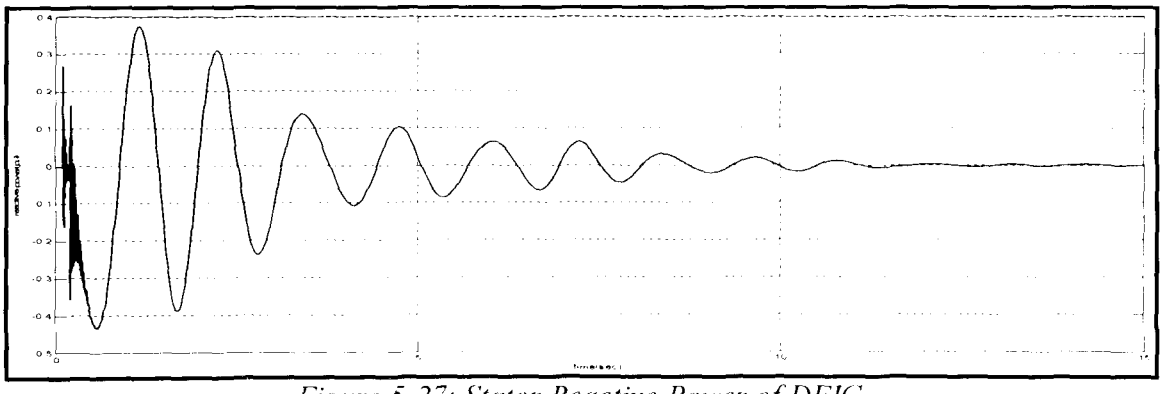

Figure 5-27: Stator Reactive Power of DFIG

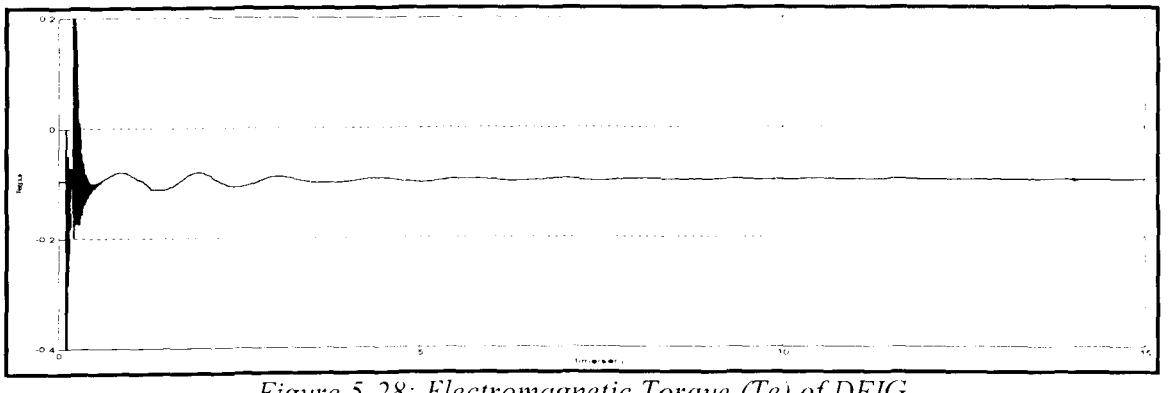

Figure 5-28: Electromagnetic Torque (Te) of DFIG

Reactive power modulation shows improvement in the oscillation damping. Here, the DFIG supplies reactive power as per the deviation of the rotor angle of synchronous generator in area 2 with the swing bus generator 1 in the first area; clearly shown by the stator reactive power. The voltage profile initially tends to oscillate which is unwanted in a transmission system. However, fast improvement in voltage profile was observed.

5.5.5. Simulation Results with DFIG with Active Power Modulation

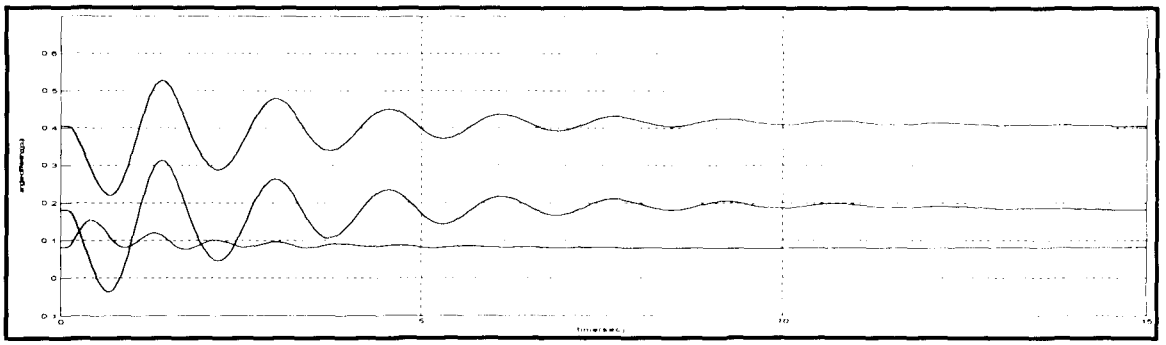

Figure 5-29: Rotor Angle Difference δ_{21}, δ_{31}, δ_{41}

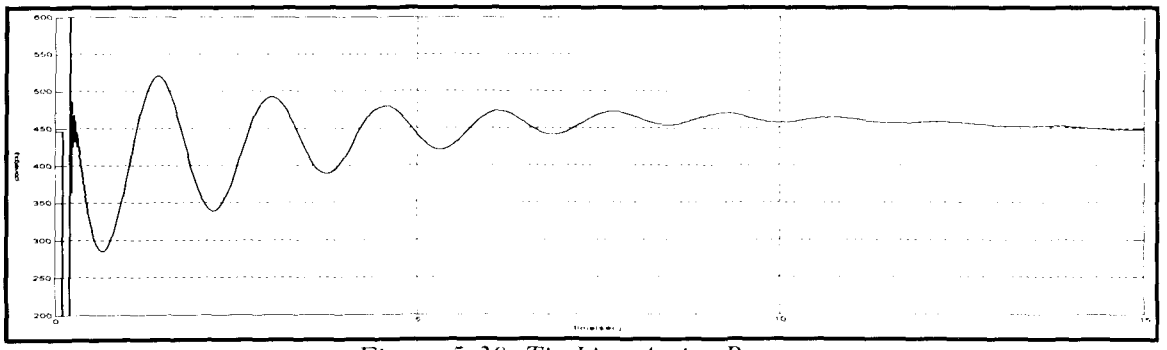

Figure 5-30: Tie Line Active Power

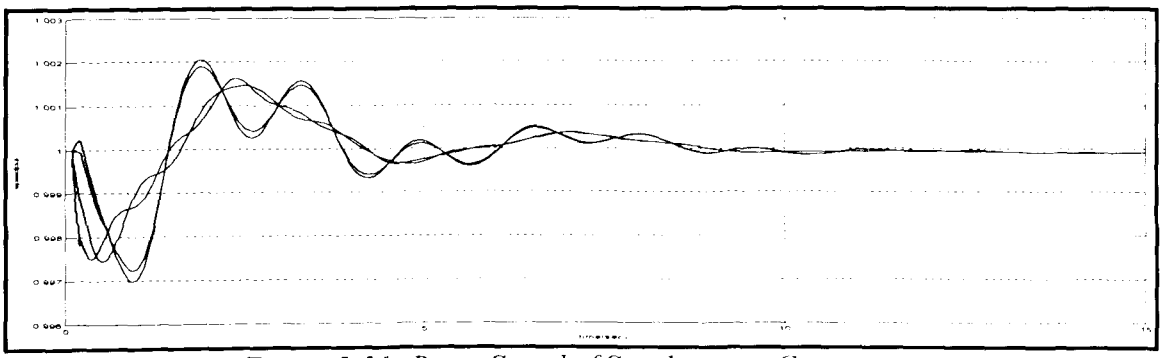

Figure 5-31: Rotor Speed of Synchronous Generators

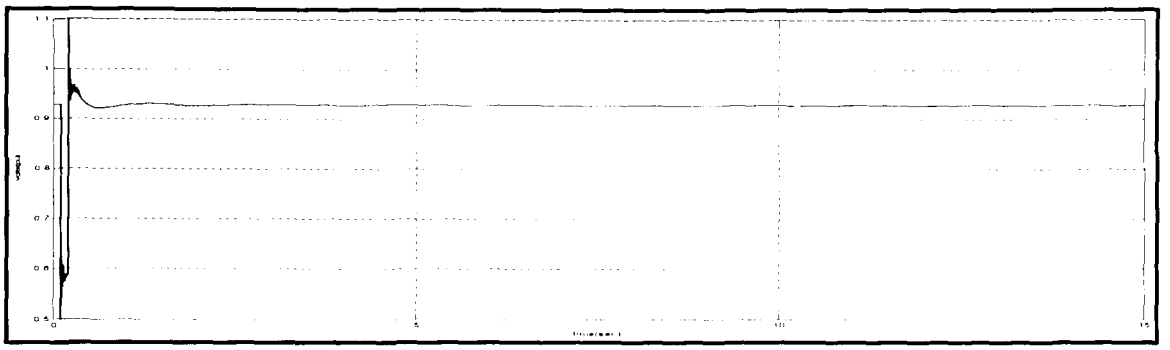

Figure 5-32: Voltage Profile at the Faulty Bus

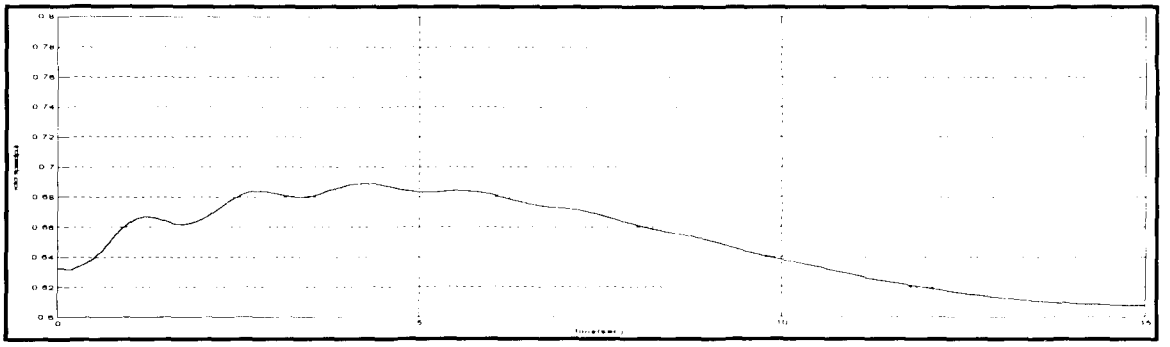

Figure 5-33: Rotor Speed of DFIG

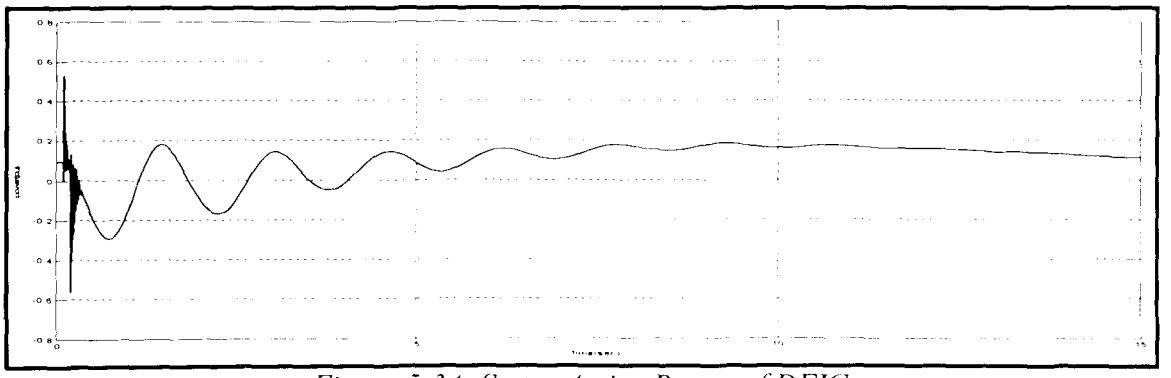

Figure 5-34: Stator Active Power of DFIG

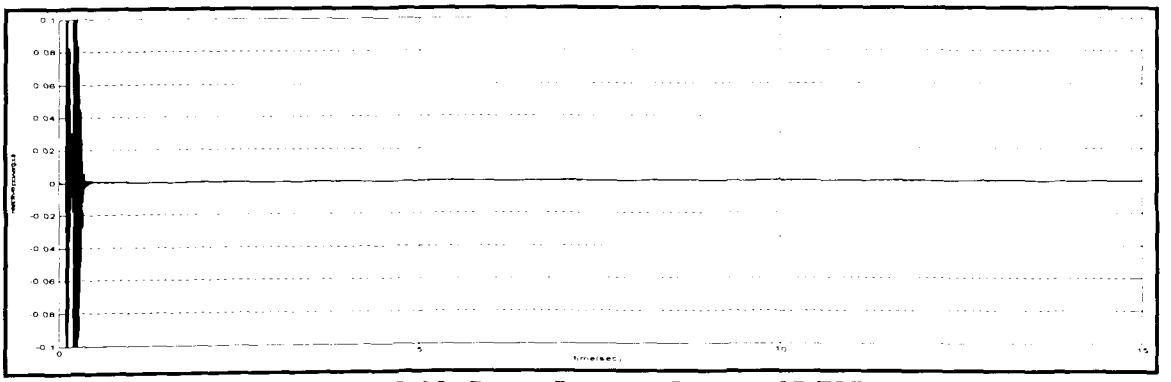

Figure 5-35: Stator Reactive Power of DFIG

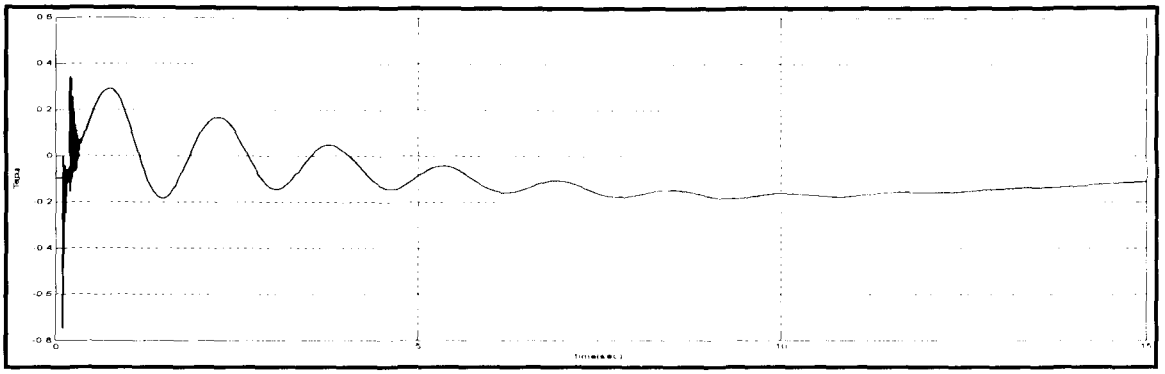

Figure 5-36: Electromagnetic Torque (Te) of DFIG

With the active power modulation technique applied, we observe the damping of the oscillations increases and tends to die out faster compared to other cases. It is depicted in the simulation diagram of rotor angle difference, transfer power oscillation and rotor speed of synchronous generators. Oscillations were observed in the DFIG rotor speed and stator active power as expected. Electromagnetic torque being directly related to active power oscillates and care should be provided to limit it as it is undesirable. Operation under such a condition generates vibration, increased losses, efficiency reduction and temperature rise that lead to reduction on insulation life.

5.5.6. Simulation Results with DFIG with Active and Reactive Power Modulation

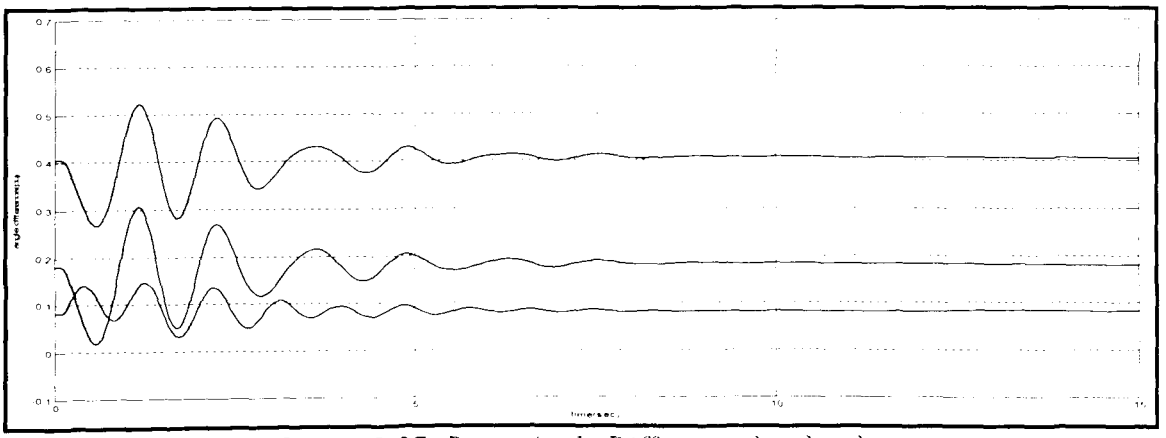

Figure 5-37: Rotor Angle Difference δ_{21}, δ_{31}, δ_{41}

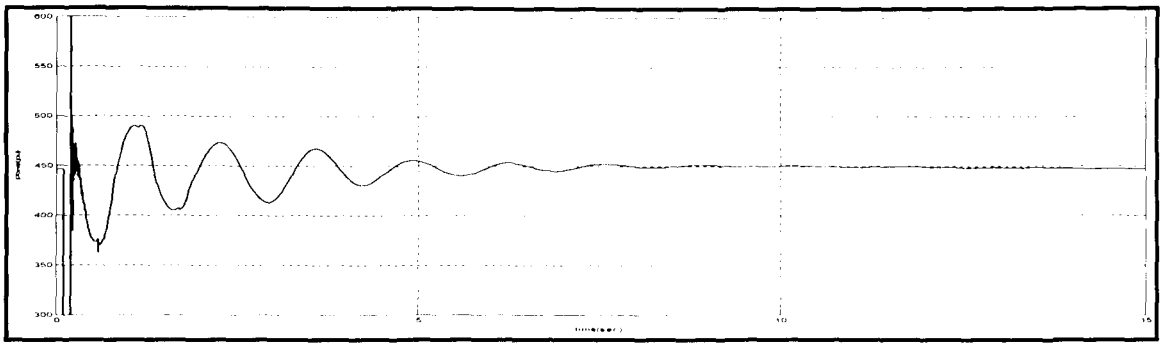

Figure 5-38: Tie Line Active Power

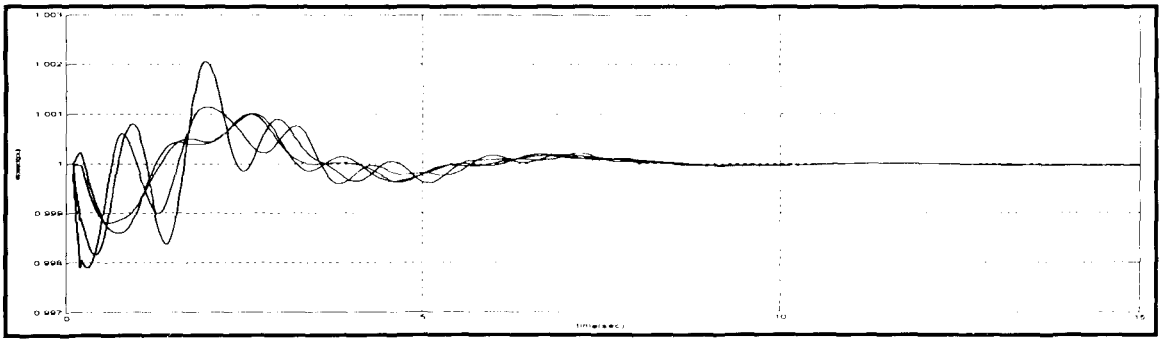

Figure 5-39: Rotor Speed of Synchronous Generators

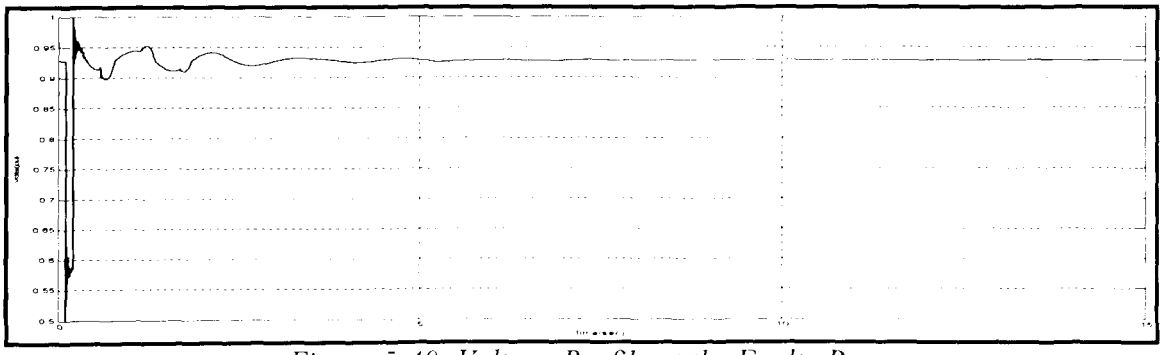

Figure 5-40: Voltage Profile at the Faulty Bus

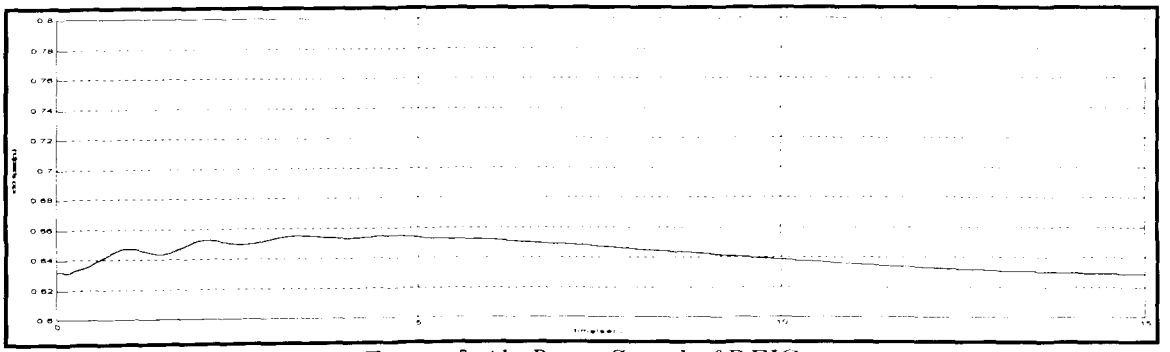

Figure 5-41: Rotor Speed of DFIG

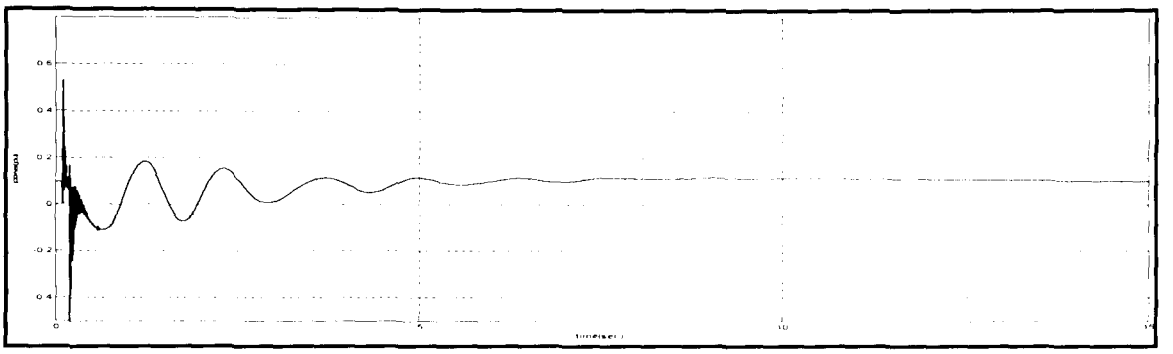

Figure 5-42: Stator Active Power of DFIG

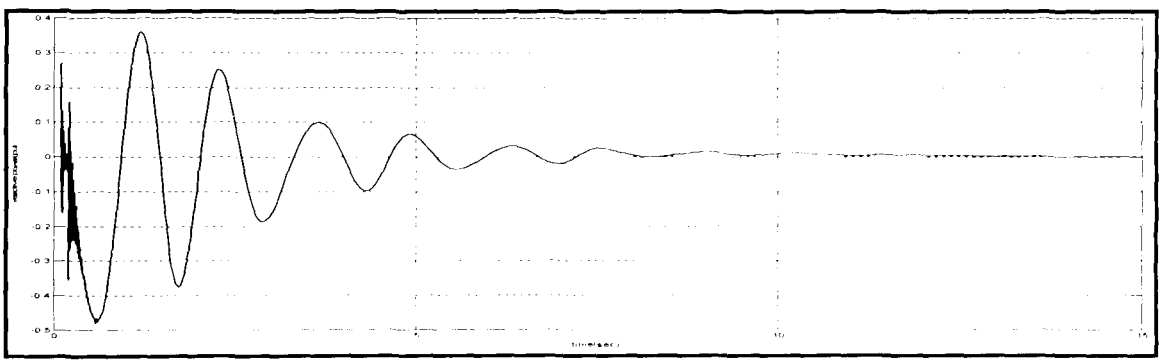

Figure 5-43: Stator Reactive Power of DFIG

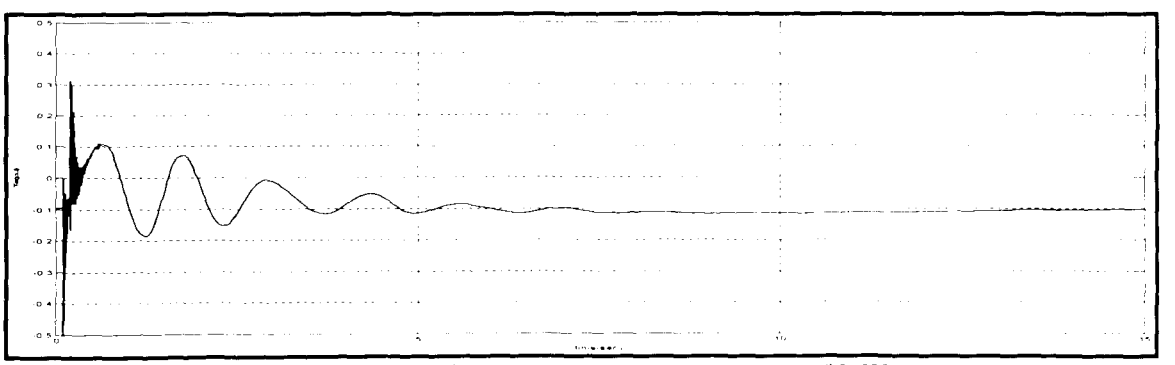

Figure 5-44: Electromagnetic Torque (Te) of DFIG

Active and reactive power modulation together at the doubly fed induction machine shows improvement in damping of the oscillation in the power systems network. The improvement is much more compared to the other cases as the oscillations were suppressed much faster. Combined effect of the two cases: active and reactive power modulation individually is observed at the faulty bus voltage, power and electromagnetic torque.

Similar damping as individual power modulation can be achieved by reduction of the gain in damping control to reduce harmful effects discussed in each of the cases.

5.5.7. Comparison of Tie Line Power Oscillation

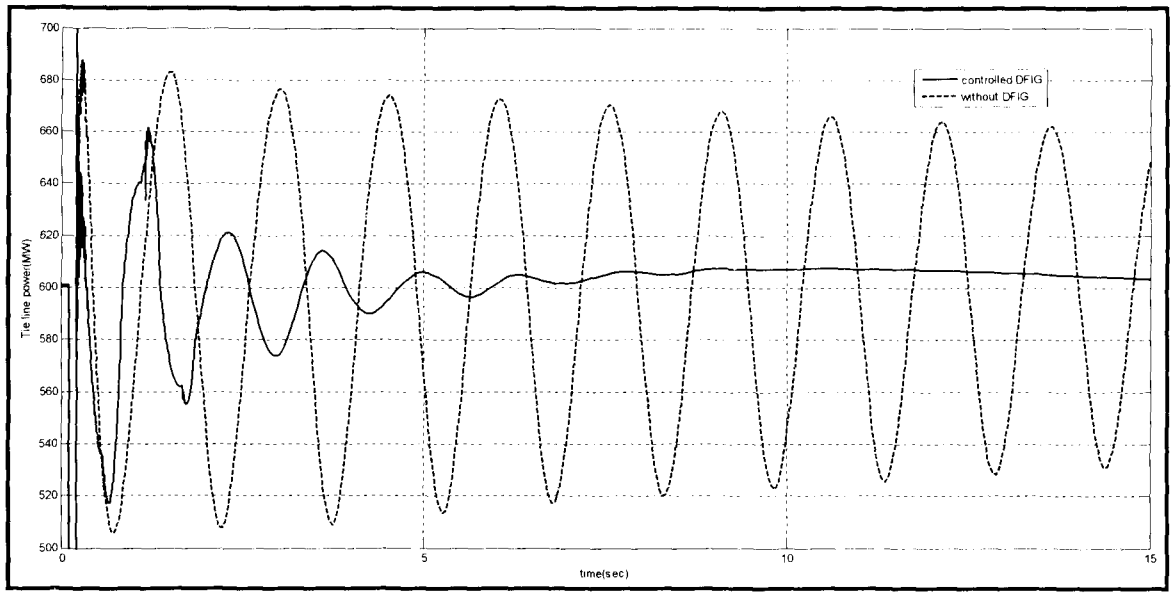

Figure 5-45: Tie Line Power Oscillation without and with DFIG for the Worst Cases in Our Study

Finally, the power oscillation in a four machine system with a tie line flow of 600MW is compared with the oscillations with a system with the improved DFIG control scheme for the same tie line flow. From time domain simulation results fast dying out oscillations in the later case clearly depicts the effectiveness of the proposed control scheme.

5.6. Summary

In this chapter eigenvalue analysis and time domain simulation results provided the effectiveness of the proposed damping control strategy. Addition of doubly fed induction generator in the system provides positive impact on damping interarea oscillation. Further modulation of simultaneous active and reactive power dampens interarea oscillation faster compared to individual cases involving modulation of active and reactive power. Modal

analysis shows that grid integration of large scale wind generation equipped with doubly fed induction generator improves the damping ratio to about 5% with the transfer of about 200MW of wind power with properly tuned controllers. Further, damping ratio is improved to about 8% with modulation of active and reactive power individually. With simultaneous modulation of active and reactive power damping ratio achieved for the system was above 10%. Damping ratio for a system above 10% is considered good for secured power systems network.

CHAPTER 6. CONCLUSION AND FUTURE WORK

6.1. Conclusion

This thesis presents research on the impact of doubly fed induction generator on power systems network. Further, control strategy to improve damping of power systems network with doubly fed induction generators is proposed and its effectiveness is verified with eigenvalue analysis and time domain simulation results.

For the study, dynamic behavior of a doubly fed induction generator under faulty condition involving oscillation was simulated in Matlab/Simulink using state space matrix/ vector control concept. Eigenvalue analysis and time domain simulation results for a power systems network were depicted. The results supported the effectiveness of the proposed control strategy to damp interarea oscillation with modulation of wind power generation.

Eigenvalue analysis showed that grid integration of large scale wind generation equipped with doubly fed induction generator provides a positive impact on interarea oscillation damping. From the various case studies done, the damping ratio was found to have improved to about 5% with transfer of about 200MW of wind power with properly tuned controllers. Further, damping ratio is improved to about 8% with modulation of active and reactive power individually. While simultaneous modulation of active and reactive power damping ratio achieved for the system was above 10%. Damping ratio for a system above 10% is considered good for secured power systems network. Finally, time domain simulation results with damped oscillation presented verified the improvements achieved.

6.2. Future Work

A single wind turbine equipped with a single mass model for a generator representing a wind farm was used for the study. Development of realistic multi turbines and multi mass models is recommended for the future work to capture accurate dynamics of the power systems network.

A simple general network system is used for the study. Whereas practical cases are vast and react differently with different configurations as for example the location of doubly fed induction generator at different location may have impacts different to doubly fed induction generator at other locations for a particular network system. So application of a particular grid network for study is a more reliable case and is recommended for the future.

Further the value of the proportional constant is chosen and is tested with the root locus plots. This is an offline method. Instead, development of a cost function to obtain the proportional constant required to resist the changes in the control signal and thus, built it as an online method is recommended as the future work.

REFERENCES

[1] "Renewables 2010 Global Status Report," available at: www.ren21.net/globalstatusreport/REN21_GSR_2010_full.pdf

[2] "Illustrated History of wind power Development," available at: www.telosnet.com/wind/

[3] "Interconnection for Wind Energy, Final Rule," Federal Energy Regulatory Commission, USA, 2 June 2005.

[4] EWEA report: "Large scale integration of wind energy in the European power supply: analysis, issues and recommendations", December 2005.

[5] P. Krause, *Analysis of Electric Machinery*. New York: McGraw-Hill, 1986.

[6] S. Heier, *Grid Integration of Wind Energy Conversion Systems*. New York: Wiley, 1998.

[7] R. Thresher, M. Robinson, and P. Veers, "To capture the wind," IEEE Power Energy Mag., vol. 5, no. 6, pp. 34–46, 2007.

[8] D. Aouzellag, K.Ghedamsi, E. Berkouk, "Power Control of a Variable Speed Wind Turbine Driving a DFIG," International Conference on Renewable Energies and Power Quality, 2006.

[9] G. Gail, A.C. Hansen, T. HartKopf, "Controller design and analysis of a variable speed wind turbine with doubly-fed induction generator," European Wind Energy Conference EWEC, 31 March-3 April 2008.

[10] S. M. Muyeen, R. Takahashi, T. Murata, J. Tamura, "Variable Speed Wind Turbine Control Strategy to Meet Wind Farm Grid Code Requirements," IEEE transaction on Power Systems, Vol. 25, pp. 331-340, Feb 2010.

[11] I.M. de Alegria, J. Andreu, J.L. Martin, P. Ibanez, J.L. Villate, H. Camblong, "Connection requirements for wind farms: A survey on technical requirements and regulation," Renewable and Sustainable Energy Reviews, 2007.

[12] B. Pal, B. Chaudhuri, *Robust control in power systems*, Springer, June 2005.

[13] L.Chang, "Wind energy conversion systems," IEEE Canadian Review, No. 40, p.2, spring 2002

[14] J. F. Manwell, J.G. McGowan, A.L. Rogers, *Wind Energy Explained: Theory, Design and Application,* New York: Wiley, 2002.

[15] B. K. Bose, *Power electronics and motor drives: advances and trends,* San Diego: Academic press, 2006.

[16] G. L. Johnson, *Wind energy systems,* Englewood Cliffs, N.J.: Prentice-Hall, 1985.

[17] P.W. Carlin, A.S. Laxson, E.B. Muljadi, "The History and State of the Art of Variable-Speed Wind Turbine Technology," National Renewable Energy Laboratory, 2001.

[18] F. Blaabjerg, Z. Chen, *Power electronics for modern wind turbines*, California: Morgan and Claypool publishers, 2006.

[19] S. Muller, M. Deicke, W. Rik, De Doncker, "Doubly fed induction generator systems for wind turbines", IEEE Industrial Application Magazine 8 (3), pp. 26–33, May/June 2002.

[20] L. Fan, S. Yuvarajan, "Modeling and slip control of a doubly fed induction wind turbine generator," North American Power Symposium, pp. 1-6, 28-30 Sept. 2008.

[21] T. Ackermann, *Wind power in power systems,* New Jersey: John Wiley & Sons, Inc., 2005.

[22] I. Erlich, M. Wilch, and C. Feltes, "Reactive power generation by DFIG based wind farms with AC grid connection," in Proc. 2007 European Conference on Power Electronics and Applications, Aalborg, Denmark, pp. 1-10, September 2007.

[23] B.Chitti Babu, K.B. Mohanty "Doubly-Fed Induction Generator for Variable Speed Wind Energy Conversion Systems-Modeling & Simulation," International Journal of Computer and Electrical Engineering, Vol. 2, No. 1, pp. 1793-8163, February, 2010.

[24] J.I. Jang, Y.S. Kim and D.C. Lee, "Active and reactive power control of DFIG for wind energy conversion under unbalanced grid voltage," IPEMC 2006 proceedings, Shanghai, vol. 3, pp. 1487-1491, Aug. 2006.

[25] R. Fernández, R. Mantz, P. Battaiotto, "Contribution of wind farms to the network stability," In: PES general meeting; 2006.

[26] J.G. Slootweg and W.L. Kling, "The impact of large scale wind power generation on power system oscillations," Electric Power System Research 67 pp. 9-20, 2003.

[27] C. Eping, J. Stenzel, M. Poeller, H. Mueller, "Impact of Large Scale Wind Power on Power System Stability," Fifth International Workshop on Large-Scale Integration of Wind Power and Transmission Networks, Glasgow, 2005.

[28] L. Meegahapola, D. Flynn, J. Kennedy, T. Littler, "Impact of Wind Generation Mix on Transient Stability for an Interconnected Power System," European Wind Energy Conference (EWEC), March 2009.

[29] L. Fan, Z. Miao, and D. Osborn, "Impact of doubly fed wind turbine generation on inter-area oscillation damping," 2008 IEEE Power and Energy Society General Meeting - Conversion and Delivery of Electrical Energy in the 21st Century, pp. 1–8, 2008.

[30] M. Klein, G.J. Rogers and P. Kundur, "A fundamental study of inter area oscillations in power systems," IEEE Transactions on Power Systems, pp. 914–921, 1991.

[31] O. I. Elgerd, *Electric Energy systems theory: An introduction,* New York, McGraw-Hill, 1971.

[32] E. Hagstrøm, I. Norheim and K. Uhlen, "Large-scale wind power integration in Norway and impact on damping in the Nordic grid," Wind Energy 8 (3) pp. 375–384, 2005.

[33] J.F. Hauer, C.J. Demeure, L.L. Scharf, "Initial results in Prony analysis of power system response signals," IEEE Transactions on Power Systems, pp. 80–89, 1990.

[34] G. Tsourakis, B. M. Nomikos, and C. D. Vournas, "Contribution of Doubly Fed Wind Generators to Oscillation Damping", IEEE Transactions on energy conversion, Vol. 24, No. 3, September 2009.

[35] G. Tsourakis, B. M. Nomikos, and C. D. Vournas, "Effect of wind parks with doubly fed asynchronous generators on small-signal stability," Electric Power System Research, vol. 79, no. 1, pp. 190–200, Jan. 2009.

[36] F.M. Hughes, O. Anaya-Lara, N. Jenkins, and G. Strbac, "A power system stabilizer for DFIG-based wind generation," IEEE Transaction on. Power Systems, vol. 21, no. 2, pp. 763–772, May 2006.

[37] P. Ledesma and C. Gallardo, "Contribution of variable-speed wind farms to damping of power system oscillations," Proceedings IEEE Power Tech., Lausanne, Switzerland, pp. 190–194, Jul. 2007.

[37] Z. Miao and L. Fan, "The art of modeling and simulation of induction generator in wind generation applications using high-order model," Simulation Model Practice and Theory, 16 (9), pp.1239-1253, 2008.

[39] Z. Miao, L. Fan, D. Osborn, and S. Yuvarajan, "Control of DFIG based Wind Generation to Improve Inter-Area Oscillation Damping," IEEE Transactions on Energy Conversion, vol. 24, no. 2 , pp. 415-422, June 2009.

[40] B.J. Jonkman, M.L.J. Buhl, "TurbSim User's Guide," National Renewable Energy Laboratory-NREL,April2007.
Available:http//wind.nrel.gov/designcodes/preprorpssors/turbsim/

[41] A.D. Hansen, P. Sorensen, F. Blaabjerg and J. Bech, "Dynamic modeling of wind farm grid interaction," Wind Eng, pp. 191–210, 2002.

[42] Z. Miao, *Modeling and dynamic stability of distributed generations*, Ph.D. thesis, West Virginia University, 2002.

[43] T. Petru, *Modeling of Wind Turbines for Power System Studies,* Ph.D thesis, Chalmers University of Technology, Department of Electric Power Engineering, Goteborg, Sweden, June 2003.

[44] B.J. Jonkman and M. L. J. Buhl, "FAST User's Guide," National Renewable Energy Laboratory, Golden, CO, Tech. Rep. NREL,August 2005. Available:http//wind.nrel.gov/designcodes/simulatos/fast/

[45] B. Boukhezzar, L. Lupu, H. Siguerdidjane and M. Hand, "Multivariable control strategy for variable speed variable pitch wind turbines," Renew. Energy 32 (8) pp. 1273–1287, 2007.

[46] E.S. Abdin and W. Xu, "Control design and dynamic performance analysis of a wind turbine-induction generator unit," IEEE Transactions on Energy Conversion Vol. 15 pp. 91–96, 2000.

[47] A. Murdoch, J.R. Winkelman, S.H. Javid, and R.S. Barton, "Control Design and Performance Analysis of a 6 MW Wind Turbine-Generator," IEEE Transactions on Power Apparatus and Systems, Vol. PAS-102, No. 5. pp. 1340-1347, May 1983.

[48] R. Aghatehrani, L. Fan, R. Kavasseri, "Coordinated Reactive Power Control of DFIG Rotor and Grid Sides Converters," Power & Energy Society General Meeting, IEEE pp. 1-6, 26-30 July 2009.

[49] N. Mohan, *Advanced Electric Drives: Analysis, Control and Modeling using Simulink,* MNPERE, 2001.

[50] P. Kundur, *Power System Stability and Control*, McGraw-Hill, 1993.

[51] A. Mullane, M. OM′ alley, "The inertial response of induction-machine-based wind turbines," IEEE Transactions on Power Systems 20 (3), pp. 1496–1503, 2005.

[52] F. Poitiers, M. Machmoum, R. L. Doeuff, M. E. Zaim, "Control of a doubly-fed induction generator for wind energy conversion systems," Proceedings of the Australasian Universities power engineering conference, 2001.

[53] N. P. Quang, A. Dittrich, and A. Thieme, "Doubly fed induction machine as generator:control algorithms with decoupling of torque and power factor," Electrical Engineering, Vol. 80, pp. 325-335, 1997.

[54] R. Datta and V. Ranganathan, "Decoupled control of active and reactive power for a grid-connected doubly-fed wound rotor induction machine without position sensors,"

Conference Record of the IEEE Industry Applications Conference. Thirty-Fourth IAS Annual Meeting, vol. 4, October 1999.

[55] R. Crowder, *Electric drives and Electro mechanical systems*, Burlington, MA: Butterworth-Heinemann, 2006.

[56] E. Larsen, J.J. Sanchez-Gasca, J. Chow, "Concepts for design of FACTS controllers to damp power swings," IEEE Transactions on Power Systems Vol. 10 pp. 948-956, 1995.

[57] H. Saadat, *Power Systems Analysis,* McGraw-Hill Primis Custom Publishing July 2001.

APPENDIX

Matlab/ Simulink Model

Matlab/simulink is widely used for time domain simulations. The test case network is built in simulink. Thus, the computer model for each of the components described in chapter three is built and connected in simulink. The basic block diagrams in development of the system are presented here. Figure A-1 shows the actual block diagram for the simulation from simulink.

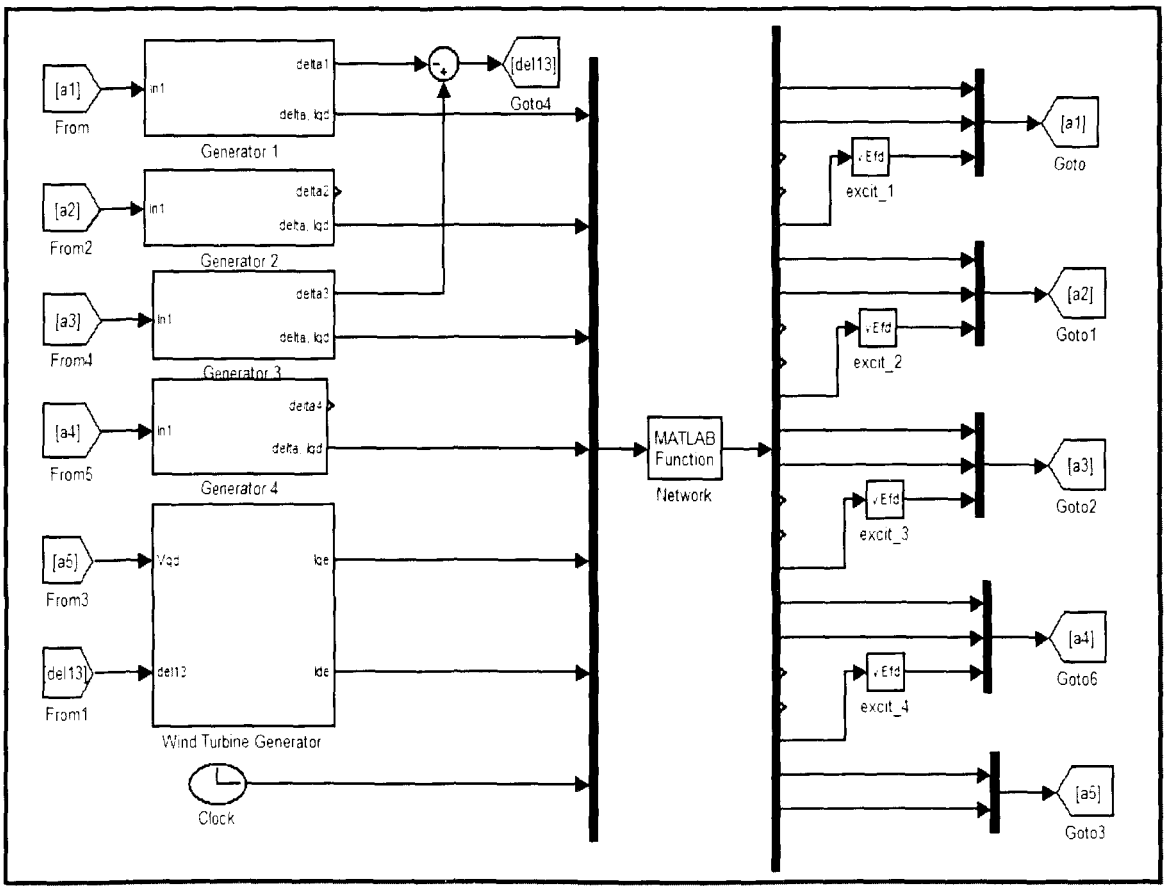

Figure A-1: Simulink Block Diagram for a Power System Network Simulation

Generators shown as subsystems are modeled with predefined blocks and Matlab code defined functions described later. The network is modeled using Matlab function with

current and power angle as inputs. The voltage at the terminals of the generating units is routed to their inputs again with signal routers as shown in Figure A-1.

Wind Turbine Simulink model

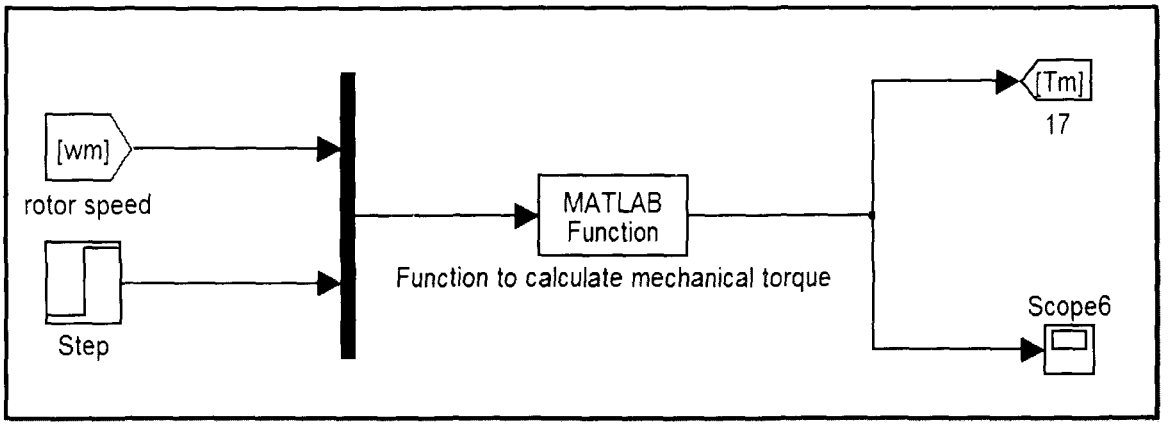

Figure A-2: Simulink Block Diagram for Wind Turbine Simulation

The wind turbine modeling can be done with the simulink defined block sets; easiness with the Matlab function to write the equations in code forms have led us chose it. Measured rotor speed and wind speed is fed to the Matlab function block. Step function provides us a constant wind speed required for the study, further a step source can be applied to observe changes due to change in wind speed.

Code for the Matlab function block in Figure A-2:-

```
Function Tm = Wind turbine (u)
wm = u (1);  % wm -- Rotor shaft speed
v = u (2);      % v -- wind speed
if v>10          % the rated wind speed beyond it the output power is constant
v=11;
end
R = 200*0.3048; %rotor size in m
A = pi*R^2;
V = v;
Wmga = wm;       % in per unit
row = 1.225; %(kg/m^3)
Beta = 0;
lambda = Wmga*R/V/2/pi;
```

```
Cp = (0.44-0.0167*Beta)*sin (pi*(lambda-3)/ (15-0.3*Beta)) -
        0.00184*(lambda-3) *Beta;
Tm = 0.5*row*A*R*Cp*V^2/lambda;
Tm = Tm/ (2*10^6);     % converting to per unit for the two MW wind turbine
```

Doubly Fed Induction Generator Simulink Model

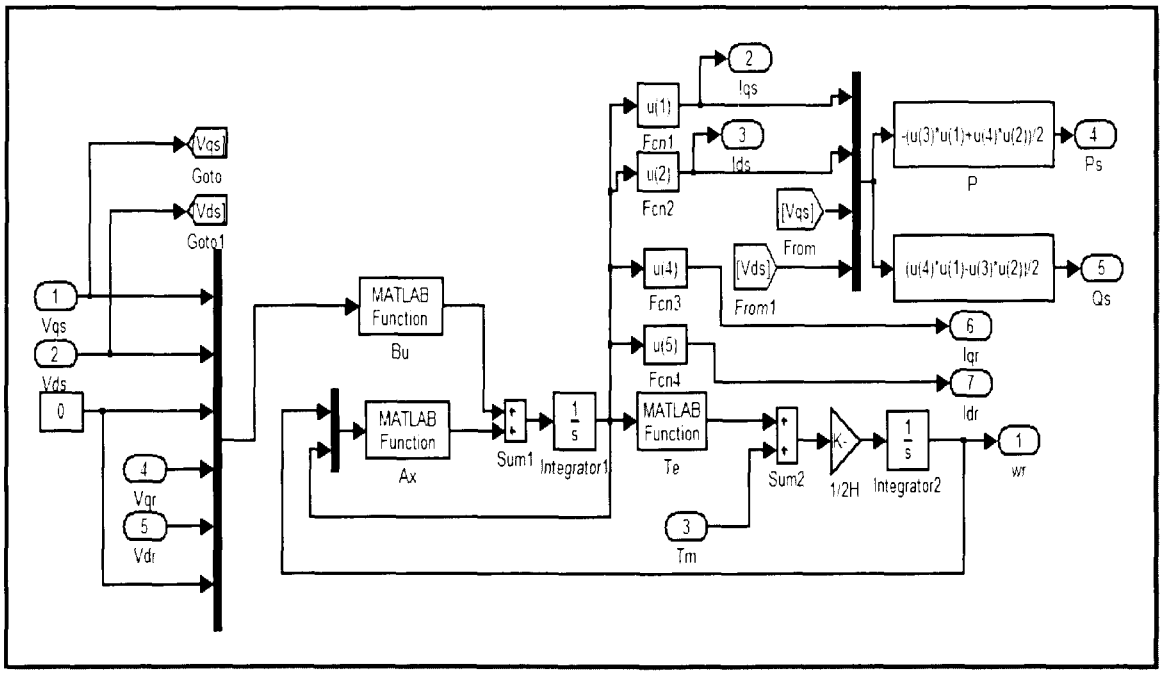

Figure A-3: Detailed Simulink Block Diagram for Induction Generator

The terminal voltage and mechanical torque are the inputs to the induction generator model. As the simulation is conducted in two phase d-q reference frame, the measured three phase voltage here is assumed to be transformed already by another block. The outputs for the model are the d-q currents, active and reactive power, rotor speed and electrical torque. Further, the major blocks for induction machine model are discussed in details.

Figure A-4 shows the block diagram for state equations for the induction generator defined as = Ax +Bu; in chapter three. Then the differential output is integrated to obtain the x matrix output i.e. is the current 'i' in the figure.

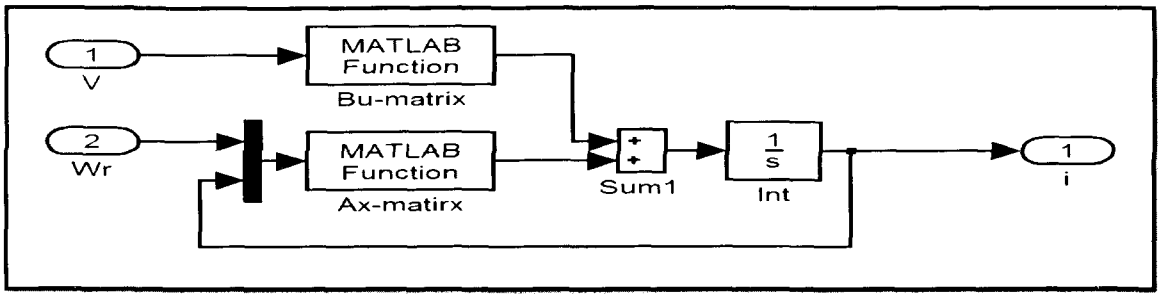

Figure A-4: Simulink Block Diagram for State Equations

Matlab codes for the function generating Ax and Bu matrix:-

```
function out = Aa(u,rs, Xss, XM, rr, Xrr, Xls,Xlr)
wr = u(1);
we = 2*pi*60;
R=[rs, Xss, 0, 0, XM, 0;
  -Xss, rs, 0, -XM, 0, 0;
  0, 0, rs, 0, 0, 0;
  0, (1-wr)*XM, 0, rr, (1-wr)*Xrr, 0;
  -(1-wr)*XM, 0, 0, -(1-wr)*Xrr, rr, 0;
  0, 0, 0, 0, 0, rr];

L=1/we*[Xss, 0, 0, XM, 0, 0;
   0, Xss, 0, 0, XM, 0;
   0, 0, Xls, 0, 0, 0;
   XM, 0, 0, Xrr, 0, 0;
   0, XM, 0, 0, Xrr, 0;
   0, 0, 0, 0, 0, Xlr];
Aa=-inv(L)*R;
out = Aa*u(2:7);
L_ind=1/we*[Xss_ind, 0, 0, XM_ind, 0, 0;
                    0, Xss_ind, 0, 0, XM_ind, 0;
                    0, 0, Xls_ind, 0, 0, 0;
                    XM_ind, 0, 0, Xrr_ind, 0, 0;
                    0, XM_ind, 0, 0, Xrr_ind, 0;
                    0, 0, 0, 0, 0, Xlr_ind];
Bb_ind = inv(L_ind);
function out = f_bb_ind(u, Bb_ind)
out = B_ind*u(1:6);
```

The swing equation in chapter three is modeled here in Matlab simulink. Then the differential of the rotor speed given by the swing equation is integrated to obtain the rotor speed.

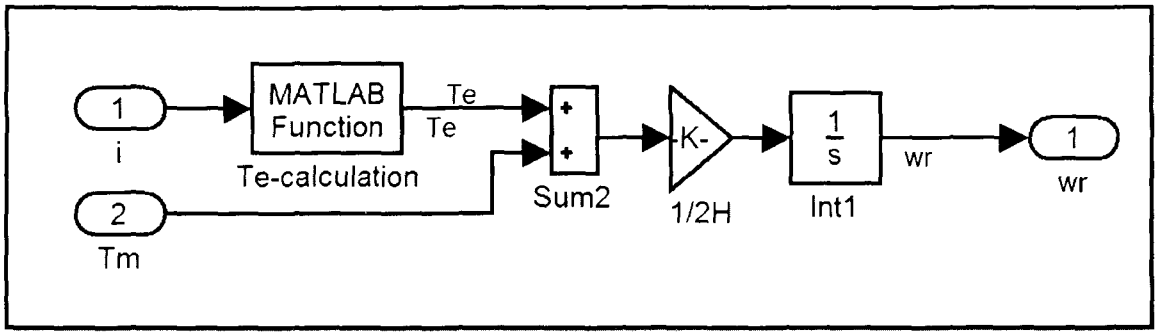

Figure A-5: Simulink Block Diagram for Swing Equation

Matlab codes for the function generating electromagnetic torque (Te):-

```
function out = Te (u, XM)
iqs = u(1);
ids = u(2);
i0s = u(3);
iqr = u(4);
idr = u(5);
i0r = u(6);
out = XM*(iqs*idr-ids*iqr)/2;
```

Coordinate active and reactive control for reactive power control was implemented.

Simulink diagram for the control is shown in Figure A-6.

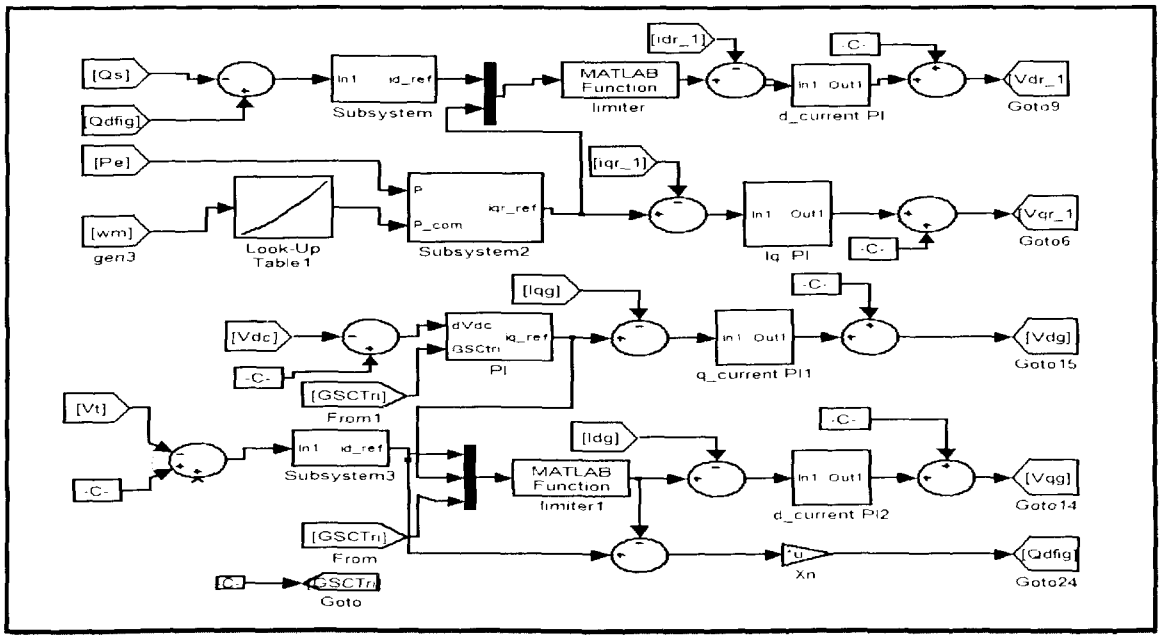

Figure A-6: Simulink Block for Coordinated Active and Reactive Power Control

A damping controller such that it operates to cancel the oscillations was added to the reference as shown in Figure A-7. The measured steady state power angle difference is subtracted so that the input from the controller remains zero during normal operation. Similar connection is added once for the reactive control loop and for both as combined active and reactive power modulation to study the impact.

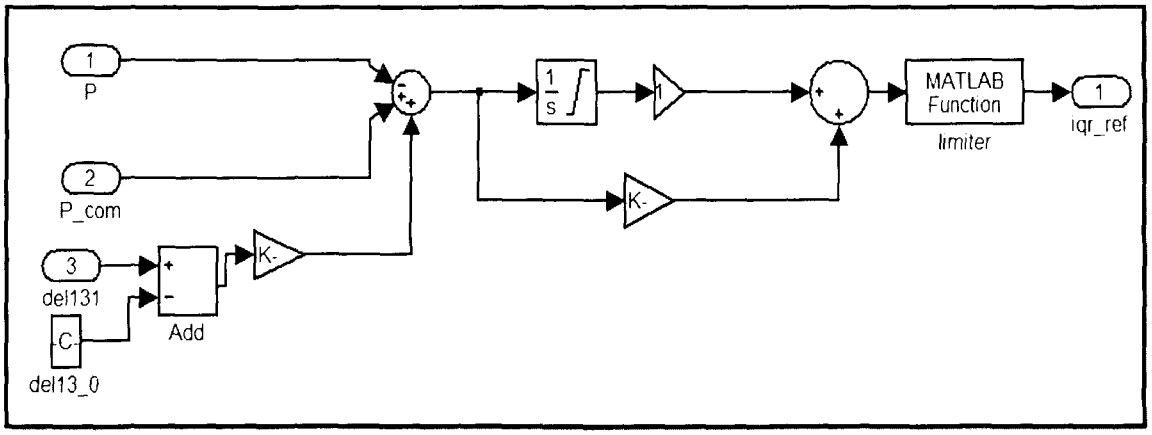

Figure A-7: Simulink Block for Damping Controller Corresponding to Active Power Modulation

Initialization

The first step in simulation is always the initialization part. Here the simulink model is initialized so that all the parameters of the machine are known. A matlab .m file is thus created with all the machine parameters assigned for the variables in simulink and run before running the model file for the system for power flow solution using PSAT (power systems analysis toolbox) toolbox.

```
clear;
bus = [...
01 1.03 0 7.00 1.85 0.00 0.00 0.00 0.00 1 99.0 -99.0 022.0; %01   G1 ->01
02 1.01 0 6.67 2.35 0.00 0.00 0.00 0.00 2 05.0 000.0 022.0; %02   G2 ->02
03 1.03 0 7.00 1.76 0.00 0.00 0.00 0.00 2 05.0 000.0 022.0; %11   G3 ->03
04 1.01 0 7.00 2.02 0.00 0.00 0.00 0.00 2 05.0 000.0 022.0; %12   G3 ->04
05 0.98 0 0.50 0.00 0.00 0.00 0.00 0.00 3 00.0 000.0 230.0; %03 wind->05
06 0.95 0 0.00 0.00 7.67 1.00 0.00 0.00 3 00.0 000.0 115.0; %04       ->06
07 1.01 0 0.00 0.00 0.00 0.00 0.00 0.00 3 00.0 000.0 230.0; %10       ->07
```

```
08 0.99 0 0.00 0.00 0.00 -3.5 0.00 0.00 3 00.0 000.0 230.0; %13        ->08
09 0.95 0 0.00 0.00 18.2 1.00 0.00 0.00 3 00.0 000.0 115.0; %14        ->09
10 0.99 0 0.00 0.00 0.00 0.00 0.00 0.00 3 00.0 000.0 230.0; %20        ->10
11 0.92 0 0.00 0.00 0.00 0.00 0.00 0.00 3 99.0 -99.0 500.0; %101       ->11
12 1.01 0 0.00 0.00 0.00 0.00 0.00 0.00 3 00.0 000.0 230.0; %110       ->12
13 0.99 0 0.00 0.00 0.00 0.00 0.00 0.00 3 00.0 000.0 230.0; %120       ->13
];
bus1=bus;
bus(:,4:9)=bus(:,4:9)/8.35;% base of 835MW

line = [...
01 07 0.00000 0.01670 0.000000 1.0 0. 0.0 0.0 0.;   % 01    10
02 10 0.00000 0.01670 0.000000 1.0 0. 0.0 0.0 0.;   % 02    20
05 06 0.00000 0.00500 0.000000 1.0 0. 1.2 0.8 .05; % 03    04
05 10 0.00100 0.01000 0.017500 1.0 0. 0.0 0.0 0.;   % 03    20
05 11 0.011/3 0.110/3 0.1925*3 1.0 0. 0.0 0.0 0.;   % 03    101
07 10 0.00250 0.02500 0.043700 1.0 0. 0.0 0.0 0.;  % 10    20
03 12 0.00000 0.01670 0.000000 1.0 0. 0.0 0.0 0.;  % 11   110
04 13 0.00000 0.01670 0.000000 1.0 0. 0.0 0.0 0.;  % 12   120
08 09 0.00000 0.00500 0.000000 1.0 0. 1.2 0.8 0.05;% 13    14
08 11 0.011/3 00.11/3 0.1925*3 1.0 0. 0.0 0.0 0.;     % 13   101
08 13 0.00100 0.01000 0.017500 1.0 0. 0.0 0.0 0.;   % 13   120
12 13 0.00250 0.02500 0.043700 1.0 0. 0.0 0.0 0.]; %  110 120

line(:,3:4)= line(:,3:4)*8.35;
line(:,5)= line(:,5)/8.35;
[m_line, n_line] = size(line);
bus=loadflow(bus,line,1e-4,10,1,'y',2);
Pgen = bus(:,4);
Qgen = bus(:,5);

% data for synchronous generator
H =5.6;
rs = 0.003;
Xls = 0.19;
Xq = 1.8;
Xd = 1.8;
rkq1 = 0.00178;
rfd = 0.000929;
Xlkq1 = 0.08125;
Xlfd = 0.1414;
rkq2 = 0.00841;
rkd = 0.01334;
Xlkq2 = 0.0939;
Xlkd = 0.08125;
D = 0.0;% worst case with damper '0'
```

```
r=rs; rF=rfd; rD=rkd;
rQ=rkq1;
kMD = 1.55; kMF = 1.55; MR = 1.55; kMQ = 1.49;
Ld=Xd; LF=kMF+Xlfd; LD=Xlkd+kMD; Lq=Xq;
LQ=Xlkq1+kMQ;

parameter1(1,:)=[Ld, Lq, LD, LQ, LF, MR, kMF, kMD, kMQ,r, rF, rD, rQ, H];
parameter1(2,:)=[Ld, Lq, LD, LQ, LF, MR, kMF, kMD, kMQ,r, rF, rD, rQ, H];
parameter1(3,:)=[Ld, Lq, LD, LQ, LF, MR, kMF, kMD, kMQ,r, rF, rD, rQ, H];
parameter1(4,:)=[Ld, Lq, LD, LQ, LF, MR, kMF, kMD, kMQ,r, rF, rD, rQ, H];
[Aa(:,:,1), Bb(:,:,1), I_0(:,1), delta_0(1), Tm0(1)]= data_syn(parameter1(1,:), Pgen(1),
Qgen(1), Va(1));
[Aa(:,:,2), Bb(:,:,2), I_0(:,2), delta_0(2), Tm0(2)]= data_syn(parameter1(2,:), Pgen(2),
Qgen(2), Va(2));
[Aa(:,:,3), Bb(:,:,3), I_0(:,3), delta_0(3), Tm0(3)]= data_syn(parameter1(3,:), Pgen(3),
Qgen(3), Va(3));
[Aa(:,:,4), Bb(:,:,4), I_0(:,4), delta_0(4), Tm0(4)]= data_syn(parameter1(4,:), Pgen(4),
Qgen(4), Va(4));
 Te1 = [0.05 0.05 0.05 0.05];
Ka  =  [0.05 0.05 0.05 0.05];
 iF0 = I_0(2,1:4);
rF=parameter1(1:4, 11);
n=length(bus(:,1));
Y=formY(bus,line);
Y_pre=Y;
bus1(5,6)=40.0;
bus1(:,4:9)=bus1(:,4:9)/8.35;
Y1=formY(bus1,line);
Y_fault=Y1;
Y0=Y_pre;
Yr_pre    =Y_pre;
Yr_fault  =Y_fault;
 %wind generator
k=1;
wm = 0.75;  % per unit
v = 7;% wind speed 9 m/s
lookup1 = [0.75, 0.85, 0.95, 1.05, 1.15 1.25];
lookup2 = [0.16, 0.245, 0.3457, 0.475, 0.625, 0.80];
H_ind = 3.5*k;
rr_ind   = 0.00549/k;  %pu
rs_ind   = 0.00488/k; % pu
Xls_ind  = 0.09231/k;  % pu
Xlr_ind  = 0.09955/k; % pu
XM_ind = 3.95279/k;
k_s = 1.0;
we =2*pi*60;
```

```
Xss_ind = Xls_ind + XM_ind;
Xrr_ind = Xlr_ind + XM_ind;
I0_ind=zeros(6,1);
TL_ind = 1.0;

L_ind=1/we*[Xss_ind, 0, 0, XM_ind, 0, 0;
        0, Xss_ind, 0, 0, XM_ind, 0;
        0, 0, Xls_ind, 0, 0, 0;
        XM_ind, 0, 0, Xrr_ind, 0, 0;
        0, XM_ind, 0, 0, Xrr_ind, 0;
        0, 0, 0, 0, 0, Xlr_ind];
Bb_ind = inv(L_ind);
V5_ind = bus(5,2)*exp(j*bus(5,3)*pi/180);
P_ind = bus(5,4)*k_s;
slip_old = 1-wm;
Vas_ind = V5_ind;
Vv_ind = V5_ind;
delta_PLL = angle(Vas_ind);
Vas_ind = abs(Vas_ind);
P_dfig = bus(5,4)*k_s
Q_dfig = bus(5,5)*k_s
Pr  = P_dfig/(1-slip_old)*slip_old;
for n= 1: 10
Ps_dfig = P_dfig+Pr;
Iaa = Pr/Vas_ind';
Is = (Ps_dfig-j*Q_dfig)/Vas_ind';
Vm = Vas_ind + Is*(rs_ind+j*Xls_ind);
Im = Vm/(j*XM_ind);
Ir = Is + Im;
Vr = Vm + Ir*(rr_ind/slip_old+j*Xlr_ind);
Vqr0 = real(Vr)*slip_old;
Vdr0 = imag(Vr)*slip_old;
wr_ind = 1- slip_old;
Ia_ind = Is;
Ig_ind = Is-Iaa;
iqs_ind = -real(Ia_ind)*sqrt(2);
ids_ind = imag(Ia_ind)*sqrt(2);
Vqs_ind = real(Vas_ind)*sqrt(2);
Vds_ind = -imag(Vas_ind)*sqrt(2);
pp=Vds_ind*ids_ind/k_s+Vqs_ind*iqs_ind/k_s;
qq=Vqs_ind*ids_ind/k_s-Vds_ind*iqs_ind/k_s;
Iar_ind = Ir;
iqdr_ind = [real(Iar_ind); -imag(Iar_ind)]*sqrt(2);
Te_ind = Te_fun_ind([iqs_ind;ids_ind;0;iqdr_ind;0], XM_ind);
TL_ind = Te_ind;
I0_ind=[iqs_ind;ids_ind;0;iqdr_ind;0];
```

```
Ir = I0_ind(4)-j*I0_ind(5);
Pr = real(Vr*slip_old*Ir'/sqrt(2));
end
R_wind = 200*0.3048; %m
A_wind = pi*R_wind^2;
V_wind = [6.2,7, 13.3, 26.6]; %m/s
luo = 1.225; %(kg/m^3)
Wmga = 17.9/60*2*pi;
Beta_wind =0;
lbda0_wind = Wmga*R_wind/V_wind(2);
Cp0_wind = (0.44-0.0167*Beta_wind)*sin(pi*(lbda0_wind-3)/(15-0.3*Beta_wind))-
0.00184*(lbda0_wind-3)*Beta_wind;
Tm0_wind =
0.5*luo*A_wind*R_wind*Cp0_wind*V_wind(2)*V_wind(2)/lbda0_wind/(2*10^6);
p_wind = pp/(-sqrt(2))*k_s;
Ki_wind = 6.2;
Kp_wind = 6.2;
wr0 = 1-slip_old;
Vv_ind = bus(5,2)*exp(j*bus(5,3)*pi/180)
w = 2*pi*60;
absG = 10^(29/20);
sita = -pi + pi/2 -(-82.8)*pi/180;
Kp = cos(sita)/absG;
Ki = -sin(sita)/absG*w;
C_iqr = Ki;
C_pqr = Kp;
C_idr = Ki;
C_pdr = Kp;

Ig = 1.0;
X= 1.0; Xtg = 0.55; %pu
for i=1:10
X = X - (X^2*Xtg-abs(Vas_ind)^2*X+Pr^2)/(2*X*Xtg-abs(Vas_ind)^2);
end
Ig = sqrt(X);
sita_g = acos(Pr/Ig/Vas_ind);
iqg = sqrt(2)*real(Ig*cos(sita_g));
idg = -sqrt(2)*imag(Ig*sin(-sita_g));
Vg = Vas_ind - Ig*(cos(sita_g)-j*sin(sita_g))*(j*Xtg);
Vqg = sqrt(2)*real(Vg);
Vdg = -sqrt(2)*imag(Vg);
vDC_0 = 1200; % volt
C = 0.07; % F
Xtg = 0.55; % pu
```